UNIVERSITY OF SOUTHAMPTON, U.K.

MODEL-BASED APPROACHES FOR RECOGNISING PEOPLE BY THE WAY THEY WALK OR RUN

Chew-Yean Yam

Doctor of Philosophy

FACULTY OF ENGINEERING
DEPARTMENT OF ELECTRONICS AND COMPUTER SCIENCE

Submitted November 2002

UNIVERSITY OF SOUTHAMPTON

ABSTRACT

FACULTY OF ENGINEERING
DEPARTMENT OF ELECTRONICS AND COMPUTER SCIENCE

Doctor of Philosophy

MODEL-BASED APPROACHES FOR RECOGNISING PEOPLE BY THE WAY THEY WALK OR RUN

by Chew-Yean Yam

Using biological traits, such as fingerprints, iris patterns and voice print, in identification and authentication has gained increasing attention due to the demand for a more secure environment. The potential of human walking as a biometric has only attracted interest in the computer vision community since the last decade. Nevertheless, the potential of human running gait as a biometric remains largely unexplored. Here, we propose an approach for an automated non-invasive/markerless person identification system by not only the walking, but also the running gait to explore the potential of these two biomechanically distinct gaits. Two motion models both invariant to walking and running, have been developed based on the concept of harmonic motion. The first is a bilateral symmetric model made up of an upper and a lower pendulum, representing the thigh and the lower leg, joined at the knee. The upper pendulum is simple harmonic motion whilst the lower pendulum uses an empirical model requiring parameter selection for the different gait mode and lacks analytical attributes. The second model has a forced coupled oscillator to describe the knee rotation as legs are considered to be imperfect pendula with energy loss.

The rhythm and pattern of gaits are automatically extracted by a temporal evidence gathering technique with the motion models as the underlying temporal templates. The spatio-temporal characteristics of the gait patterns are described by a Fourier representation, which are in turn used to create unique gait signatures for the purpose

of identification. Performance analysis demonstrates the potential of gait as a biometric, with running being more potent. This technique not only performs well in discriminating individuals, but also appears capable of distinguishing the gender and gait mode. Moreover, analysis shows that the knee rotation contributes significantly to discrimination capability.

Based on the hypothesis that human walking and running gaits are intimately related by the musculo-skeletal structure and that the walking pattern is the phase-modulated version of running (or vice versa), a unique mapping/transform between individuals' walking and running gait is developed, making the signature invariant to gait mode. Furthermore, this mapping can be used alone as a compressed signature or to buttress the original signature to further improve the recognition capability. Then, a generic relationship between walking and running has been investigated via a neural network. Due to the current size of the experimental dataset, the structure of the two signature spaces could not be drawn, at least not by this approach. However, results do suggest its possible existence.

The effect of different camera views is an important application issue. The gait pattern perceived by machine vision at different viewpoints has been investigated. The frequency description of the gait pattern is linearly dependent on the camera sagittal view angle. The changes of both the magnitude and the phase component are symmetric about the fronto-parallel view. This linearity offers a convenient way to map the angular motion obtained from various camera sagittal views to the true motion, for the convenience of gait analysis. More importantly, this linearity can be exploited to develop view invariant gait signatures.

The new and interesting findings of this work not only benefit biometrics research, but may also draw attention from other communities such as biomechanics and graphics applications.

Table of Contents

List of Tables

List of Figures

Glossary

Bilateral symmetry	Symmetry of left and right.
Double float	Period when both limbs are not on the ground, i.e. airborne.
Double support	Period when both limbs are in contact with the ground.
Forced walk	A walk with a prescribed step frequency or step length and speed.
Free/Preferred walk	A walk in which a person adopts whatever speed and step length or step frequency he/she chosen.
Gait cycle	The basic unit of measurement in gait analysis. It is defined as the period from the initial contact of one foot to the following initial contact of the same foot, i.e. two steps. In other words, it is the time interval between successive instances of initial contact of the same foot.
Heel strike	The instance when the heel contacts the ground.
Kinematics	The description of motion of joints but does not consider the forces that cause the actions.
Kinetics	Study of the internal forces (i.e. muscle forces) and external forces (ground reaction forces) that cause movement.
Single support	Period when only one limb is in contact with the ground.
Speed controlled walk	A walk with specified speed: i.e. treadmill walking.

Step	The period from heel strike of one foot to heel strike of the other foot.
Step length	The projected distance between two positions of the same anatomical point on the left and right feet along an anterior-posterior line drawn in the direction of ambulation
Step/stride frequency	The number of steps/stride per unit of time.
Stride length	The projected distance between two positions of an anatomical point on the same foot along an anterior-posterior line drawn in the direction of ambulation.
Swing phase	The period of single support during the gait cycle.

Acknowledgements

I am indebted to my supervisors, Prof. Mark S. Nixon and Dr. John N. Carter, colleagues and friends who have directly and indirectly guided and helped me in the course of my research. Millions of thanks. I would like to acknowledge Robert T. Boston for the human synthesiser and Georgia Tech Research Institute for the human gait data.

I also gratefully acknowledge partial support by the European Research Office of the US Army under Contract No. N68171-01-C-9002.

Chapter 1 : Prelude

An average human does not exist!

V. T. Inman, *Human Walking*, 1981.

Today's crime, ever more hostile and involving more advanced technology, has fanned the demand for a more secure environment. Attempts range from the simple, like locking a door, to more sophisticated (or experimental) methods, such as employing biometrics in identification and authentication. Scanning iris and fingerprints, voice prints and entering a PIN (Personal Identity Number) to gain access to controlled premises is no longer limited to the scenes in Hollywood movies. Rather, they are daily practices in today's society, as much technology has been infused into sophisticated security measures. An emerging and fast-growing worldwide crime is identity theft, increasing nearly 500% a year in the United Kingdom alone [Penycate'01]. Identity fraud may become one of the most serious crimes and can result in significant financial loss, or even terrorist acts. To counter-attack this intolerable crime, biometrics have gained increasing attention and momentum.

1.1 What are Biometrics

Biometrics concern any human physiological and/or behavioural characteristics [Jain'99] which are *(i) universal*, every person should have that characteristic; *(ii) unique*, no two people should be the same in terms of that characteristic; *(iii) permanent*, invariant with time; and *(iv) collectable*, can be measured quantitatively. Since biometrics are concerned with using one's biological characteristics, it provides a more reliable means in countering identity fraud. The concept of identifying people based on physical characteristics is not new. Human and animals recognize one another by their physical characteristics, voice and odour. Archaeological artifacts show that our ancestors recognised the individuality of fingerprint impressions on their picture drawings [Moenssens'71]. Biological characteristics that have been explored for their potential as biometrics so far are face, fingerprints, hand geometry, keystrokes, hand vein geometry, iris patterns, retinal scan, signature, voice print, facial thermograms, body odour, DNA (DeoxyriboNucleic Acid), gait and ear. As many are still in their infancy, not all have been deployed in the real world.

Aiming to address the huge losses due to credit card fraud, a trial scheme asking shoppers for their thumbprint on the back of cheques or credit card receipts (in addition to the traditional signature recognition [Fairhurst'94]) is already underway in the UK. In order to improve security and speed in immigration, some airports now employ biometrics. For example, Iceland's main airport will employ face-recognition technology to help improve security, whereas Saudi Arabia will use iris patterns and fingerprints to prevent terrorism in the month of the Hajj pilgrimage. The attractive advantages of biometrics are the combination of high speed processing with a high level of security. Hong Kong is preparing to introduce one of the world’s most advanced identity cards in an attempt to curb illegal immigration. An embedded computer chip on the card will hold personal details as well as the owner’s thumbprints. This will help to speed up border checks. There are approximately 200,000 people travelling across the border between the former UK colony and the mainland China a day. The idea of using biometric identity checks such as fingerprints, iris pattern, hand geometry or voice print in a "smart" passport has also attracted the

interest of the UK Passport Office, aimed to prevent identity fraud. Many biological traits, be it physical or behavioural, could be a novel and feasible idea to be used as a biometric. However, the primary question is to design a system which can meet the ever increasing application requirement with currently available technology, of which most are in their infancy.

A typical biometric system operates in two modes, *enrolment* and *identification*. The e*nrolment* phase will capture biometric measurements from a given subject. Relevant information from the raw measurement is then harvested by a feature extractor, and feature information is stored in a database. Some form of label associated to a subject may be generated. This is essentially a computer vision problem (for visual-based biometrics). Here, *identification* is synonymous with classification. The system senses the biometric measurements from a subject, extracts features from the raw measurements, and searches for possible matches within the database using the features thus extracted. This is essentially a pattern recognition problem.

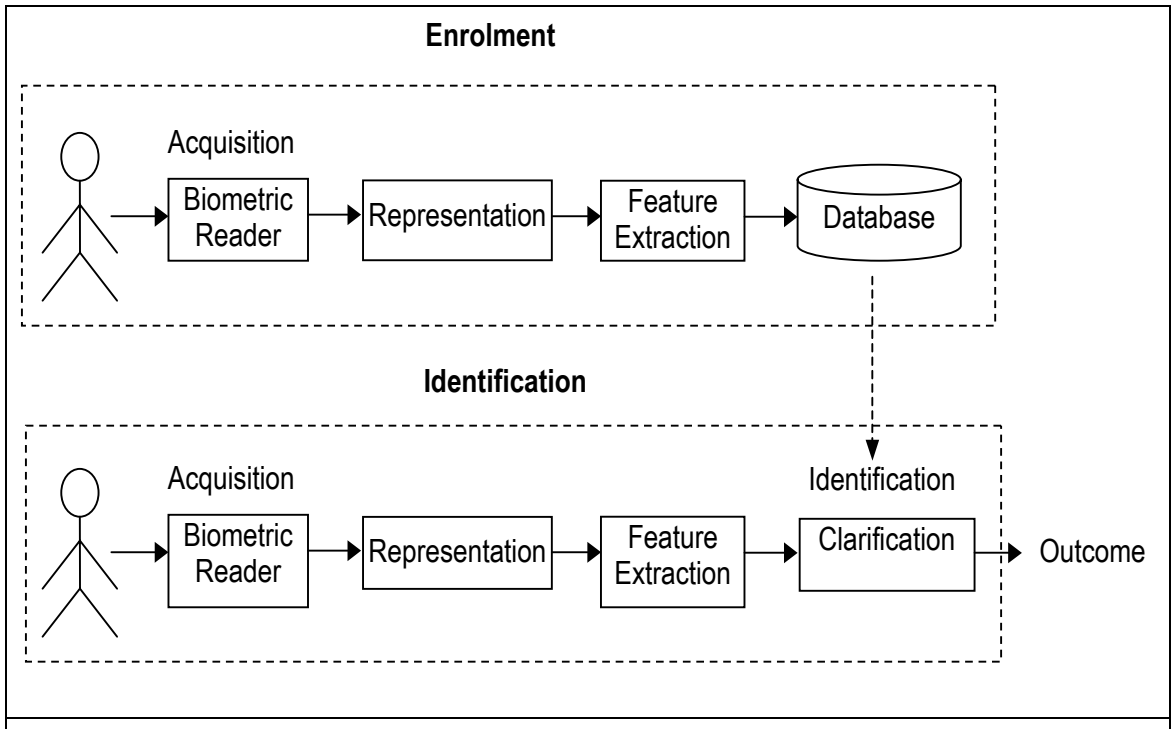

Figure 1.1: Architecture of a typical biometric system.

Figure 1.1 illustrates the architecture of a typical biometric system. This system consists of four vital interdependent components: *acquisition*, *representation*, and *feature extraction* (in both the *enrolment* and *identification* mode), and *classification* (in *identification* mode only).

(i) Acquisition

Often, acquisition will affect the performance of the system. This concerns the quality and suitability of the input data and also the segmentation process. Here, the biometric reader is a digital video camera and the data acquired is a sequence of digital images capturing a moving person. The separation of the *input data* from *irrelevant information* is critical. *Input data* in computer vision generally refers to an object of interest whilst *irrelevant information* often refers to the background. In our approach, as we shall see later, the desired object is the moving thigh and lower leg described by edge information. However, the 'ultimate' *input data* is the angular motion of the thigh and lower leg (desired information for creating the signature vector), while *irrelevant information* is the complement of that (such as the background and noise, or even any moving or articulating objects that do not move like human lower limbs).

(ii) Representation

Given a complex digital representation, in this case, a sequence of digital images, a system must be able to automatically extract desired features or objects and describe them by some (hopefully meaningful) representation. Furthermore, this representation should be common across the population, and yet unique on an individual basis. As human locomotion is all about dynamic characteristics, the angular motion of the lower limb is extracted automatically and the angles will be a meaningful representation, rather than intensity values of a series of digital imagery. An efficacious acquisition technique should extract only the dynamics of the human lower

limb and not just any moving object, for example, a pair of articulating chopsticks is not desired!

(iii) Feature extraction

Feature extraction is the essence of the entire system. Promising features for recognition are representations that differ minimally for the same identity (minimum intra-class variance), and differ maximally for those belonging to different identities (maximum inter-class variance). At this stage, important information from a series of images have been reduced and represented by the motion angles. In our approach, Fourier magnitude and phase are used to describe the spatio-temporal characteristics, the essence of human unique walking and running dynamics. Thus, these features are used to form the gait signature for identification purposes.

(iv) Classification

Classification is eventually a similarity function which quantifies the difference between two instances of measurements to associate the test data with a possible class within a database, or to reject the test data if the similarity measurement is below a threshold. This is effectively an identification process. Here, a basic and simple classifier has been employed in attempt to reveal the genuine discriminatory capability of the selected feature sets.

1.2 Gait as a Biometric

Before asking the question why gait is well suited as a biometric, let us define what is gait. Gait is defined as a particular manner of locomotion. Recall that the criteria of a biometric are *universality*, *uniqueness*, *permanence* and *collectability*. Gait is *universal* as every normal person does move on foot. As yet, there have been few studies providing quantitative measurements on the *uniqueness* of gait. Nevertheless, encouraging experimental results from many gait recognition techniques (most using

walking gait) do suggest that gait is indeed unique. Furthermore, this is supported by medical and psychology observations. However, the *permanence* of gait is not as enduring as other biometrics such as fingerprints. Gait will change with age [Samson'01], that is a child's gait is different from an adult's gait, whilst an adult gait is yet different from an elderly person's gait. Besides, gait may be affected by mood [Bader'99], drunkenness, pregnancy [Foti'00], disease (e.g. Parkinson's), footwear and load [Zwick'98]. However, these factors do not hinder an attempt to unleash the potential of human locomotion as a means of identification. In practice, gait may not be as prominent as other established biometrics such as fingerprints, though, it can be used together with other biometrics to achieve demanding performance or to act as an identity filter in a large population. Since CCTVs are not unusual in today's society (there are approximately 200,000 CCTV in the UK and this number is increasing), gait as a biometric will have no difficulty in gaining public acceptance. Furthermore, recognition by the way one walks has least impact on privacy issues, unlike one's DNA.

Any biometric has its strengths and limitations, which often concern application and social issues. Whether a particular biological characteristic is a valid biometric is dependent upon the requirement of a given application. Fingerprint, iris and retinal patterns may enjoy uniqueness across large populations, but can be difficult to collect, as they require substantial co-operation from the subjects. On the other hand, face, ear and signature can be easily acquired, but they may be easily obscured or disguised. Gait may have the potential to overcome these limitations. One of the unique advantages of using gait as a biometric is that it can be perceived from a distance, making acquisition non-invasive and convenient. Biometrics such as the iris and retinal patterns and face require high resolution images but surveillance cameras are often of poor resolution. Gait will not suffer from this shortcoming because the body has a proportionally larger area compared with the eyes or face. Furthermore, gait cannot be easily disguised without impeding one's natural gait (which will only attract attention). Thus, gait appears to be a potential biometric.

1.3 Allied Research

```
CASSIUS: 'Tis Cinna; I do know him by his gait;
         He is a friend.
         [Enter CINNA]
                  Julius Caesar - W. Shakespeare
```

There is considerable evidence in the literature that humans have the natural ability in recognising friends by the way they walk; psychological studies confirmed that we can discriminate the gender of a walker [Kozlowski'77]. We can also recognise ourselves and acquaintances by a dynamic light display of the walking pattern [Cutting'77] without familiarity cues. It is suggested that gait could be used as a reliable means of discriminating individuals, especially when the face is obscured [Stevenage'99] because individuals show unique characteristics in their walking mechanics [Bianchi'98]. Thus, not only walking gait patterns display individual uniqueness, but also gender and age differences. Studies of human locomotion found that male walkers tend to swing their shoulders more while female walkers tend to swing their hips more [Mather'94]. Recently, the walking styles of children and adult have been categorised via computer vision techniques [Davis'01].

1.4 Current Approaches

Human motion analysis has gained increasing attention from computer vision researchers motivated by a wide spectrum of applications such as surveillance, medical, man-machine interface and animation. The major areas of research are motion analysis [Akita'84, Chen'92], tracking [Cai'96, Polana'94], recognizing biological motion [Boyd'97, Campbell'95], and as an emerging biometric. Investigation on gait as a biometric only began less than a decade ago. Perhaps the earliest work derived a gait signature from a spatio-temporal pattern of a walking person for recognition purposes [Niyogi'94]. Murase et. al. projected images of human walking in eigenspace and used the eigenvectors for gait recognition [Murase'96]. Then, dense optical flow [Little'98] was exploited where an instantaneous motion description that varies with the type of

motion and the moving objects was developed. Huang combined canonical space transformation based on Canonical Analysis with eigenspace transformation for feature extraction to extract a gait signature [Huang'99]. The potential of image self-similarity [Abdelkader'01], area-based metrics [Foster'01], static body parameters [Johnson'01], velocity moments [Shutler'01] and symmetry [Hayfron-Acquah'01] have been used to generate gait signatures. Recently, stride and cadence has been investigated as gait parameters for recognition [Abdelkader'02], besides, continuous Hidden Markov Models have been applied to explore the structural and transitional characteristics of gait [Kale'02]. Gait recognition is not only limited to the computer vision community, another medium, an in-air sonar-based method, has been deployed in recognising walking people [Sabatini'98]. Gait can also be combined with other more established biometrics such as face [Shakhnarovich'01] or fingerprint to further improve performance. Current approaches discussed so far are mainly based on statistical measurements. A statistical approach assumes a statistical basis to describe whole body motion for pattern classification. This approach may not have in-built knowledge of the gait pattern or characteristics, and may require much training to achieve good performance.

However, the significant information in (or the characteristics of) a gait pattern is not merely the presence, or even the numerical values of a set of features. Rather, it is the interaction and inter-relationship of the structural description. In a model-based approach, one must be able to quantify and extract structural information, and access the structural similarity of the gait. It is a formulation of a hierarchical description of a more complex system that is built up from primitive attributes. For example, a human lower limb resembles a pair of articulated sticks joined at a point. Biological modelling is exceptionally intricate, partly because nature has infinite variations and there are numerous (uncontrollable) factors, both internal (the human body itself) and external (e.g. the environment) to be considered. Although there exist methods for modelling human walking, these have not been deployed for identification purposes. Perhaps, the only model-based approach in human gait recognition was pioneered by Cunado and Nash who explored the potential of the Velocity Hough Transform (VHT) [Nash'97]

and simple pendular motion described by a Fourier series [Cunado'99a]. This approach models human walking as a pendulum representing the thigh, with the fulcrum at the hip joint. It combines the VHT with a Fourier series to extract the motion of the hip and thigh within a gait cycle. The gait signature is then derived from the Fourier series. Visually, leg movements during walking and running resemble a compound pendulum, that is the leg periodically swings at a fulcrum. Thus, adapting pendular motion to model human locomotion is natural. This idea has also been elaborated by the biomechanicists into two directions [Zatsiorky'94]: i) leg movement as *free oscillation*, and ii) leg movement as *forced oscillation*. As discussed, both the statistical- and model-based approaches demonstrate encouraging results and undoubtedly, more techniques are emerging.

1.5 Next Questions

Until now, a considerable amount of research has focused on human walking, with encouraging results confirming the potential of using walking gait as a biometric. This leads to a question on whether human running gait can offer equivalent, if not better, quality for identifying people. Although walking and running are distinct gaits as defined by biomechanics, interestingly, it has been demonstrated that there occur topological similarities in the co-ordination patterns between the thigh and the lower leg in walking and running, which co-existed with functional differences throughout a gait cycle [Li'99]. The next question is: can these two distinct gaits be described by the same structural motion model incorporating their inter-dependency? Since walking and running are intimately related by the skeleto-muscular structure, there must exist some correlation between them. The next irresistible question is: can we, (or how can we) describe this intimate relationship?

1.6 Objectives

Our objective here is to develop a new approach for an automated non-invasive model-based human identification system by walking and running. We will need to extract a series of measurements of leg motion by computer vision techniques, taking

into account spatial and temporal properties. In order to do so a model invariant to gait mode, as such able to describe both walking *and* running, is essential. Meaningful labelling associating the unique pattern of walking and running is significant in order to achieve a convincing recognition rate. As walking and running are intimately related, we aim to seek the relationship between these two distinct but systematically related gaits and attempt to create signatures that are invariant to these gaits. Furthermore, generalisation capabilities such as immunity to noise, resolution, and camera view angle shall be incorporated into the approach.

1.7 Contributions

The major contributions to this area of biometrics research are as follows:

1. A novel approach to an **automated non-invasive person recognition system** has been developed using computer vision techniques. We have explored the potential of using walking and running gaits as biometrics, with running gait being more potent [Yam'02b].

2. Two new motion models invariant to walking and running have been developed based on the concept of pendular motion and the biomechanics of human locomotion: firstly a **bilateral symmetric** model [Yam'01] and secondly a **forced coupled oscillator** model [Yam'02a]. These models can be extended, if necessary, to describe both legs simultaneously by introducing a phase-lock of a half a period.

    a. The **bilateral symmetric** model which requires only 13 parameters (in implementation) is capable of describing both the thigh and the lower leg motion of walking and running. This model requires fewer parameters as compared with the earlier model [Cunado'99b] which demands 18 parameters to describe only the thigh motion for walking. The thigh motion is described by a simple harmonic motion whilst the lower leg rotation is empirical and therefore, selection of one parameter

is necessary for different gait modes. This model can extract the motion of both gaits well when used as the underlying temporal template within a feature extractor.

b. The **forced coupled oscillator** model consists of two pendula: an upper pendulum with a simple harmonic motion representing the thigh, and a lower pendulum (which is influenced by the force introduced by the upper pendulum) representing the lower leg. Despite the gait mode, this model is capable of capturing the motion of the thigh and lower leg distinctly well as compared to that of the bilateral symmetric model when used within the feature extractor. Furthermore, this model does not require any parameter selection.

3. The **gait signature** is formed by multiplying the corresponding phase and magnitude components of the Fourier description, yielding a phase-weighted magnitude spectrum. It proved to be a useful representation achieving higher discriminatory capability as compared to using magnitude components alone. As human locomotion is defined by *kinematics* (range of joints' motion) and *kinetics* (forces that cause the motion), and the fact that it satisfies spatial- and temporal-symmetry, magnitude and phase, together play a significant role in describing the dynamics.

4. Statistical measurements and performance analysis show that the **knee rotation** contributes significantly to discrimination capability as compared with the thigh rotation. This could be due to the fact that knee rotation has more variations across the population and also the range of motion is of a relatively greater magnitude. Furthermore, it is also demonstrated that the class separation within the signature space of running gait is higher then that of walking, and this effect is reflected in the performance analyses. Therefore, **running** gait is a more potent cue for recognition. This is also supported by biomechanics observations that there are several styles of running. Performance analyses show that this biometric approach which uses the **forced coupled oscillator** as the underlying

temporal template outperforms the one that uses the bilateral symmetric model by an average increase of 15.2% and 10.6% recognition rate (on a dataset of 20 subjects and 6 samples for each subject) for the cases of running and walking, respectively. Also, this approach can tolerate various application issues including **noise** and **resolution**. Moreover, it can classify not only individual, but also **gender** and **gait mode**.

5. A novel method employing the concept of phase-modulation has been found useful in describing the unique relationship of an individual walking and running patterns [Yam'02c]. This **unique mapping** also provides a convenient means of transforming one gait mode to the other. Gait signatures are made invariant to gait mode by exploiting this transform. The mapping, which can capture the motion features of both gaits, is highly unique across the population, achieving perfect classification rates (in this dataset). This can be used as a condensed form of signature, or to buttress the original gait signature.

6. A neural network has been employed to investigate the existence of a generic relationship between the walking and running patterns across a population. Observations do suggest that this **generic mapping** may exist. However, due to the size of this dataset, conclusions are that the structure of such a relationship could not be drawn.

7. The automated evidence gathering extraction technique successfully extracted the angular motion of both the thigh and the lower leg within the range of -50^{o} to 50^{o} **camera sagittal view angle**. More importantly, the Fourier description of the lower limb's dynamics are found to be linearly related to the camera sagittal view angle. Interestingly, both the magnitude and the phase change is symmetric about the fronto-parellel view. Thus, gait signatures can be made invariant within a limited range of sagittal view angle by exploiting this linear transformation.

8. The new feature extraction technique together with the human locomotion model has been found beneficial in aiding automated non-invasive and markerless leg motion extraction for **clinical application** [Yam'02d].

1.8 At a Glance

Chapter 2 reviews the biomechanics of walking and running gaits while **Chapter 3** illustrates the data acquisition phase and feature extraction. **Chapter 4** reveals the development of the bilateral symmetry and forced coupled oscillator model describing the angular motion of human walking and running gaits and the comparison of both models. Also, the relevancy of using pendular motion in describing human motion is drawn. **Chapter 5** illustrates the creation of the gait signature, the classification process, performance analyses under various conditions, and the significance of lower leg rotation in discriminating between individuals. **Chapter 6** explores the relationship of individuals' walking and running gaits, and also the generic relationship of a population's walking and running patterns, whilst **Chapter 7** investigates how the camera sagittal view angle is related to the gait signature and how the signature is made view angle invariant. Last but not least, **Chapter 8** draws the conclusions and discusses future work beside suggesting possible deployment of these new findings in other areas.

Chapter 2 : Human Gait

Gait is a manner or a particular way of locomotion. Humans and humanoids have been walking and running for thousands of years, and it is critical for survival and evolution. Yet, only recently have we had the tools to study human locomotion scientifically. This chapter will introduce some early studies of human locomotion and the biomechanical similarities and differences between walking and running, which form the essential foundation of this work. Besides the pattern of human gait, some possible gait parameters for deployment in biometrics are also discussed.

2.1 Early Studies of Human Locomotion

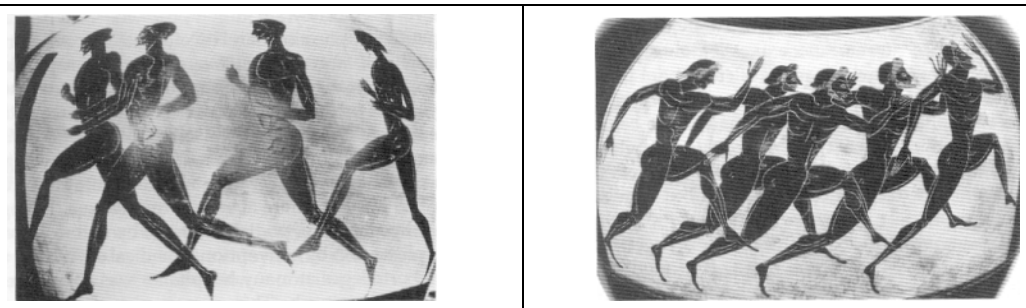

(a) (b)

Figure 2.1: Ancient Greek illustration depicting the difference of (a) running and (b) sprinting gait with individual uniqueness.

Even 2500 years ago, the study of human locomotion (sprinting, running and walking) was reflected in ancient Greek art, see **Figure 2.1**. There is a rich treasury of illustrations which depict the differences between sprinting, running and walking as well as the variations among different individuals. Aristotle (384-322 B.C.) was the first person to study the gaits of animals, including that of humans. He observed that when one walks, the gait is symmetric and the body moves in an undulating manner. His observations read

> " … for just as tall men walk with their spines bellied (undulated) forward, and when their right shoulder is leading in a forward direction their left hip, rather inclined backwards, …"
>
> Part 7, On the Gait of Animals – Aristotle

> " If a man were to walk parallel to a wall in sunshine, the line described by the shadow of his head would be not straight but zigzag, becoming lower as he bends, and higher when he stands and lifts himself up."
>
> Part 7, On the Gait of Animals – Aristotle

Artists have also shown interest in human locomotion. Leonardo da Vinci (1452-1519) was aware of the complexity of human movement and the difficulties in studying gait without appropriate tools such as photographic equipment. He observed and illustrated the principles of human motion in order to accurately represent human locomotion activities in his paintings. He also observed that the anatomy of the human body is symmetric and that the need to maintain balance while moving is essential, as depicted in **Figure 2.2**.

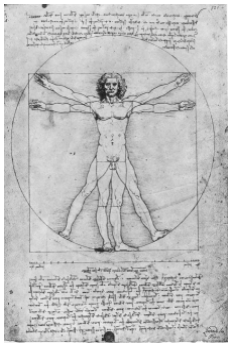

(a)

(b)

Figure 2.2: (a) Illustration of human body symmetry and (b) a fragment of a variety of human locomotion. ***From Leonardo da Vinci's Elements of the Science of Man (pp 175) by K.D. Keele, 1983, New York: Academic Press.***

Then, the study of human locomotion was revisited by Borelli (1608-1679) [Cavanagh'90] who was interested in the mechanical principles of locomotion, representing the starting point for the study of biomechanics of locomotion. Later, the Weber Brothers (1836) investigated human gait, both walking and running with simple instrumentation, and suggested that the lower limbs act like a pendulum. However, these awaited scientific justification. More advanced mathematical techniques and reliable instrumentation were necessary to probe into the study of locomotion. Muybridge (1830-1894) was the first to employ photographic techniques extensively to record locomotion, see **Figure 2.3**. These quality sequential images allowed researchers to scrutinise the motions and counter-balance the inadequacy of the human eye. This offers new insights for scientists in studying human locomotion.

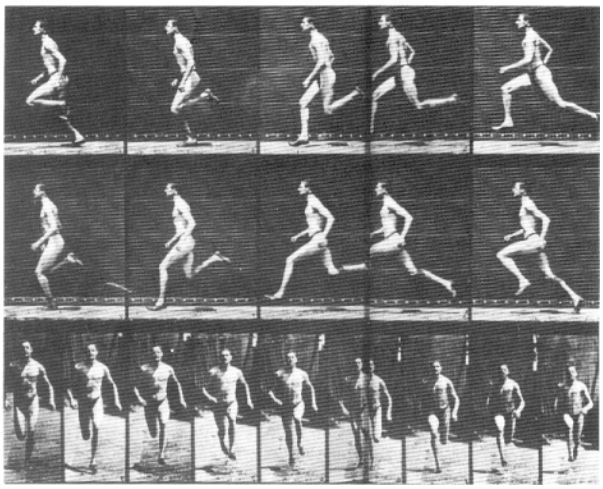

Figure 2.3: A plate from Muybridge's image sequences showing a man running at a distance pace. ***From The Human Figure in Motion (plate 18) by E. Muybridge, 1955, New York: Dover.***

Nevertheless, gait has only been quantified very recently. Murray was the first to characterise walking gait for pathologically normal men and women [Murray'67, Murray'64, Murray'70]. Simultaneous displacements of walking patterns are obtained by interrupted-light photography where the subjects are attached with reflective markers at specific anatomical landmarks. This marked the beginning of systematic scientific studies of human locomotion employing more sophisticated tools and techniques.

2.2 Biomechanics of Walking and Running

Gait is known as one of the most universal and yet one of the most complex forms of all human activities. This rhythmic motion involves a high level of interaction between the central nervous system and various muscles. Functional and independent locomotion entails the ability to *(i)* support the upright body; *(ii)* maintain balance in the upright position; and *(iii)* execute the stepping movement. *The Encyclopaedia of Science and Technology*, volume 2 (pp 699-702), defines *biomechanics* as the field that

combines the disciplines of biology and engineering mechanics and using the tools of physics, mathematics and engineering to quantitatively describe the properties of biological materials. The biomechanics of locomotion can be studied in two different lights. *Kinematics* is the description of motion of joints but does not consider the forces that cause the actions. *Kinetics* is a study of the internal forces (e.g. muscle forces) and external forces (e.g. ground reaction forces) that cause those movements. Here, we are more interested in *kinematics* rather than *kinetics* in describing gait as we are only concerned with the output of this biomechanical system. That is, computer vision sees nothing more than the appearance!

Running is a natural extension of walking, with significant biomechanical differences [Ounpuu'94, Thordarson'97]. The running cycle, however, is not solely discriminated from walking by velocity; you cannot just walk fast to claim that you are running! By biomechanics definitions, walking and running are distinguished firstly by the *stride duration*, *stride length*, velocities and the range of motion made by the limbs. That is, the *kinematics* of running differs from that of walking where the joints' motion increases significantly as the velocity increases. A second difference concerns the existence of periods of *double support* or *double float*. This is determined by the duration of the *stance phase*. A *gait cycle* is divided into the *stance phase* and the *swing phase*, which usually comprises approximately 60% and 40% respectively of a normal walking cycle, see **Figure 2.4(a)**. A normal walking gait cycle may also be described in terms of *double support* and *single support*. On the other hand, there are two periods of *double float* in running, see **Figure 2.4(b)**. *Double float* is when neither foot is in contact with the ground, which can also be seen clearly on **Figure 2.3**. Therefore, for running, the *stance phase* must be less than 50% of the *gait cycle* and correspondingly, the *swing phase* must be more than 50% of the *gait cycle* (i.e. the remainder). The duration of the *stance phase* and the *swing phase* depends on the running velocity. The *stance phase* duration is inversely proportional to the velocity while the duration of the *swing phase* is proportional to the velocity. Unlike walking, there are several manners in which the foot contacts the ground. During walking, the heel contacts the ground followed by a foot-flat stance. For running, the majority

(approximately 80%) of runners (rear foot or heel strikers) make initial ground contact along the posterolateral border of the foot while the minority (midfoot striker) initially contact the ground with the midlateral border of the foot. This will give a range of variation in running patterns. One interesting point to note is that the range of motion of the hip increases as the progression speed increases in the case of walking, but it decreases in the case of running [Hreljac'95].

Interestingly, there exist some similarities between these two distinct gaits under certain conditions. Li et. al. compared the co-ordination patterns of walking and running at similar speed and *stride frequency* [Li'99]. They observed that under similar speed and *stride frequency*, there occurs topological similarities in the co-ordination patterns between the thigh and the lower leg in walking and running. These co-exist with functional differences throughout the gait cycle, especially in the transition from the *stance* to *swing phase*. The thigh and the lower leg co-ordination pattern for running and walking is quite similar except between 20% - 40% of the gait cycle. They also observed that during walking, the thigh swings forward at toe-off, but it swings backward during running.

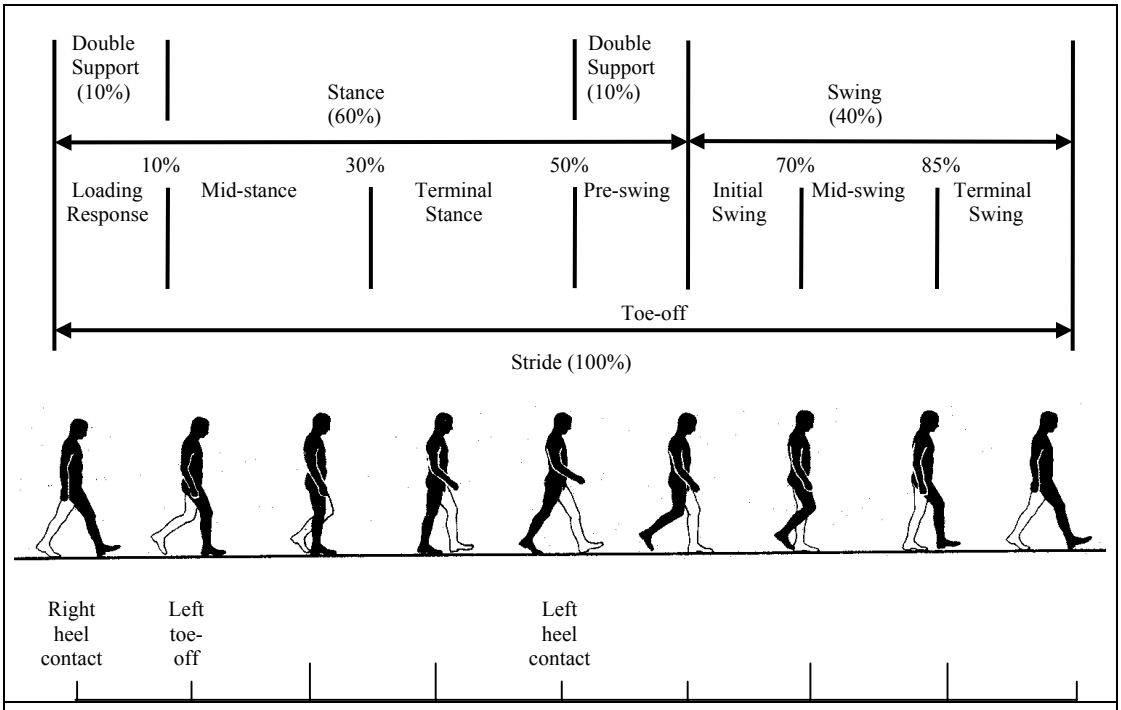

(a) Gait cycle and terminology used for walking.

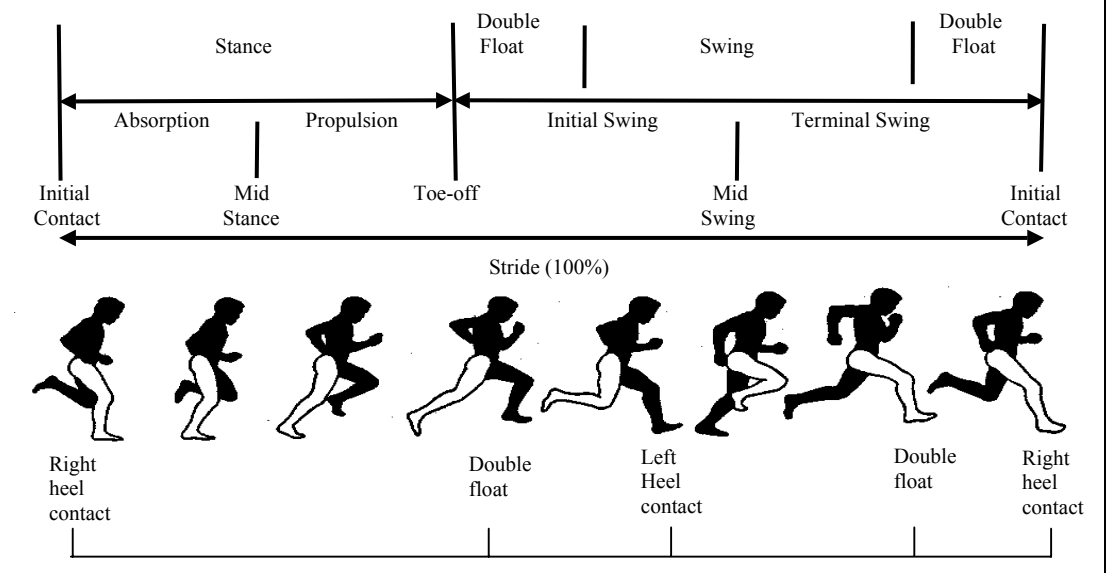

(b) Gait cycle and terminology used for running.

Figure 2.4: Comparison of the gait cycle for walking and running. [Ounpuu'94, Thordarson'97]

2.3 Gait as a Pattern of Movement

Gait has a composite set of consistent characteristics or style for an individual, and is rhythmic and periodic. Therefore, gait is a pattern of movement. This section illustrates the variability for multiple simultaneous patterns of the angular motion of human lower limbs while walking and running. **Figure 2.5** shows manually labelled sample data obtained from a particular subject for a gait cycle. When a person walks or runs, there are vertical and forward hip motions. In our case, the overall forward motion is not our concern due to the data acquisition process and also the technique used for the feature extraction which will be described in **Chapter 3**. **Figure 2.5(a)** shows the hip's vertical oscillation relative to the average vertical motion. The body (or trunk) oscillates through two vertical peaks and two valleys in each cycle as one gait cycle consists of two steps. The peaks and the valleys are dependent on the lower limb's positions. When walking, the valleys occur during the *double support* phase and the peaks occur during the *single support*, that is, when the body and the lower limbs are upright. Interestingly, the shape of the graph for walking is a phase shifted version of that for running. During running, the valleys occur during *heel strike* while the peaks occur during *double-float*. **Figure 2.5(b-c)** shows the absolute angles of the thigh and the lower leg rotation, respectively, for a gait cycle of a particular subject. As depicted, the range of the joint's motion increases when running, as discussed in the previous section.

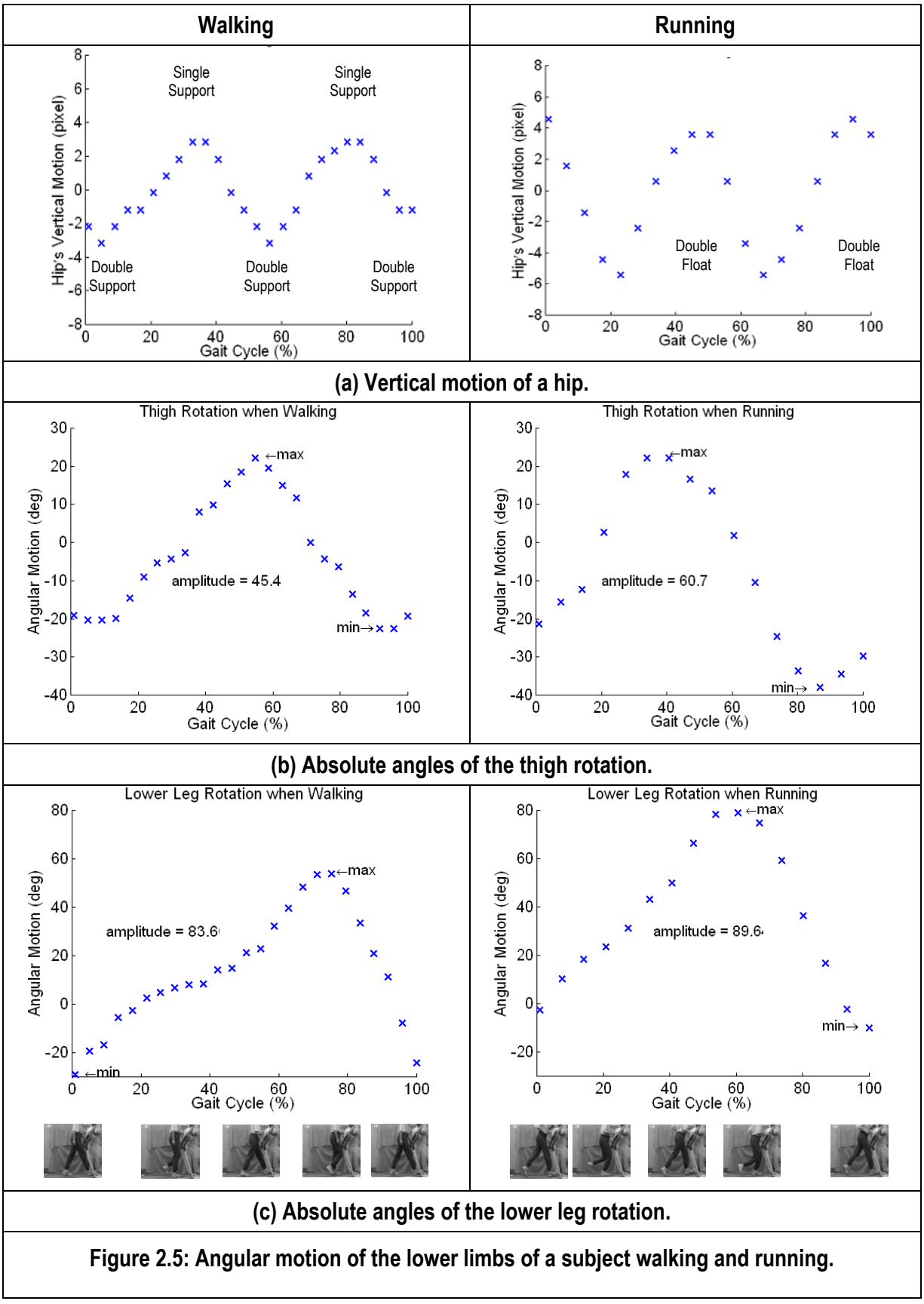

Figure 2.5: Angular motion of the lower limbs of a subject walking and running.

Human locomotion is naturally rhythmic producing a co-ordinated oscillatory behaviour [Stewart'99] which is believed to be controlled by a Central Pattern Generator. Gait not only satisfies *geometrical symmetry* (step length is similar for both heel strikes) but also *dynamical symmetry* (the frequency content of both lower limb's motion is similar). As the consequence, these motions which operate in space and time, satisfy the rules of *spatial symmetry* (sequence of oscillation, i.e. swapping legs and arms) and *temporal symmetry* (generally a phase-lock of half a period).

One of the unique characteristics of walking and running is *bilateral symmetry*, which gives the name of our first motion model. It means symmetry of left and right, or, if there exists some reflection that is invariant. That is, when one walks or runs the left arm and right leg interchange direction of swing with the right arm and left leg, and vice versa, with half a period phase shift. To further illustrate the bilateral symmetry of walking and running, **Figure 2.6** shows a support graph (where the dots represent which foot is in contact with the ground) of these gait patterns. Unsurprisingly, the second half of the gait cycle is a reflection (about the midpoint of the cycle) of the first half for both the cases of walking and running.

●		●	●
●	●	●	

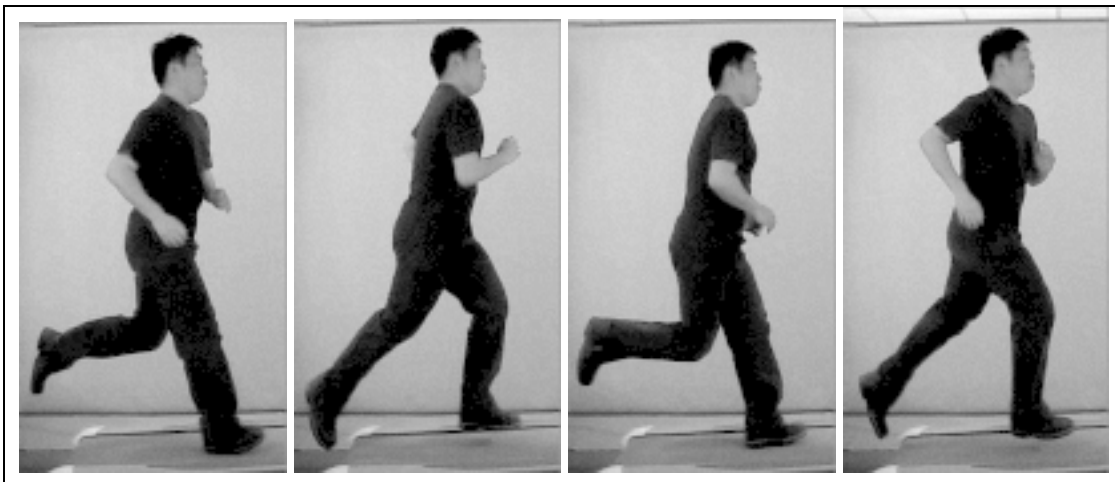

		•	
•			

Figure 2.6: Support graphs illustrating bilateral symmetry in walking and running gait patterns.

Figure 2.7 shows the manually labelled absolute angles of rotation for the thighs and lower legs. This shows that the motions of the left and right leg are coupled by half a period phase shift. However, this is only a generalisation for normal gait. Gait symmetry or asymmetry is still in debate [Sadeghi'00] and could be of significant importance for clinicians. As our purpose is to develop a model to guide a biometric system in extracting leg motion, gait symmetry can be assumed. Hence, if necessary the same model can be extended to describe both legs simultaneously as both perform the same motion but with a phase-lock of a half a period. If one's gait is lack of symmetry, or when symmetry is of great importance, then both legs can be modelled by two distinct but systematically coupled oscillators (with fixed relative phase difference).

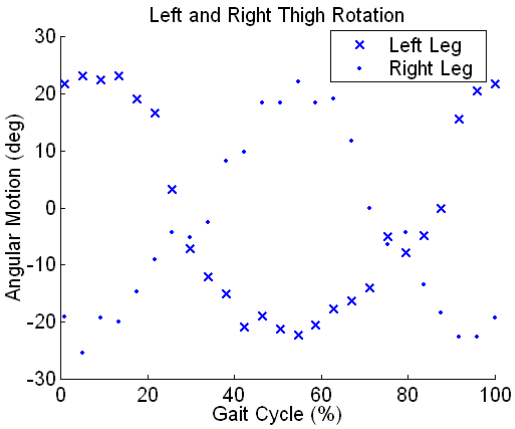

(a)

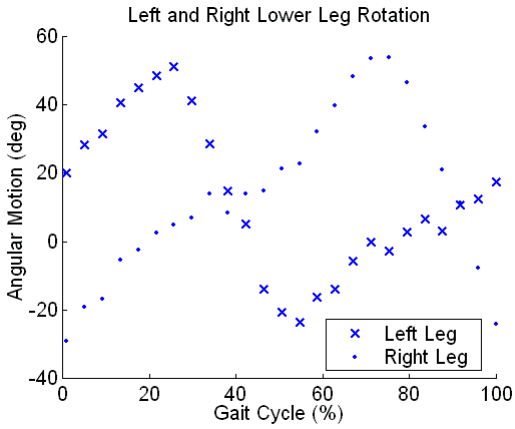

(b)

Figure 2.7: Thigh and lower leg rotation of the left and right leg.

These together form the foundation for the development of the new human locomotion models (described in **Chapter 4**), which serve as the basis for the novel automated non-invasive person recognition approach.

2.4 Gait Parameters for Recognition

Although there are extensive studies on the biomechanics of human locomotion, they have been mainly interested in understanding motions for sports injury and efficiency, and not for recognition purposes. For a gait biometric system to be efficacious, gait parameter selection is critical as they have direct impact on the performance. Many characteristics can be derived from human locomotion patterns. They can be characterised into four categories:

(i) *Kinematics*

Any characteristic that is caused by *kinetic* factors such as hip, knee and ankle angular rotation patterns, body/trunk ambulation, step length, step width, speed etc.

(ii) *Kinetics*

Any characteristics such as forces, moments or torques acting on a body.

(iii) *Dynamics*

Any characteristic (usually derived from kinematics and kinetics characteristics) that entail continuous changes such as symmetry of the limbs' angular motion, ambulatory velocity etc.

(iv) *Physiological*

Any quantifiable biological characteristics such as body height, leg length etc.

Recently, various gait parameters have been used for identification purposes. Some examples are cycle time, stance/swing ratio and double support time [Davis'02]; and stride and cadence [Abdelkader'02]. Here, we are concentrating on dynamic characteristics, owing to the fact that gait operates in space and time. We favour the thigh and lower leg angular motion to recognise people only by the way they walk or run, rather than by their physiological traits or any static aspects of gait. That is, it is all about motion! Although, computer vision can only perceive appearance which are usually kinematic and physiological features, they can be further manipulated or transformed into a suitable representation to benefit the recognition process.

2.5 Conclusions

The study of gait is not new, it attracts not only scientists, but also artists. However, only recently have we had the tools and facilities to study gait quantitatively. Although human walking and running are two distinct gaits, as defined by biomechanics, there exist topological similarities in the co-ordination patterns. This encourages the development of a motion model that is invariant to both gaits (**Chapter 4**). Human walking and running patterns are periodic, satisfying *spatial* and *temporal symmetry*. Therefore we favour dynamic characteristics including the thigh and the knee rotation in developing the recognition strategy. Dynamic characteristics of gait facilitate analysis in the frequency domain which benefits the investigation of the correlation between these two gaits (**Chapter 6**) and also the development of unique gait signatures (**Chapter 5**). The following chapter will illustrate the development of the subject dataset and the feature extraction process.

Chapter 3 : Data Acquisition and Feature Extraction

The first stage of a biometric system is the data acquisition followed by the feature extraction. During data acquisition, video clips are taken when the subjects are walking or running on a motorised treadmill. In the first stage, feature extraction is to pre-process the images to simplify the data representation for computational efficiency. Then, an evidence gathering technique which consists of two phases will capture the dynamics of the leg motion within a gait cycle. **Figure 3.1** illustrates the acquisition and feature extraction process.

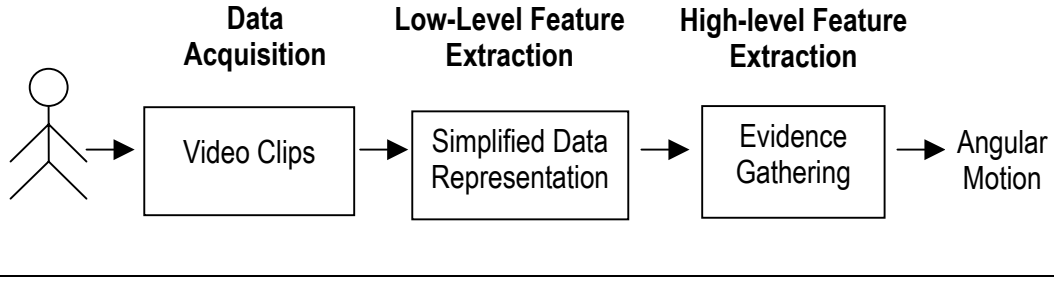

Figure 3.1: Schematic diagram for data acquisition and feature extraction.

3.1 Data Acquisition

There is a wide range of methodologies and equipments available for gait analysis, mainly designed for clinical and laboratory environments. The most common systems are based on electrogoniometry, electromagnetics and imaging.

An electrogoniometer is an electronic device which is fixed to a joint to measure the rotation. Although data can be obtained immediately, the major drawbacks are alignment problems of the device and the joints, and the repeatability of device placement. Some examples of imaging systems are optoelectronics, cinematography and videography. Optoelectronics automate much of the process: they use active markers, such as LEDs which are placed on a subject and are triggered by a computer. However, this system is encumbered by interference from the reflections off the floor and requires complex cabling. The electromagnetic system detects the motion of sensors placed on each segment in an electromagnetic field and can provide real time 6-degree of freedom data. The limitations are complex cabling, large number of sensors and high cost. On the other hand cinematography is more versatile and less sensitive to the environment. The major advantage is that it provides better image quality. The problem that always haunts clinicians is that currently there are few automated systems for quantifying the data. Videography is the most frequently employed approach to automated motion analysis. In clinical environments, this system usually automatically tracks reflective markers. However, the disadvantages are poor image resolution and obstruction and/or movement of markers.

Here, we employed a non-invasive digital videography system which is markerless, eliminating the problem of marker occlusion. Subjects are filmed walking and running on a motorised treadmill in their own choice of clothing, at their *preferred speed*, by a digital video camera. Then, video clips are split into individual image files for pre-processing.

3.1.1 Experimental Dataset

The experimental dataset consists of the fronto-parallel views of 20 subjects, with 6 samples or sequences of each subject. Each monocular image sequence is a full gait cycle, i.e. 2 steps. The dataset is summarised in **Table 3.1.** Various application issues are also incorporated in the dataset for performance analyses. Images are contaminated with 25% salt and pepper grey scale noise to simulate poor quality video, and at half the original resolution (65 × 95) for performance analyses. This dataset has more subjects than some previous studies in gait recognition [Cunado'99a, Huang'99] and is the first to contain the same subjects walking and running. Subject's enrolment is chosen randomly.

Attribute	Range	Mean	Standard Deviation
Age (years)	22 – 45	27.4	5.58
Weight (kg)	45 – 100	67.0	13.78
Height (cm)	156 – 192	171.1	8.48
Walking Speed (km/h)	2.8 - 5.5	4.35	0.67
Running Speed (km/h)	6.5 - 13.9	9.13	1.84
Gender	5 females, 15 males	-	-

Table 3.1: Summary of the subjects information of the experimental dataset.

3.1.2 Treadmill or Track

Treadmills offer many advantages in human locomotion analysis. Space requirements are constrained, environmental factors can be controlled, steady-state locomotion speeds are selectable, and successive repetitive strides can be documented. The issue of whether treadmills will alter the pattern of walking and running remains a constant topic of discussion among the biomechanics, psychology and rehabilitation communities. One study suggests that walking on an 'ideal' treadmill, when the supporting belt moves with a constant speed, does not differ mechanically from

walking over ground, except for wind resistance, which is negligibly small during walking [Zatsiorky'94]. The only difference between the two conditions is perceptual: the environment is stationary when a treadmill is used [Schenau'80]. However real treadmills are not ideal! Murray found that during treadmill walking, subjects tend to use a faster cadence and shorter stride length than during floor walking. However, in general, treadmill walking was not found to differ markedly from floor walking in kinematics measurements [Murray'85]. Whether a treadmill will affect one's gait will also depend on the habituation of the subjects to treadmill walking [Wall'80]. For this reason, all the subjects were familiarised to the treadmill for at least 15 minutes before measurements were taken. The differences of walking over ground in comparison to walking on a treadmill may be of great importance to the biomechanics community. For our purposes we assume all subjects to be affected equally as they were all filmed under the same conditions. Thus, the features may change, but with respect to one another, these changes are assumed to be subtle. We assume that the general trend and principles apply to all subjects. As subjects tend to look down while walking and running at the treadmill, a mirror was placed in front of the subject, so that they keep their head up and maintain their natural posture but more importantly this aids to maintain stability.

3.2 Feature Extraction

Feature extraction here involves two different levels, one is *low-level* and the other is *high-level*. *Low-level* feature extraction will require no prior knowledge about the shape or structure of the image to extract basic features such as edge information and operates on the basis of a single pixel's (or a small) neighbourhood. *High-level* feature extraction here concerns finding articulated moving shapes by evidence gathering based on a motion template (which will be described in **Chapter 4**). Thus, the two levels of extraction (edge detection and an evidence gathering technique) are used to extract the dynamic features of interest: the angular motions of the thigh and the lower leg.

3.2.1 Low Level Feature Extraction

Video clips are split into individual colour image files (**Figure 3.2(a)**), and then cropped to reduce computational cost. To reduce the complexity of the colour image, the Sobel edge operator is used to obtain the edge information. The Sobel edge detector consists of two masks, M_x (which detects vertical edges) and M_y (which detects horizontal edges) where the coefficients are derived from Pascal's triangle giving the effect of Gaussian smoothing within the template itself [Nixon'02]. A condition, which effectively thresholds the M_x-component's magnitude of the Sobel edge operator (**Figure 3.2(b)**) is applied to obtain the leading edge. If the convolution of the M_x template with the image is bigger than zero, then the edge magnitude is the length of the vector of M_x- and M_y-components. Assuming that subjects are in front of a bright background, this process is applied to the three layers of colour (red, green, blue), see **Figure 3.2(c)**. The edge magnitude of the three layers are then summed and thresholded at 255 (for 8-bit images), to produce prominent edges (**Figure 3.2(d)**). The leading edge is most suited to automated feature extraction because clothing tends to adhere to the front of the moving leg (**Appendix A**). These single-edge images are then passed into the *high-level* feature extractor.

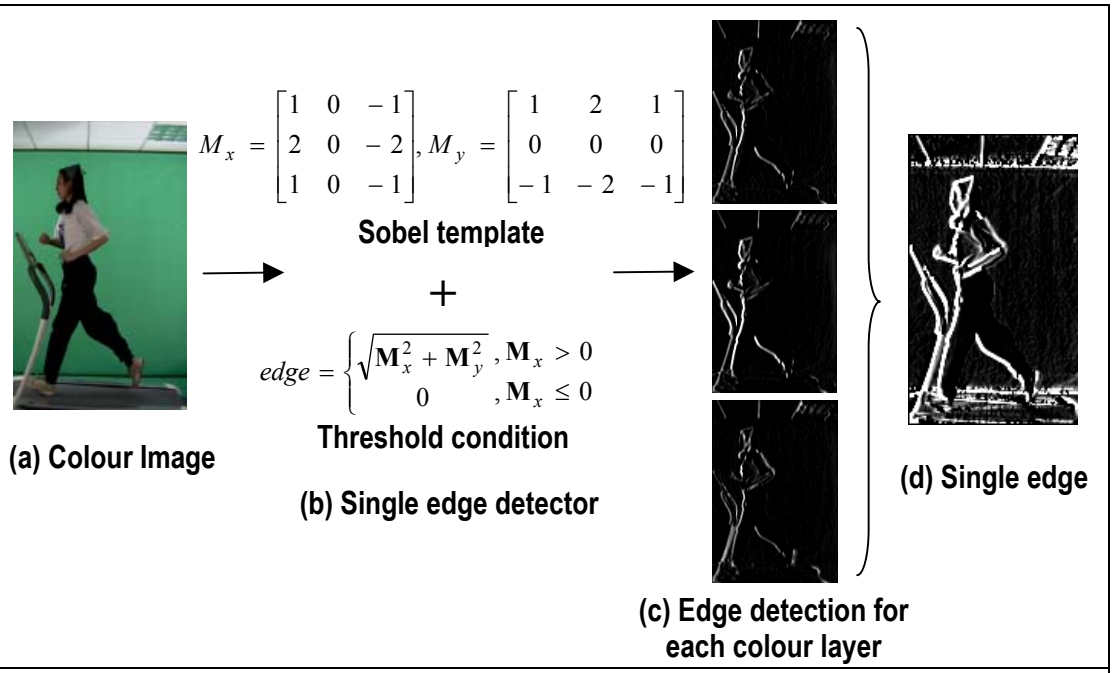

Figure 3.2: Process of transforming a colour image into a single-edge data via the Sobel edge detection with a threshold condition on the M_x- component of the operator.

3.2.2 High Level Feature Extraction by Evidence Gathering

The evidence gathering technique used here comprises two phases: *i) temporal template matching* and, *ii) local template matching*. The aim of *temporal template matching* is to search for the best motion model that can describe the leg motion from global information, i.e. over a gait cycle. That is, this will gather evidence for the best gross motion of a complete gait cycle. Essentially, this process is to match a line which moves according to the structural and motion model (temporal template) described in **Chapter 4**, to the edge maps of a whole sequence of images to find the desired articulating edges of the thigh and the lower leg. This process is described by

$$Temporal\_Template\_Match = \sum_{t \in r} \sum_{i \in x} \sum_{j \in y} \left(P_{i,j}(t) \cap T_{i,j}(t) \right) \qquad \textbf{(3.1)}$$

where P is an x by y image, T is the temporal/motion template, r is the total number of frames and t is the time index. The union operation describes the intersection of the edge points with the template; it is described as evidence gathering since the number of

intersecting points is counted to give the match over the sequence of r frames. A temporal template can be thought of as a sub-image that varies in time in a manner described by a model. That is, a representation of moving objects in a sequence of images embedding the nature of a motion. The idea of using a temporal template in extracting an arbitrary moving arbitrary object [Grant'02] has demonstrated successful results, even in extracting a moving person. The evidence gathering process will accumulate evidence which is essentially the intensity level of the edge maps that fall within the moving template, enabling the calculation of the best set of parameters for the underlying motion model. As an example, **Figure 3.3(a)** shows a slightly distorted simple harmonic motion (SHM), superimposed with the best-fit motion model found using this method. As shown, it attempts to search for the best motion model that resembles the distorted SHM. Having found the best set of parameters for the motion model, the angles for each frame are then generated. The search is refined by employing a *local template matching* technique. This is achieved by searching within a range based on this angle to ensure that the best-fit angle is found in each frame, an example result is shown in **Figure 3.3(b)**. Therefore, any deviation from the norm can be filtered or extracted at this stage. This process is described by

$$Template\_Match = \sum_{i \in x} \sum_{j \in y} \left(P_{i,j} \cap T_{i,j} \right) \qquad \textbf{(3.2)}$$

where evidence is gathered over a single frame, not a sequence.

A similar process is applied to extract the lower limb's angular motion for each subject. **Figure 3.4** illustrates the process of extracting the angular motion of the thigh and lower leg. Each individual will have his/her own norm of motion (extracted by temporal evidence gathering) and unique deviation from the norm (determined by local evidence gathering). *Temporal template matching* will search for the best hip and thigh motion followed by the lower leg motion for each subjects. Once the parameters describing the best gross motion are found, angles of rotation are generated. Then, *local template matching* will search within a range to determine the deviations from each individual's norm. Hence precise measurements can be obtained, which is then used to create gait signature for recognition purposes.

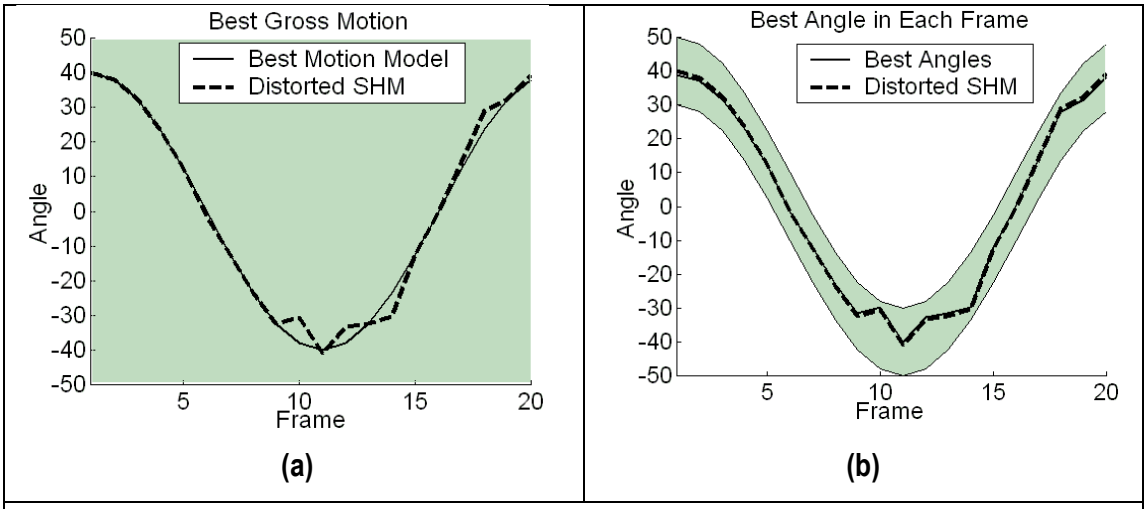

Figure 3.3: Results of (a) temporal template matching and (b) local template matching to search for the gross motion and the deviation from each individual norm, respectively. The shaded area is the search-area.

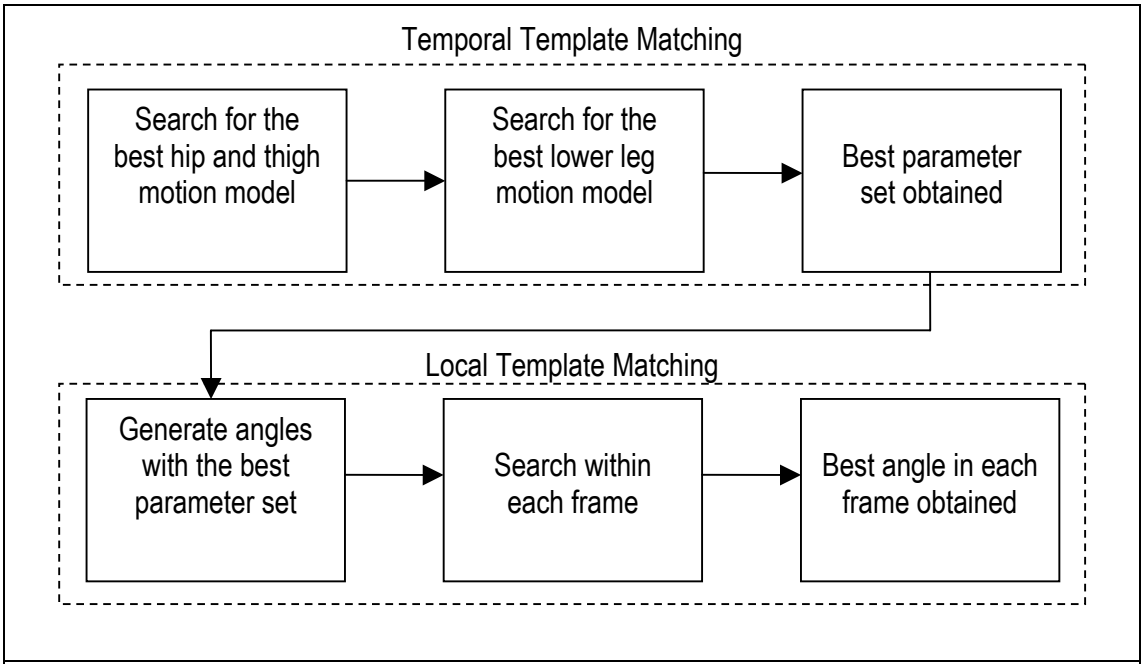

Figure 3.4: Extraction of the lower limb motion.

3.3 Conclusions

A dataset consists of the clean, noisy and low-resolution images of 20 subjects, each with 6 samples of walking and running on a treadmill has been developed. A treadmill was used because it offers various advantages in data acquisition and processing. There are two levels of feature extraction. *Low-level* feature extraction simplifies the raw data to single-edge data by using the Sobel edge detector. Then, *high-level* feature extraction (comprises two processes) is designed to extract the most accurate possible angular motion of the leg from a complete sequence of gait cycle. This *high-level* feature extractor is to be used with an underlying motion model detailed in the next chapter.

Chapter 4 : Describing Motion

The motion model which serves as the underlying temporal template of an evidence gathering technique in feature extraction, is one of the most vital elements in a model-based approach for person recognition by gait. We have developed two new motion models invariant to walking and running: the bilateral symmetric (BS) model and the forced coupled oscillators (FCO) model, each with their unique strengths and limitations. A structural model for the lower limb is also described. Results of feature extraction using these two models are illustrated. The appropriateness of using oscillators as the underlying model for human locomotion is now discussed.

4.1 Motion Models

There are many ways of modelling human leg motion. The most accurate way may be using Fourier series (as this can describe any periodic waveform) but at the expense of complexity and computational cost. Here, we suggest an alternative way to model human locomotion aiming to achieve automated angular motion extraction with reasonable accuracy for the purpose of biometrics via computer vision.

4.1.1 Bilateral Symmetric Model

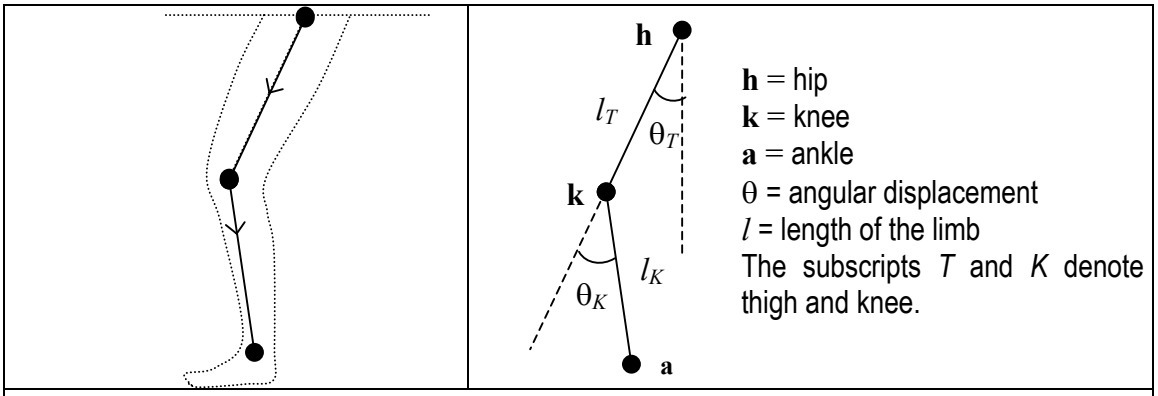

Figure 4.1: Structural model of a lower limb: upper and lower pendulum represents the thigh and the lower leg, respectively, connected at the knee joint.

The bilateral symmetric (BS) model is developed based on the observations of the apparent movement of the human leg. The leg is modelled by two pendula joined in series, as illustrated in **Figure 4.1**. By the biomechanics convention, the knee rotation of this model is relative to the thigh rotation, as opposed to that of the forced coupled oscillator model which will be described in the next section. As subjects are filmed walking and running on a motorised treadmill at constant velocities and the resolution of the images used is relatively low, the horizontal motion of the hip is subtle compared with the other motions, such as the hip's vertical oscillation and the motion of the thigh and the lower leg. The vertical motion of the hip is essential as it differs from walking to running. As depicted in **Figure 4.2**, during running the amplitude of the displacement is greater and has a relative phase shift with respect to that of walking. The motion model for the hip's vertical displacement, S_y, is

$$S_y(t) = A_y \sin(2\omega t + \phi_y) \qquad \textbf{(4.1)}$$

where A_y is the amplitude of the vertical oscillation, ω is the fundamental frequency, ϕ_y is the phase shift and t is the time index for a normalised gait cycle. Since a gait cycle consists of two steps, the frequency is twice that of the thigh motion which will be described later. That is, every time we make a step, the body lowers and lifts, which gives the variations shown in **Figure 4.2**. For visualisation purposes, all the plots are normalised to a complete gait cycle. The superimposed graphs reflect the veracity of this simple model, by comparing the model generated vertical motion of the hip with that of manually labelled data. The structure is clearly identical and agrees with biomechanical studies acquired by other marker-based systems [Murray'67, Ounpuu'94].

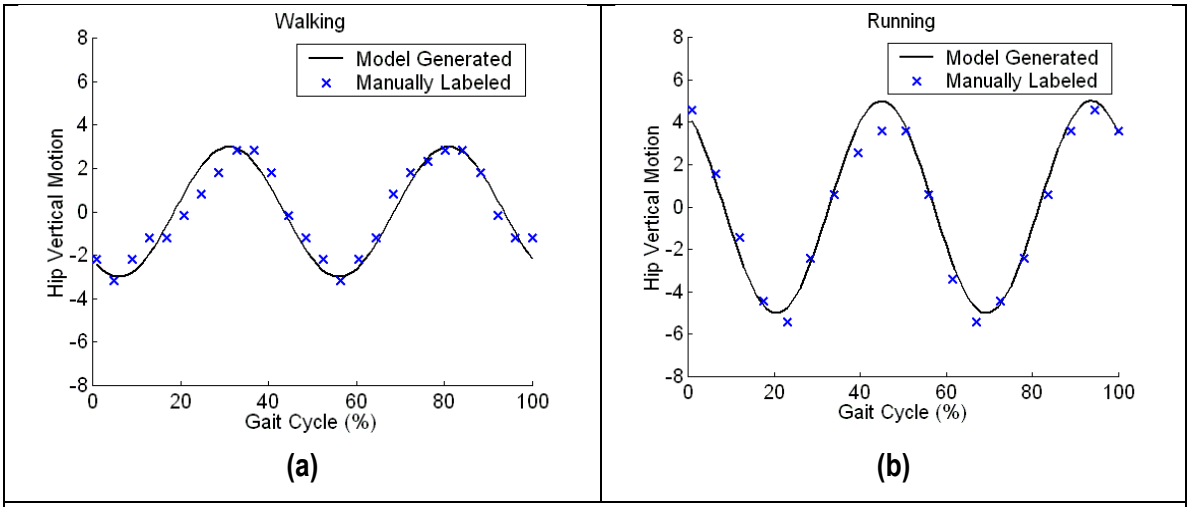

Figure 4.2: Relative vertical displacement of hip during walking and running.

The thigh rotation, $\theta_T(t)$, is a simple harmonic motion described by **Eq. 4.1**, where A_T is the amplitude of the thigh rotation and C_T is the offset.

$$\theta_T(t) = A_T \cos(\omega t + \phi_T) + C_T \qquad \textbf{(4.2)}$$

C_T is important for implementation (but not in describing the dynamics) because when walking or running, the human leg does not move about equilibrium as a normal pendulum does. **Eq. 4.2** can be applied for both running and walking. **Figure 4.3(a-b)**

show the model-generated thigh rotation superimposed on the manually labelled angles for a particular walker and runner, respectively. Results show that the model describes the motion well. Based on observations, the knee rotation, $\theta_K(t)$, can be described as

$$\theta_K(t) = \begin{cases} A_{K1} \sin^2(\omega t) + C_{K1} & ,0 \le t < p \\ A_{K2} \sin^2(\omega t + \phi_K) + C_{K2} & , p \le t < 1 \end{cases} \quad \textbf{(4.3)}$$

where A_{K1} and A_{K2} are the amplitudes of the knee rotation, C_{K1} and C_{K2} are the offsets, ϕ_K is the phase shift and p is the time when the *swing phase* starts. For walking, p appears to be 0.4 whereas p is approximately 0.3 when running. This is because the swing phase starts earlier when running. This also marks the start of the second *double support* and the *double float* for the cases of walking and running, respectively. The $\sin^2$ term models well the basic motion as depicted in **Figure 4.3(c-d)**. However, the knee rotation model requires parameter selection as it is an empirical model. The 13 parameters of interest extracted from the motion models are A_y, ϕ_y, A_T, ϕ_T, A_{K1}, A_{K2}, ϕ_K, p, C_T, C_{K1} and C_{K2}, (where the last three offsets are only important in implementation), and the initial coordinate of the hip's position, $h_x(0)$ and $h_y(0)$ which will be explained in **Chapter 4.2** . This model is able to describe the motion of the thigh and the knee of both walking and running gaits. If necessary, it can also be extended to couple the left and right leg by a phase-lock of a half a period shift. As such, a model achieving fewer parameters as compared with the earlier model [Cunado'99a] which demands 18 parameters only to describe the thigh motion. Again, the results agree well with biomechanical observations [Murray'67, Ounpuu'94].

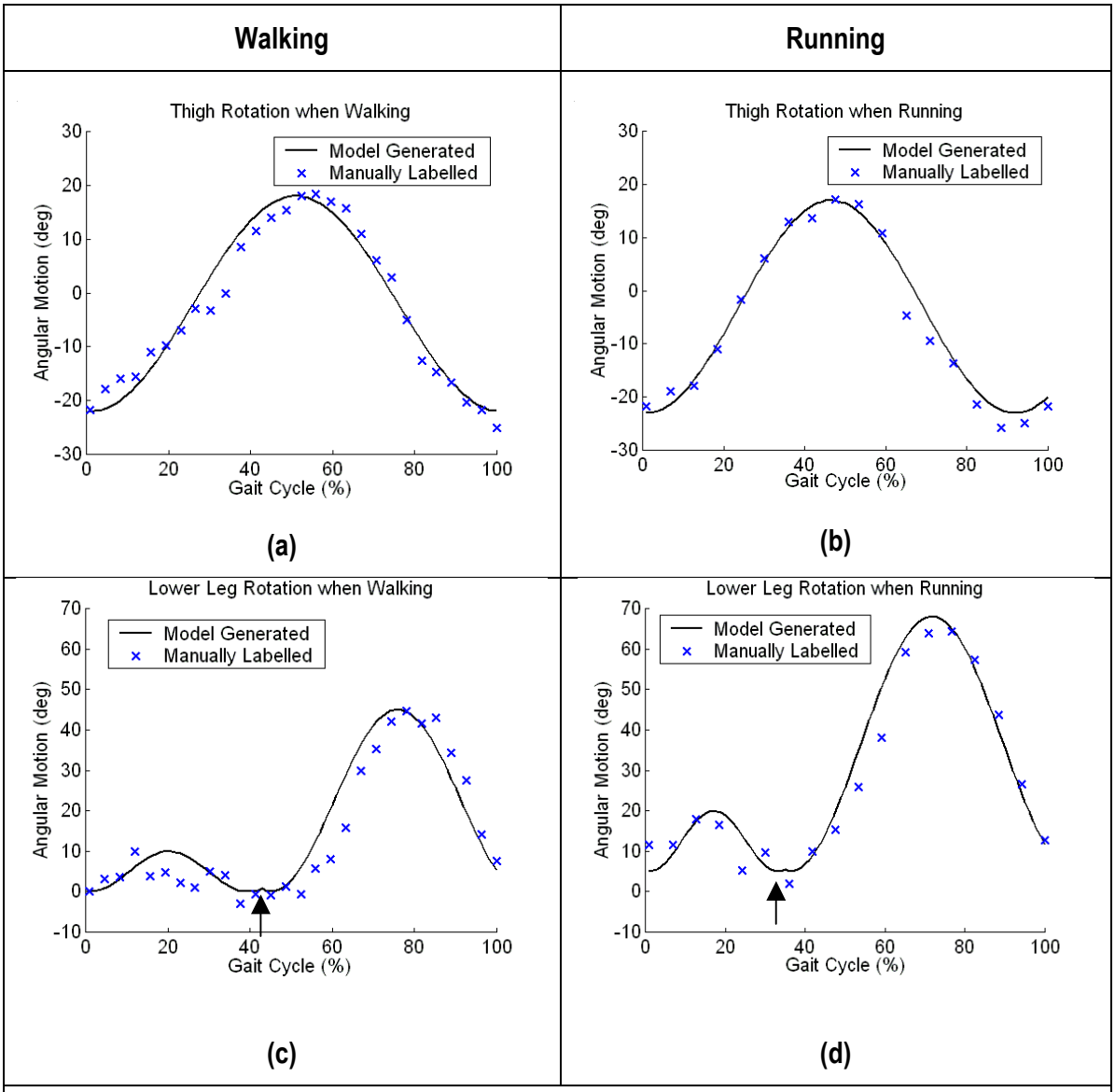

Figure 4.3: Model generated thigh and knee rotation (relative measurement) for walking and running superimposed with the manually labelled angles of a particular subject.

4.1.2 Forced Coupled Oscillator Model

Although the bilateral symmetric model illustrated earlier describes the motion well, there are a few drawbacks. First of all, the model lacks analytical attributes, and secondly the need to select the mode of gait (i.e. the value for the parameter p). In this extended analytical model, the human lower limb is again represented by two pendula joined in series, where $\theta_K(t)$ is measured with respect to the vertical (absolute angle) as

opposed to the one in the bilateral symmetric model which is relative to $\theta_T(t)$, see **Figure 4.4**. We exploit the concept of a forced coupled oscillator to create a model invariant to walking and running gaits, as legs are considered to be an imperfect pendulum with substantial energy loss [Zatsiorky'94]. Biomechanics studies show that a driven harmonic oscillator provides a good representation for human walking [Holt'90]. However, this is only a simple pendulum representing mainly the thigh motion. McGeer had also proposed a 2-legged machine (that only walks downhill) using only down slope as a source of energy [McGeer'90a] and claimed that its motion is comparable to that of human walking. This machine consists of two rigid legs with mass and inertia, joined at the hip with a mass at the hip, and semicircular feet. Later, he proposed another passive dynamic walking structure with knees [McGeer'90b]. This also gave impressive results.

This new forced coupled oscillator model, which requires no parameter selection for different gait mode, solves the differential equations obtained from the dynamic motion of these two pendula. The upper pendulum swings with a simple harmonic motion while the lower pendulum is influenced by the force introduced by the upper pendulum. To avoid notational overload, note that the notations for the corresponding labels remain the same as the previous model. The hip motion remains as described by **Eq. 4.1**.

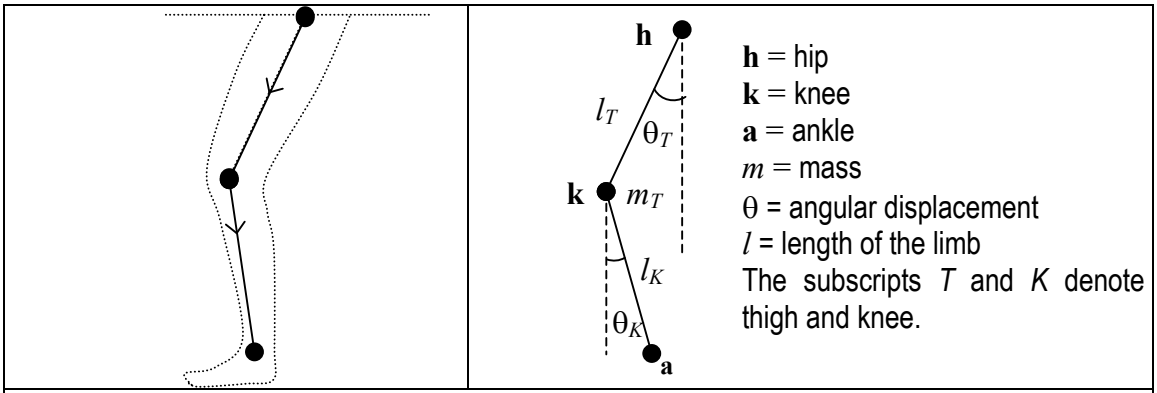

Figure 4.4: Structural model of the thigh and lower leg: upper and lower pendulum models the thigh and the lower leg, respectively, connected at the knee joint. Motions are measured by absolute angles.

Referring to **Figure 4.4**, the upper pendulum representing the thigh can be modelled by simple harmonic motion as

$$\ddot{\theta}_T + \omega_T^2 \theta_T = 0 \qquad \textbf{(4.4)}$$

where θ_T is the angular displacement from the vertical, $\ddot{\theta}_T$ is the angular acceleration, and ω_T is the fundamental frequency. The solution is the motion model for thigh rotation given by

$$\theta_T = A\cos(\omega_T t) + B\sin(\omega_T t), A > B \qquad \textbf{(4.5)}$$

where A and B are constants, and t is a time index which varies from 0 to 1, representing the start and end of the gait cycle, respectively. As the thigh rotation is of cosine nature, thus, the coefficient of the cosine term is more significant and is accounted for the amplitude of this rotation.

In reality, human walking and running is a highly sophisticated system involving multiple factors interacting simultaneously. As we seek a model providing a foundation for a person recognition system, realistic modelling of an individual's locomotion is unnecessary. We shall assume that the lower leg can be modelled as a driven oscillator where the force applied to it is related to the motion of the upper pendulum. Following an analogy of Newton's laws, by differentiating **Eq. 4.5** twice, we have

$$\ddot{\theta}_T = -\omega_T^2 \left[A\cos(\omega_T t) + B\sin(\omega_T t) \right] \qquad \textbf{(4.6)}$$

which contributes to the driving force to the lower pendulum. This force is given by

$$\mathbf{F}(t) = -m_T \omega_T^2 \left[A\cos(\omega_T t) + B\sin(\omega_T t) \right] \qquad \textbf{(4.7)}$$

Similar to **Eq. 4.4**, the motion equation for the lower pendulum is

$$\ddot{\theta}_K + \omega_K^2 \theta_K = -\mathbf{F}(t) \qquad \textbf{(4.8)}$$

Substituting **Eq. 4.7** into **Eq. 4.8**, yields

$$\ddot{\theta}_K + \omega_K^2 \theta_K = m_T \omega_T^2 \left[A\cos(\omega_T t) + B\sin(\omega_T t) \right] \qquad \textbf{(4.9)}$$

The solution for θ_K will comprise the general solution, θ_{Kg}, and the particular solution, θ_{Kp}. The general solution is obtained by setting $\mathbf{F}(t) = 0$ in **Eq. 4.8** to give

$$\theta_{Kg} = C\cos(\omega_K t) + D\sin(\omega_K t) \qquad \textbf{(4.10)}$$

where C and D are constants. A Wronksian method [Kreyszig'93] is used to find the particular solution, and the result is

$$\theta_{Kp} = -\frac{m_T \omega_T^2}{(\omega_T{}^2 - \omega_K{}^2)} (A\cos\omega_T t + B\sin\omega_T t) \qquad \textbf{(4.11)}$$

Recalling that $\theta_K = \theta_{Kg} + \theta_{Kp}$, by substituting **Eq. 4.10** and **Eq. 4.11**, the complete solution for θ_K yields the basic motion model for the lower leg rotation, which is

$$\theta_K = C\cos\omega_K t + D\sin\omega_K t - \frac{m_T \omega_T^2}{(\omega_T{}^2 - \omega_K{}^2)} (A\cos\omega_T t + B\sin\omega_T t), \omega_K > \omega_T \qquad \textbf{(4.12)}$$

where, ω_T and ω_K are constrained not to be equal, otherwise **Eq. 4.12** will introduce a singularity. Also, ω_T shall be greater than ω_K to ensure that the shape of a double-bump is achieved. And, ω_T should not be similar to ω_K, otherwise this equation will be effectively similar to that of the thigh rotation (**Eq. 4.5**). A few offsets (M_T, E and M_K) are required to be added to **Eq. 4.5** and **Eq. 4.12** for implementation purposes, yield

$$\theta_T = A\cos(\omega_T t) + B\sin(\omega_T t) + M_T \qquad \textbf{(4.13)}$$

$$\theta_K = E\left[C\cos\omega_K t + D\sin\omega_K t - \frac{m_T \omega_T^2}{(\omega_T{}^2 - \omega_K{}^2)} (A\cos\omega_T t + B\sin\omega_T t) \right] + M_K \qquad \textbf{(4.14)}$$

The motion models derived may not guarantee a precise approximation in implementation. This is because humans do not walk or run like a pendulum. If we did, we would not move at all! One obvious reason is that our legs do not swing about equilibrium points. Here, we had only borrowed the concept of pendular movement to aid the automatic motion extraction process. As this new model is invariant to walking and running gaits, no parameter selection is needed for this model to differentiate between walking and running subjects.

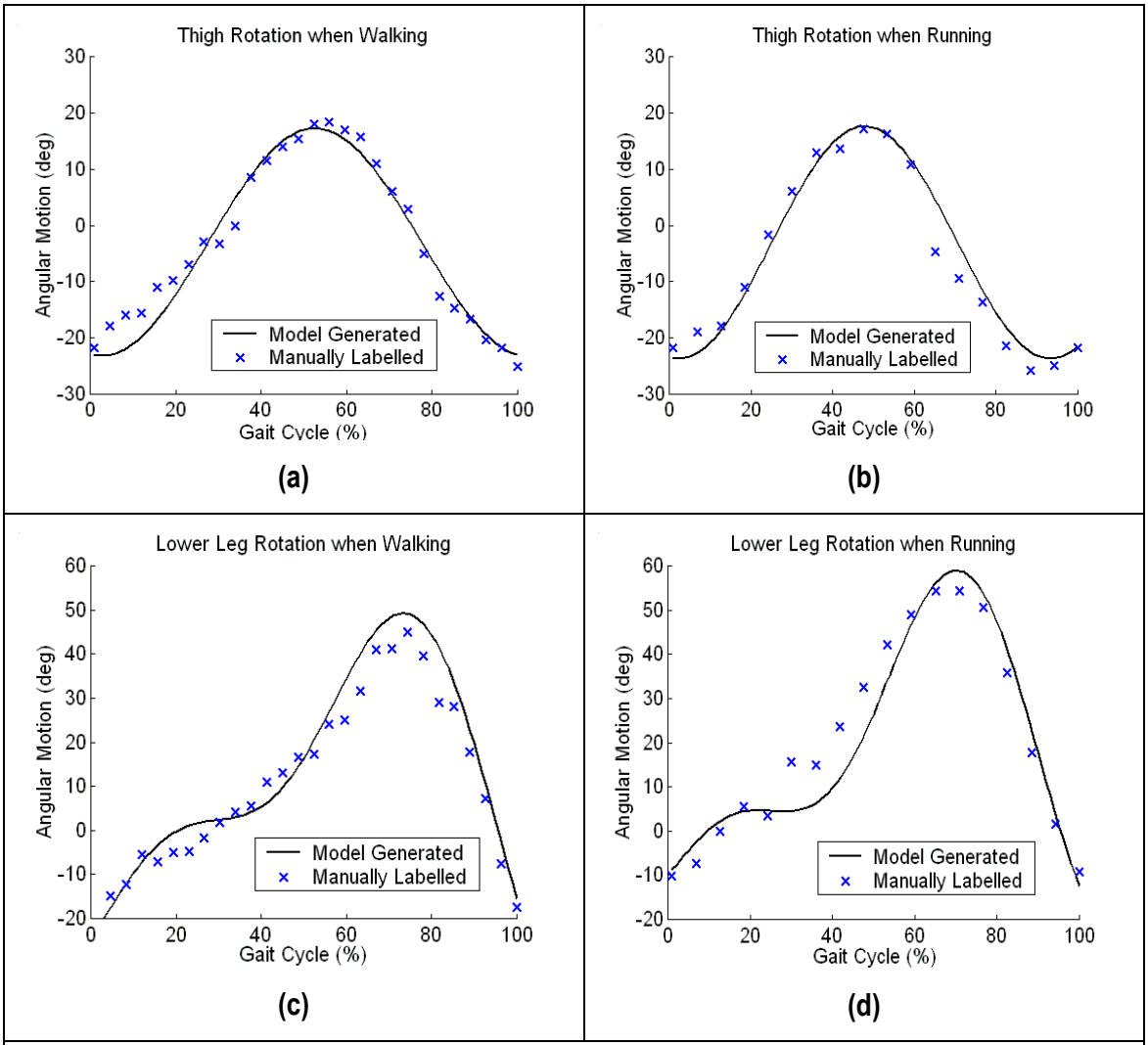

Figure 4.5: Sample output of the thigh and lower leg motion model (absolute measurement) superimposed with the manually labelled angles of a particular subject.

Example waveforms that can be produced by the thigh and lower leg motion models described by **Eq. 4.13** and **Eq. 4.14**, with appropriate value of parameters, are shown in **Figure 4.5**. The structure of the response of the model appears very close to that of the manually labelled data. As expected the simple model does not match the rotation precisely, but it can describe the gross motion of the lower leg, over a single gait cycle. This model is periodic over a larger time interval but not within the gait cycle. It is designed to describe motion within a single gait cycle as for recognition purposes, we only need features from within a single gait cycle. Naturally, the position of the leg at the end of one cycle could be used to initialise search for its position in the following cycle. However, only the labelled single cycle data is used for recognition here. As we shall see, it serves as a model to automatically extract gait motion for one cycle via computer vision techniques. It is more likely that a better model of gait itself, employing Fourier descriptors could incur better characterisation capability but at the expense of complexity. However the results here suggest such an approach is unnecessary.

4.2 Structural Model

Referring to **Figure 4.4**, the structure of a thigh can be described by a point **h** that represents the hip and the line passing through **h** at an angle θ_T. The knee is then

$$\mathbf{k}(t) = \mathbf{h}(t) + l_T \mathbf{u}_T(t) \qquad (\mathbf{4.15})$$

where $\mathbf{u}_T(t)$ is the unit vector of the line direction, **h** is the position of the hip and l_T is the thigh length, as $\mathbf{u}_T(t) = [-\sin\theta_T(t), \cos\theta_T(t)]$ and $\mathbf{h}(t) = [h_x(0), h_y(0) + S_y(t)]$, where $h_x(0)$ and $h_y(0)$ are the initial hip coordinates. Decomposing **Eq. 4.15** into constituent parts yields the coordinates of the knee point as,

$$k_x(t) = h_x(0) - l_T \sin\theta_T(t) \qquad (\mathbf{4.16})$$

$$k_y(t) = h_y(0) + S_y(t) + l_T \cos\theta_T(t) \qquad (\mathbf{4.17})$$

Similarly, the structure of the lower leg is given by a line which starts at the knee, that passes through **k** at an angle θ_k. The ankle **a** is

$$\mathbf{a}(t) = \mathbf{k}(t) + l_K \mathbf{u}_K(t) \quad \textbf{(4.18)}$$

where $\mathbf{u}_K(t)$ is the unit vector of the line direction, $\mathbf{k}(t)$ is the position of the knee and l_K is the lower leg length, as $\mathbf{u}_K(t) = [-\sin(\theta_K(t)), \cos(\theta_K(t))]$ and $\mathbf{k}(t) = [k_x, k_y]$, where k_x and k_y is the point of the knee. Decomposing **Eq. 4.18** into constituent parts yields the coordinates of the ankle as,

$$a_x(t) = k_x(t) - l_K \sin(\theta_K(t)) \quad \textbf{(4.19)}$$

$$a_y(t) = k_y(t) + l_K \cos(\theta_K(t)) \quad \textbf{(4.20)}$$

Together with the motion models described earlier, these form the basis of the temporal template to be used within feature extraction to find the moving lines that correspond to a subject's leg.

4.3 Implementing an Evidence Gathering to Extract a Gait Model

The best-fit motion model is obtained by an evidence gathering technique as described in **Chapter 3**. Each edge point that falls within a predefined region at the centre of each image of a sequence, is a set of possible initial coordinates indicating the hip position. The first stage of this evidence gathering technique will search within that predefined area according to **Eq. 4.1** and **Eq. 4.13** to determine the best-fit models for the hip and the thigh rotation simultaneously. The parameters of interest are the axes of the accumulator space. The cells in the accumulator space that corresponds to each parameter combination for a given edge point are incremented.

Once the best values for the parameters of interest are obtained, then, the values of parameters that are inherited from **Eq. 4.13** (i.e. A and B) are used when searching for the best-fit model for the lower leg rotation. Similarly, evidence is accumulated in the accumulator space defined by the parameters from **Eq. 4.14** when the given edge

point falls into the corresponding parameter combination. Here, m_T in **Eq.4.14** is set to unity as it can be absorbed into other scaling parameters. The parameters of interest extracted from all the three motion models describing the hip, the thigh and the lower leg rotations are A_y, ϕ_y, A, B, M_T, C, D, E, ω_K and M_k. And, $h_x(0)$ and $h_y(0)$ which are the initial coordinate for the hip's position. All these describe the first stage of this evidence gathering technique.

As illustrated by **Figure 3.4**, once the best-fit models are achieved, angles are then generated in the second stage of this evidence gathering technique. Based on these angles, a local template matching is employed to search within a predefined range derived from medical reports [Murray'67] for the best angles in each frame. Thus, the best possible angles describing the angular motion of the leg are obtained.

4.4 Example Results

The high-level feature extractor is initialised with parameters obtained from the averaged manually labelled angular motion of 20 subjects (each with one sample), representing the norm of human walking and running pattern in this experimental dataset. **Figure 4.6** shows the result of the automated angular motion extraction using the bilateral symmetric model as the underlying temporal template for the evidence gathering technique, superimposed on the manually labelled data. Extraction for the thigh when walking and running appears reasonably accurate, see **Figure 4.6(a-b)**. However, the results for the knee rotation may have room for further improvement. There are some discrepancies on the knee rotation between the manually labelled data and the extraction throughout the whole gait cycle in the examples shown in **Figure 4.6(c-d)**. Nonetheless, the broad structure is clearly there. That the results for the lower leg extraction are not as promising may be due to the relative angular measurement. That is, if there are errors in the thigh extraction, then the lower leg angular measurements are bound to be affected.

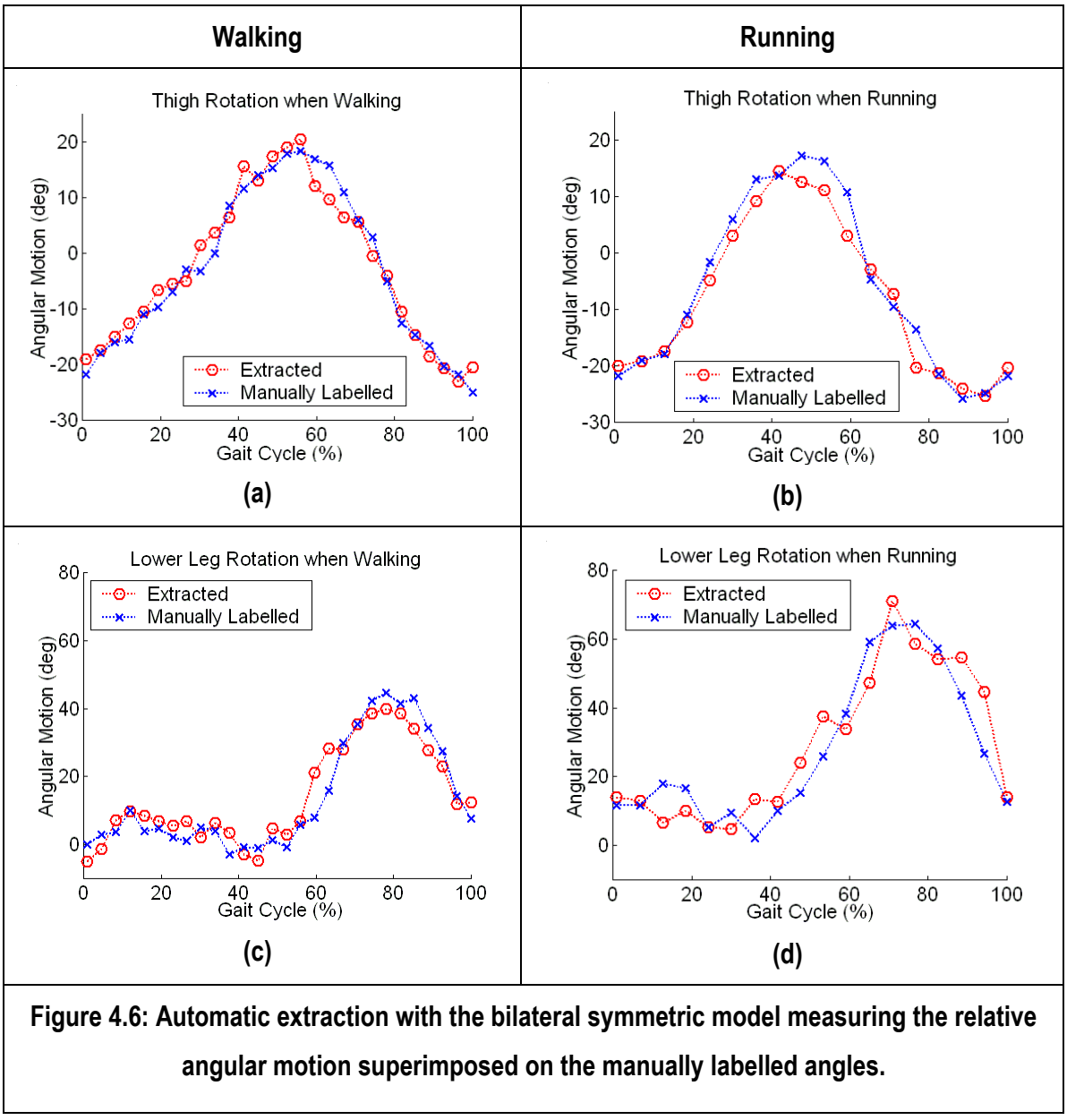

Figure 4.6: Automatic extraction with the bilateral symmetric model measuring the relative angular motion superimposed on the manually labelled angles.

Bear in mind these comparisons are made between the automatically extracted angles to that of manually labelled. Manually labelled data are not the ground truth, but rather, serve as a reference for comparison purposes. Nevertheless, manually labelled data are used to show close-to-ground truth measurement. **Figure 4.7** shows manually labelled data superimposed on the result of this evidence gathering technique with the forced coupled oscillator model as the underlying template. In general, the superimposed graphs demonstrate a considerable amount of veracity of the model and the manual labelled data. As depicted in **Figure 4.7(a)**, the thigh rotation of walking

extracted is very accurate (compared to those in the previous figure) and similarly for those of the lower leg rotation. For the case of running, results do show some discrepancies, however, the structure for both the thigh and the lower leg motion both follow closely the results of manual labelling.

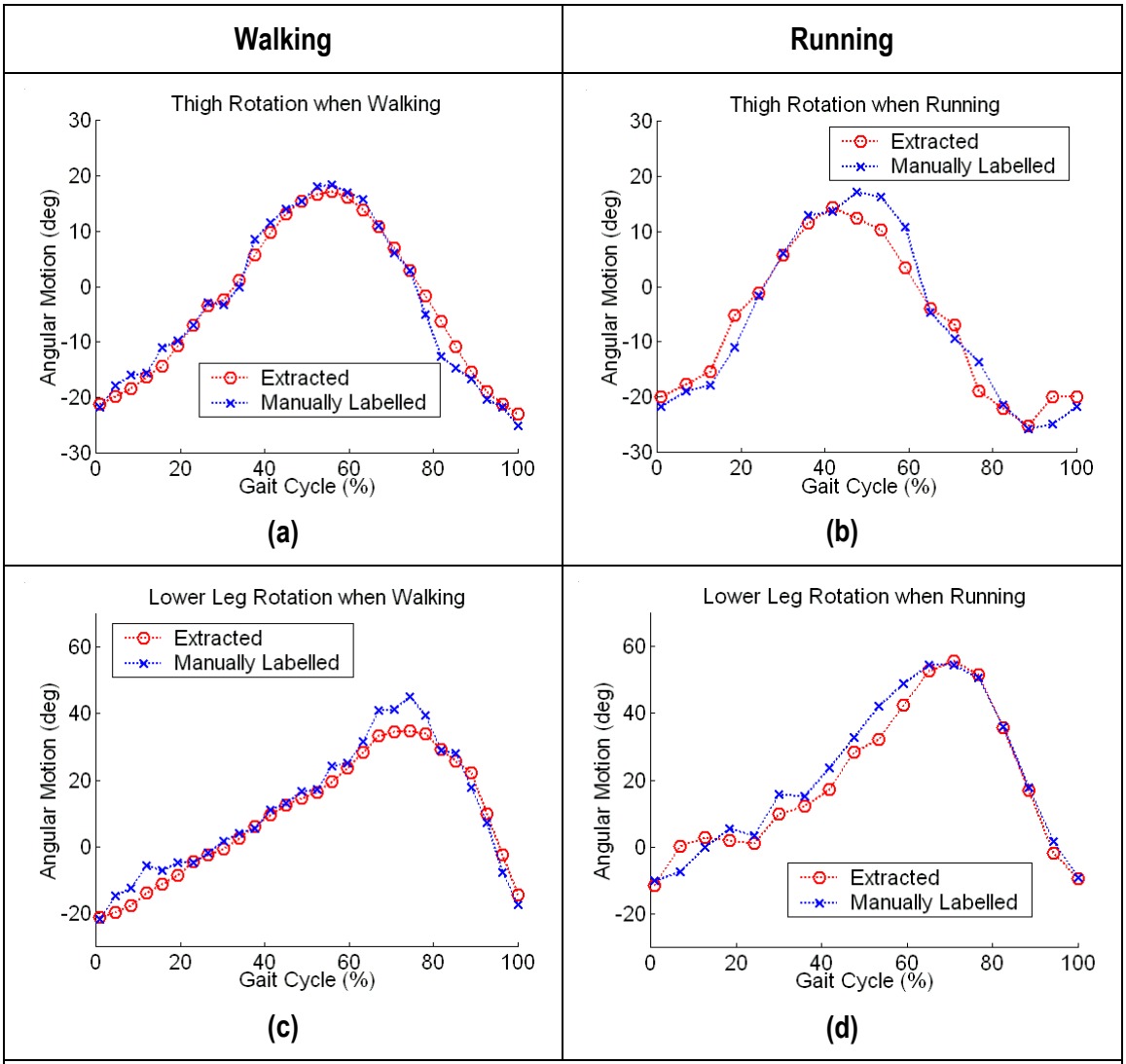

Figure 4.7: Automatic extraction with the forced coupled oscillator measuring the absolute angular motion superimposed on the manually labelled angles.

When comparing the results obtained from using the bilateral symmetric model and the forced coupled oscillator, immediate differences can be perceived except for the motion of the thigh. As illustrated in **Figure 4.6 (a-b)** and **Figure 4.7(a-b)**, the results are comparable. The two motion models for the thigh are conceptually identical. As for the extraction of lower leg motion, the forced coupled oscillator model outperforms the bilaterally symmetry model, compare **Figure 4.6 (c-d)** and **Figure 4.7(c-d)**. When comparing different gaits, results suggest that extraction for running may be more challenging. Angular motions extracted via these two models for the case of walking appear more accurate than that of running, at least in this dataset.

As manually labelled data are merely a reference, visual comparison of the automatically extracted angular motion superimposed on the image itself would be more reliable. **Figure 4.8 - 4.11** shows encouraging results when the forced coupled oscillator model is used within the feature extraction technique. Despite differences between gait modes, this highly automated technique can extract the angular motion for both the thigh and the lower leg well, even when one leg is occluding the other or when arm is occluding the hip. Furthermore, extraction is not confused when the leg is near and/or parallel with the bar of the treadmill as depicted in **Figure 4.11**. In **Figure 4.8**, the motion of walking leg is well extracted, except for frame 18-23 where the angle extraction for the lower leg during the *swing phase* is less accurate. Nonetheless, the thigh motion is extracted accurately throughout the whole gait cycle. Similarly, in **Figure 4.11**, this technique extracts the thigh motion (when running) accurately but not the lower leg motion as shown in frame 11-14. Interestingly, this happened to both female subjects despite the gait mode. Further work is necessary to determine if this is merely a coincidence. As revealed by the psychology studies (that males and females have their own unique gait pattern), in the future a more accurate model describing the gait of different gender shall be investigated. As depicted in **Figure 4.9** and **4.11**, this technique can extract the thigh and lower leg motion accurately for these two male subjects when walking and running. Even though running is a fast motion, **Figure 4.10** shows impressive results as the angle extraction for both the thigh and the lower leg are distinctly accurate.

Figure 4.8: Examplar result of a female walker's leg motion extracted by automatic evidence gathering, showing discrepancy in some images especially frame 18-23.

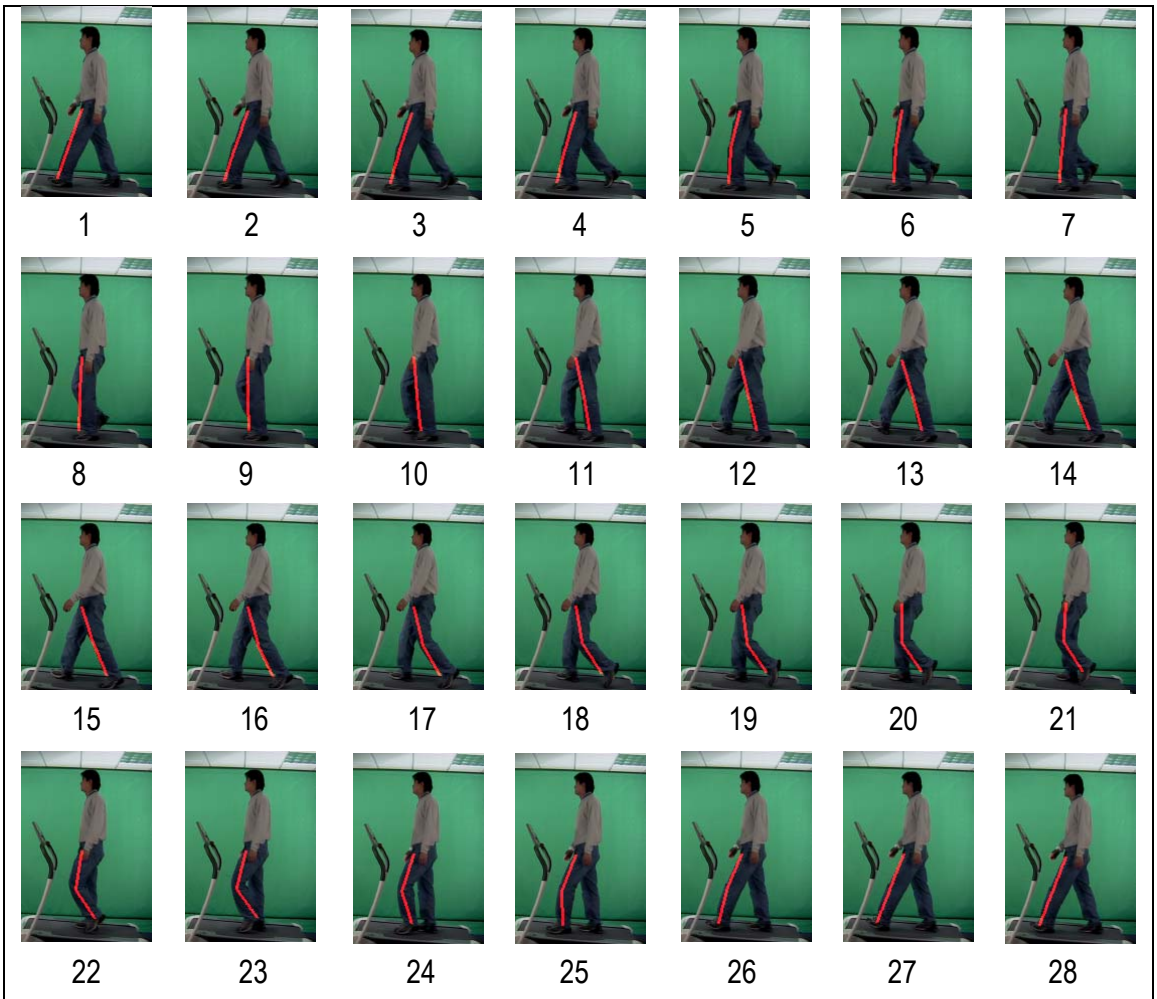

Figure 4.9: Examplar result of a male walker's leg motion extracted by automatic evidence gathering.

Figure 4.10: Examplar result of a male runner's leg motion, showing accurate extraction.

Figure 4.11: Examplar result of a female runner's leg motion, showing inaccuracy in

frame 11-14.

4.5 Discussion

We realise there are limitations on the BS and the FCO models, but we shall later show how they can indeed meet the desired (recognition) aims. They are alternative methods and the FCO is potentially a more accurate model. A better approach is to use Fourier series, but this requires greater computational cost. There are other potential models to describe the leg motion other than the two approaches described. A damped pendulum driven by a periodic force introduced by its suspension point that has periodic rotation may be a suitable model for the knee rotation, as described in **Eq. 4.21**. The response shown in **Figure 4.12** depicts its adherence to the lower leg motion, when it reaches a steady state.

$$\ddot{\theta}_K + \gamma\dot{\theta}_K + \left(\omega^2 + a\cos(2\pi ft)\right)\theta_K = a\sin(2\pi ft) \qquad (4.21)$$

where γ and a are constant coefficients.

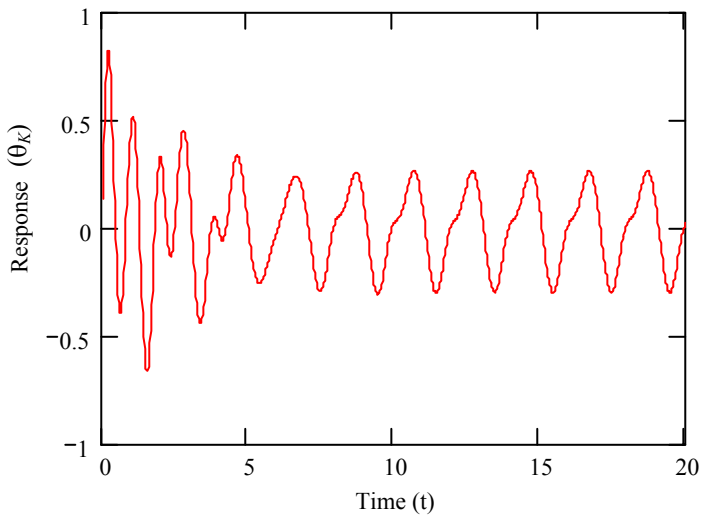

Figure 4.12: Response of a damped and driven pendulum.

In order to obtain the motion model, we have to solve **Eq. 4.21**. Although this is a linear differential equation, the sum of two solutions is no longer a solution

because of the inhomogeneous term on the right hand side. Hence, it cannot be solved analytically in terms of standard functions. One of the coefficients is not a constant, but time dependent and periodic, in this case. Although by Floquet theorem [Wolfram], there exists a set of fundamental solutions which can be written in this form

$$\theta_K(t) = c(t)e^{\lambda t} \tag{4.22}$$

where $c(t)$ is periodic with period T and λ is the Floquet exponent. However, it is a truncated Fourier series and it is not known explicitly. If the solution contains a Fourier series, then, this solution does not fulfil our purpose here, as our aim here is to achieve simplicity in modelling with sufficient accuracy for the ease of implementation.

As suggested by Weber as early as 1836 that leg movement resembles a free pendular movement [Weber'36]. Approximately fifteen decades later, Braune and Fisher [Braune'87] wrote, "*the swinging of the leg results much more from the action of the muscles than from gravity*". This is intuitively true or else the muscles would be of no use and we could not advance at all if our legs swing at a fulcrum about equilibrium. This was confirmed experimentally [Bernstein'35]. Perhaps a better representation would be employing a driven oscillator, as suggested by Holt [Holt'90]. Therefore, although pendular motion has gained attention in gait modelling, this is not the only approach to human locomotion modelling. Nature knows best. As written by McGeer [McGeer'90b], "*Thus might the engineer's sleek machinery soon dispense with nature's awkward contrivances. But a closer comparison reveals that nature is not so easily outdone. How many more examples of nature's dynamical sensitivity lie waiting to beguile the engineer?* "

4.6 Conclusions

There exist many ways to describe human locomotion. We have shown that oscillatory motion can be used as the underlying concept in modelling human leg. It may be a free oscillator, a coupled oscillator, a forced oscillator, or a combination of them. We have suggested a few alternative models: the first being an empirical model,

the second and third are analytical models. However, only the first two models, namely the bilateral symmetric and the forced coupled oscillator model have been tested. There are strengths and limitations for each model described. Automated extraction using the bilateral symmetric model as the underlying temporal template achieves good results. However, this model lacks analytical attributes and requires a parameter selection. Nonetheless, overall performance merit is gained by the forced coupled oscillator model as it does not require any parameter selection for different gait mode and more importantly it achieves higher accuracy in motion extraction. And we shall later see how this model helps in achieving the aim of this thesis. Alternative models are possible and yet await investigation to determine if they can present a technique of better efficiency than those already developed.

Chapter 5 : Gait Signature and Recognition

In order to identify an individual from a population, a unique label is associated to a particular subject. A Fourier description is employed in creating this unique label called a gait signature. Statistical analysis is used to aid the selection of prominent features and also analyses the discriminatory capability of the knee rotation. Then, a simple classification algorithm is used to examine the genuine discrimination capability. The potential of both walking and running gaits and the performance of the forced coupled oscillator and the bilateral symmetrical model are compared. This approach is also tested on generalisation capability such as noise and resolution. **Figure 5.1** illustrates the process of person identification.

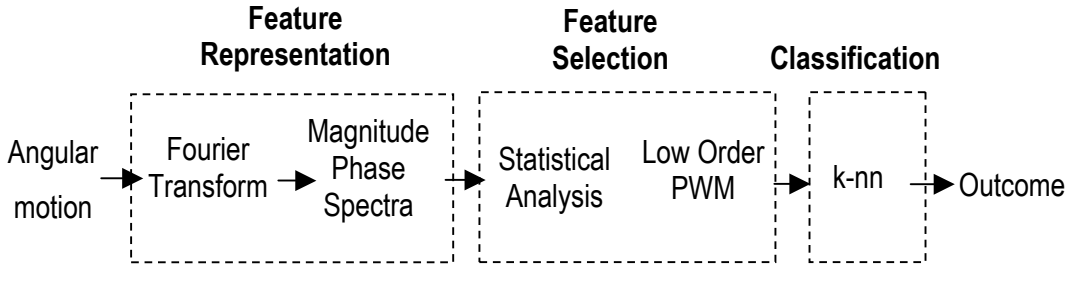

Figure 5.1: Process of person identification.

5.1 Fourier Descriptions and Gait Signature

Biological motion is always regarded as a complex activity with constant fluctuation from its own norm. An example to illustrate the fluctuation in behavioural traits is normal speech, having two persons speak with exactly the same intonation or manner is extremely rare. Just like every zebra has stripes, having two zebras with exactly the same pattern of stripes will be unusual, giving anecdotal evidence illustrating inconsistency in biological traits. In order to study the order behind the universal activity of human locomotion, yet with individual uniqueness, we first have to break the complex representation down to the underlying building blocks. This will facilitate investigation of individual characteristics of this universal activity. Here, Fourier analysis is employed because it can describe a complicated waveform as the summation of a set of simple waveforms.

Gait is not only characterised by the range of motion, but also involves the Central Pattern Generator and musculature that together control the way the limbs move. That is, walking and running are not only distinguished by their *kinematics*, but also significantly related by their *kinetics*. These suggest that phase information will have a certain degree of significance in describing gait patterns. A subject is associated with a meaningful and unique form of identification called a gait signature. The gait signature of a particular subject consists of the phase and the magnitude spectra of the Fourier description of the thigh and lower leg rotation measured from a gait cycle. This ensures the dynamics for both the spatial and temporal characteristics are captured. A scale change in the time domain signal results a scaling in the Fourier transform (**Eq. 5.1**), however, a delay in time alters the phase (**Eq 5.2**).

$$\mathcal{F}\{f(at)\} = |a|^{-1} F\left(\frac{s}{a}\right) \qquad \textbf{(5.1)}$$

$$\mathcal{F}\{f(t - t_0)\} = F(s) \quad e^{j\omega t_0 s} \qquad \textbf{(5.2)}$$

As relative timing is equivalent to the phase in the frequency domain, alignment of the time domain signal is critical. Hence, the time domain signals are aligned to start at the same point, which is the minimum of the thigh rotation and the corresponding instance of time of the lower leg rotation. This ensures the validity of the inclusion of the phase components when creating the gait signature for comparison. In the dataset collection procedure, subjects are encouraged to walk, if possible, at a constant pace. The motorised treadmill helps to achieve stability in pace, too. By using data between two successive minima, recognition becomes invariant to speed as data within a complete gait cycle is used. In recognition of the importance of phase-locking in perceiving gaits, Boyd introduced video phase-locked loops [Boyd'01] to benefit human gait analysis.

As explained earlier, to capture the essence of gait pattern, the signature shall contain both the magnitude and the phase component of the Fourier description. Therefore, the magnitude components are multiplied by their respective phase components, to yield the phase-weighted magnitude (PWM),

$$\mathrm{PWM}(\omega_n) = \left|\Theta\left(e^{j\omega_n}\right)\right| \bullet \arg\left(\Theta\left(e^{j\omega_n}\right)\right) \qquad \textbf{(5.3)}$$

where $\Theta\left(e^{j\omega_n}\right)$ is n^{th} the Discrete Fourier Transform component of the measured angle of rotation, and $\bullet$ denotes the multiplication of each element in the vector, thus increasing discriminatory capability. This will be described in the next section. The zero-order term is ignored to eliminate the effect of any offsets, so the gait signature contains only the features of the pure motion dynamics of a gait cycle. Letting the phase, $\arg\left(\Theta\left(e^{j\omega_n}\right)\right)$, range from $-\pi$ to π will introduce discontinuity at point $\pm\pi$, that is, even though they are the same point, they appear to be "numerically" far apart in the feature or signature space. This will cast a negative effect on the classification process. To eliminate this, the phase is represented in complex form to ensure continuity and also the one-to-one mapping which in turn ensures validity in implementation.

5.2 Feature Selection

Statistical analysis is necessary to establish the basis for determining which features should be used to create a signature for filtering identity. This will in turn increase the correct classification rate (CCR). A statistical measure that describes the distribution of subjects, or class, clusters in the feature space is employed. The separation, **S**, between the class means, normalised with respect to class covariances, is used. The separation, $\mathbf{S}_{i,j}$, between subjects i and j is given by a form of the Bhattacharyya distance as,

$$\mathbf{S}_{i,j} = \left[\mathbf{m}_i - \mathbf{m}_j\right]^T \left[\frac{\Sigma_i + \Sigma_j}{2}\right]^{-1} \left[\mathbf{m}_i - \mathbf{m}_j\right] \qquad \textbf{(5.4)}$$

where $\mathbf{m}_i$ is the mean and $\sum_i$ is the covariance class i. The mean signature $\mathbf{m}_i$ for each class i is given by

$$\mathbf{m}_{i,n} = \frac{1}{M}\sum_{l=0}^{M-1} \mathbf{x}_{l,n}^i \quad , n = 1,2,...N \qquad \textbf{(5.5)}$$

where M is the number of experiments or samples for class i, N is the number of Fourier harmonics used and $\mathbf{x}^i$ is an M x N data matrix of signatures for class i. The covariance matrix, $\sum_i$, is

$$\Sigma_i = \frac{1}{M}\sum_{l=0}^{M-1}\left(\mathbf{x}_l^i - \mathbf{m}_i\right)\left(\mathbf{x}_l^i - \mathbf{m}_i\right)^T \qquad \textbf{(5.6)}$$

Discriminatory capability can be deduced from the cluster separation. if the value of $\mathbf{S}_{i,j}$. is large, either the clusters are well separated and/or have low variance. Conversely, poor discriminatory capability derives from clusters which are closely spaced and/or with high variance. The advantage of measuring the variance within a class and the distance between different classes simultaneously is that measurements are less sensitive to any outliers in the feature space. The values of the mean separation $\bar{S}$ and the variance of the separation measurements σ^2, are directly proportional to the

overall discriminatory capability of a certain set of features. **Table 5.1** summarises the value of $\bar{S}$ and σ^2 for all cases including using the magnitude component only, the lower order phase-weighted magnitude and those with higher order phase-weighted magnitude of the Fourier description. As depicted, the PWM has a greater value of mean and variance, meaning that the distance between each cluster is greater compared with the signatures formed from the magnitude alone. When higher orders of PWM are included as part of the signature, the value of $\bar{S}$ decreases and is the smallest here. Even though the mean of the magnitude is larger than that of the PWM with higher order, the variance of both measures is relatively small compared to that of PWM and this holds true for both walking and running. Thus, they are less discriminative. Accordingly, this suggests that the PWM should offer best discriminatory capability, with running appearing to be more potent.

Figure 5.2 illustrates the pair-wise values of **S** between classes in each case. The brighter the square, the higher the separation, and hence better discriminatory capability. The darker the square, the closer the feature clusters, so the diagonal is the darkest reflecting the zero distance between the same feature sets.

	Walking		**Running**	
	$\bar{S}$	σ^2	$\bar{S}$	σ^2
Magnitude	0.0623	0.0086	0.0512	0.0064
PWM	0.1506	0.0264	0.1710	0.0175
PWM higher order	0.0151	0.0052	0.0140	0.0072

Table 5.1: Values of $\bar{S}$ and σ^2 using different features: magnitude alone, PWM and PWM with higher orders.

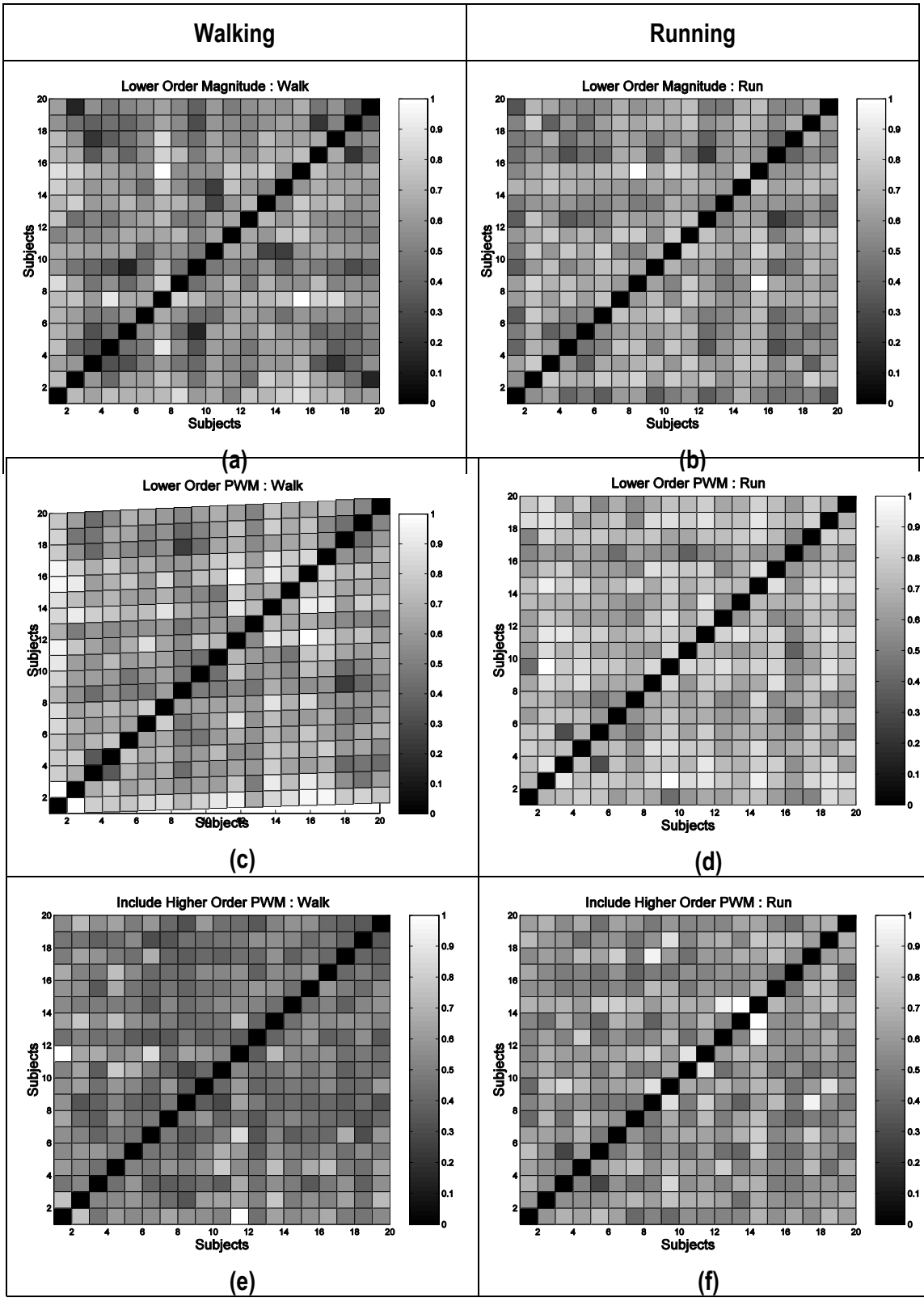
Walking
Running
Lower Order Magnitude : Walk
Lower Order Magnitude : Run
Lower Order PWM : Walk
Lower Order PWM : Run
Include Higher Order PWM : Walk
Include Higher Order PWM : Run
Subjects
(a)
(b)
(c)
(d)
(e)
(f)

Figure 5.2: Pair-wise cluster separation of various feature vectors.

As depicted by the pair-wise pseudo-greyscale plot in **Figure 5.2(a-b)** and **Table 5.1**, the magnitude component alone does show some discriminatory capability. However, gait is not only defined by the range of motion made by the limbs, but also by how the limbs are moving. This would suggest the significance of including phase in the signature. As shown in **Figure 5.2**(**c-d**), the inter-class separation increases (the squares are brighter) when the phase is multiplied by the magnitude (PWM). The lower order components (comprising of the 1^{st} - 2^{nd} harmonic of θ_T and 1^{st} – 3^{rd} harmonic of θ_K) are chosen to form the gait signature. This is because the PWM components of the thigh and lower leg rotation are dominated by the lower order due to their greater magnitude values as shown in **Figure 5.3**, where the error bars indicate the standard deviation computed from a population of 20 subjects, each with 6 samples. **Figure 5.2(e-f)** and the value of $\overline{S}$ show that the inter-class separation decreased tremendously when higher orders (1^{st} – 10^{th}) are included in the signature vector. **Figure 5.4** is the phasor plot of PWM for 20 subjects (each subject has one sample) where the radius to each point is the magnitude component and the direction from the origin is the phase component. Here, only the phase and magnitude (of the first three harmonics) of the leg motion of running is shown. The magnitude of the higher order harmonics is relatively small and they are more likely to be dominated by noise. Features shown confirm the general trend of the leg motion (the relative size of the harmonics) with some variation across the population, as expected. This is supported by medical studies which suggest that the maximum frequency content of human walking is 5Hz [Angeloni'94], that is only the first five harmonics are sufficient to describe human locomotion.

Walking	Running
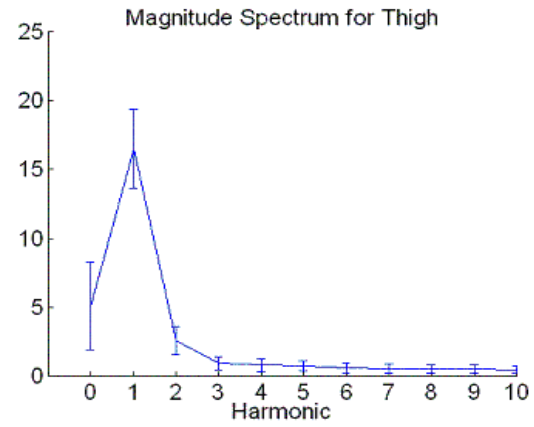 (a)	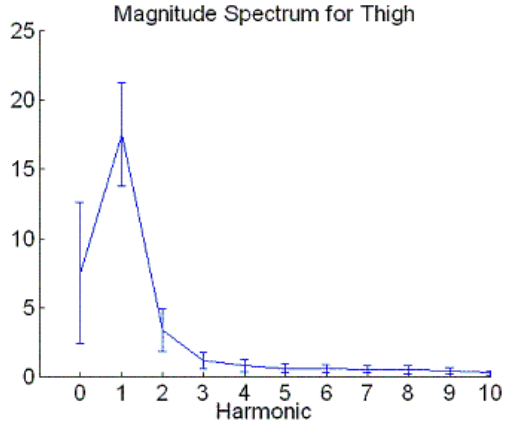 (b)
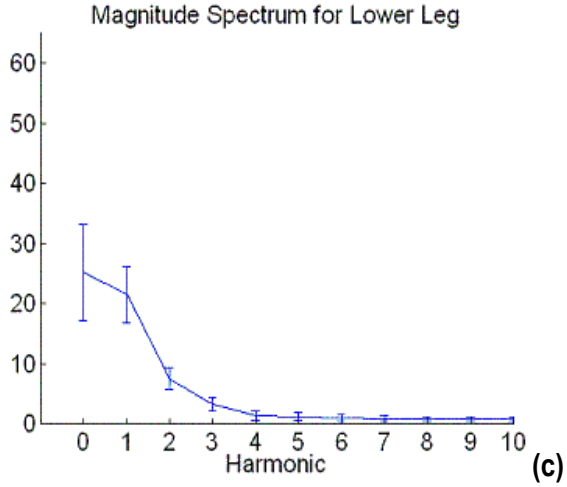 (c)	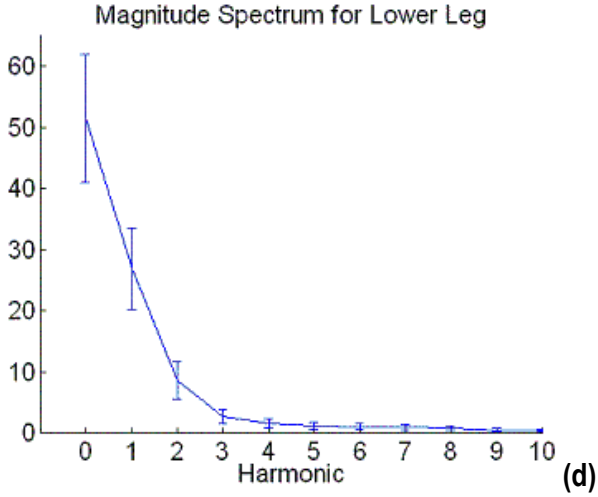 (d)

Figure 5.3: Magnitude spectrum of the thigh and the lower leg rotation when walking and running, with standard deviation.

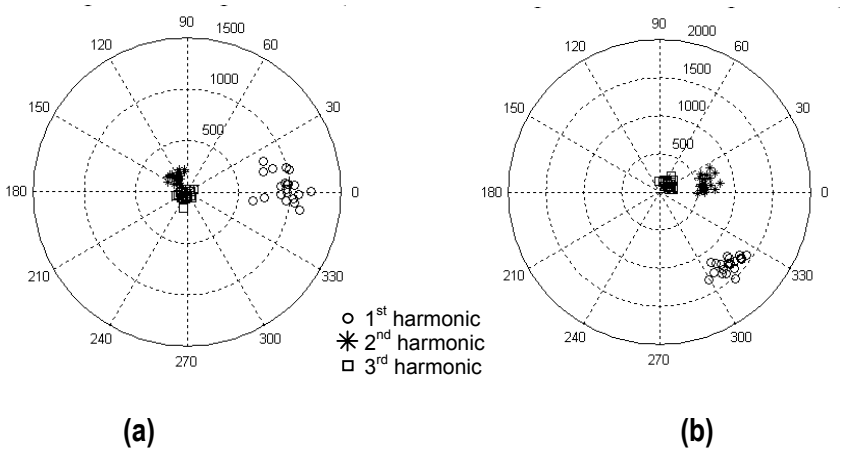

Figure 5.4: Phasor plot of the magnitude and corresponding phase components of the (a) thigh, and the (b) lower leg rotation in the case of running.

Suggested here is a way of combining the phase and magnitude, but not the only method, for recognition purposes. There may be other better ways of combining them to achieve better discriminatory capability and this shall be investigated in the future.

5.3 Identifying an Individual

Classification is done via the *k*-nearest neighbour (*k*-nn) and cross-validated with the leave-one-out rule. No doubt a more sophisticated classifier would be prudent, but the interest here is to examine the genuine discriminatory ability of the features. This method uses the Euclidean distance between the position of a test feature vector and the position of the surrounding training feature vectors to find the *k*th nearest neighbour in the feature space. The feature vector under test is then classified as the class that has the greatest population in *k*. The Euclidean distance, *D*, is calculated by

$$D = \sqrt{\sum_{n=0}^{N} \left(\mathbf{x}_n - \mathbf{y}_n\right)^2} \qquad (\mathbf{5.7})$$

where *N* is the number of harmonics used in the feature vector, **x** and **y** are the values of the *n*th harmonic for the test feature vector **x** and the training feature vector **y**,

respectively. By this means, a subject can be associated to the nearest or statistically correct class, otherwise to be rejected (if the similarity value is below a threshold).

5.4 Performance Analysis

The features are extracted via the evidence gathering technique (described in **Chapter 3**), with the motion models (described in **Chapter 4**) as the underlying temporal template. Performance analyses were carried out on both the bilateral symmetric and the forced coupled oscillator model and their results are discussed in the following subsections. This technique has been evaluated for individual, gender and gait mode (**Chapter 6**) discrimination, and the importance of the knee rotation. The practicality of this technique is also evaluated on noisy and low resolution images, see **Figure 5.5**. Images are contaminated with 25% grey scale random noise to simulate poor quality images in real life. Also, images are reduced to half of their original size, i.e. 65×95 to simulate poor resolution video.

(a) Clean

(b) 25% grey scale noise

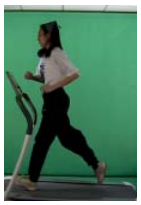

(c) ½ original resolution

Figure 5.5: Images used for performance analysis.

5.4.1 Performance of Bilateral Symmetric and Forced Coupled Oscillator Model

Figure 5.6 shows the signatures formed from the thigh and lower leg rotation using the forced coupled oscillator (FCO) model. For visualisation purposes, only 3 of the PWMs of 4 subjects are shown. Different symbols represent different subjects, each subject with 6 samples of walking and running. As depicted, there are well-

defined intra-class boundaries for both gaits. Walking gait appears to be more stable than running as the clusters for walking have lower variance then those of running. On the other hand, running appears to have greater inter-class variability. This is depicted by increase in distance in the feature space which is also depicted by the value of $\bar{S}$ in **Table 5.1**. This is also reflected by improvement in the recognition rate. Furthermore, this is supported by biomechanical observations: running involves increasing muscle activities and force [Ounpuu'94]; and there exist various manners in which the foot contacts the ground [Thordarson'97]. The features appear to have an individual mapping between the feature space of walking and running on an individual class basis. This may suggest that a mapping might exist that could make the signatures invariant and will be discussed later.

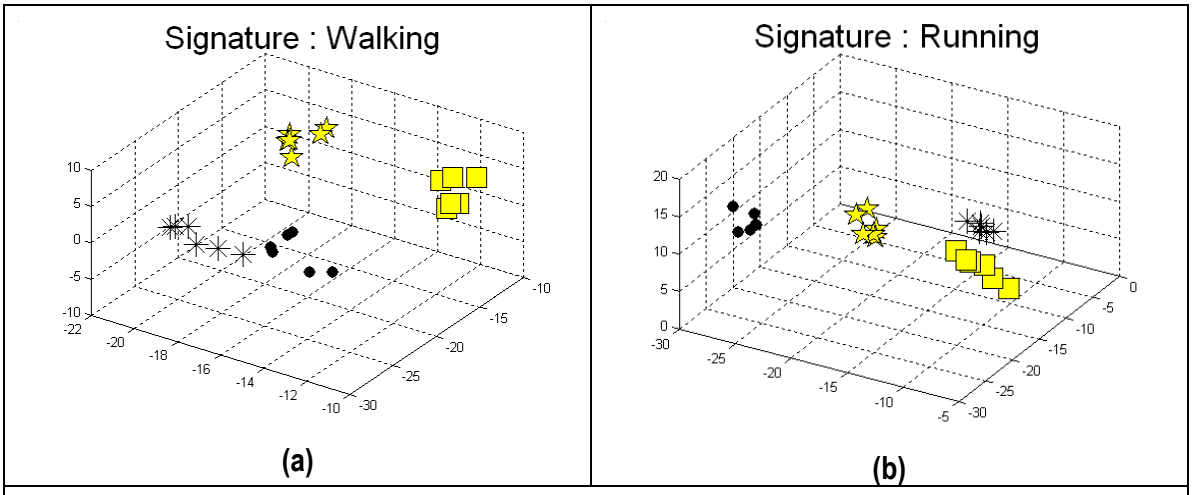

Figure 5.6: Signature space of 4 walking and running subjects. x: 1st component of θ_T; y: 2nd component of θ_T ; z: 1st component of θ_K .

In the *k*-nn with the values of *k*=1, 3 and 5, results are depicted in **Figure 5.7**. The recognition rates over 20 subjects (with 6 samples each) of both walking and running with the underlying FCO model improved over the rates where angles are extracted using the bilateral symmetric (BS) model, for both gaits. The probability of correctly classifying each subject from a population of 20 subjects at random is 0.05. The correct classification rate has a 15.2% and 10.6% increased for the cases of running and walking, respectively. As expected, the recognition rate for running is

more encouraging as running has more variability across the population compared with walking. This variability does suggest that change in running with time could be a performance issue in application.

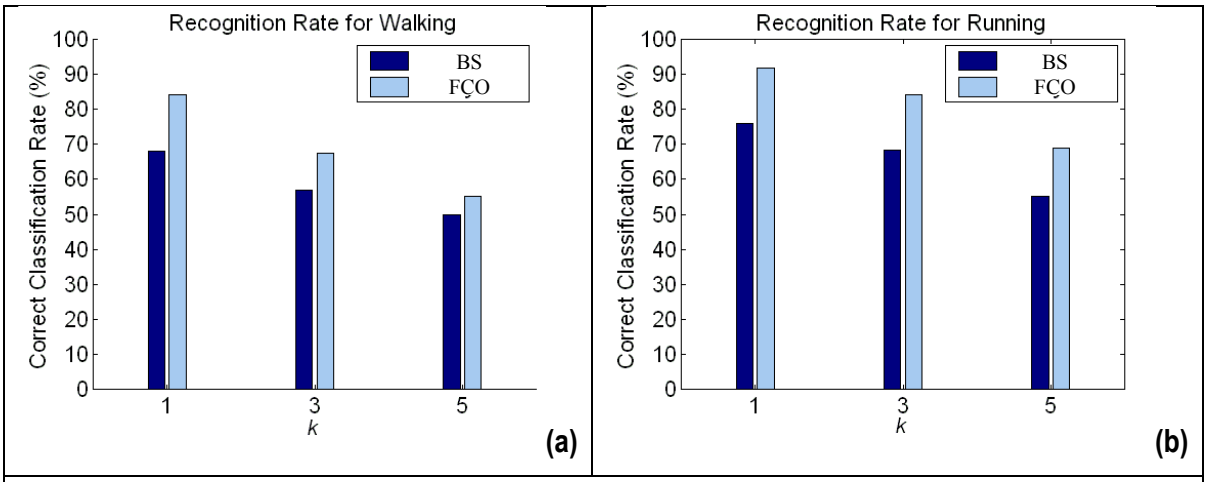

Figure 5.7: Recognition rates for walking and running via the *k*-nn with Euclidean distance metric for the bilateral symmetric and the forced coupled oscillator motion model.

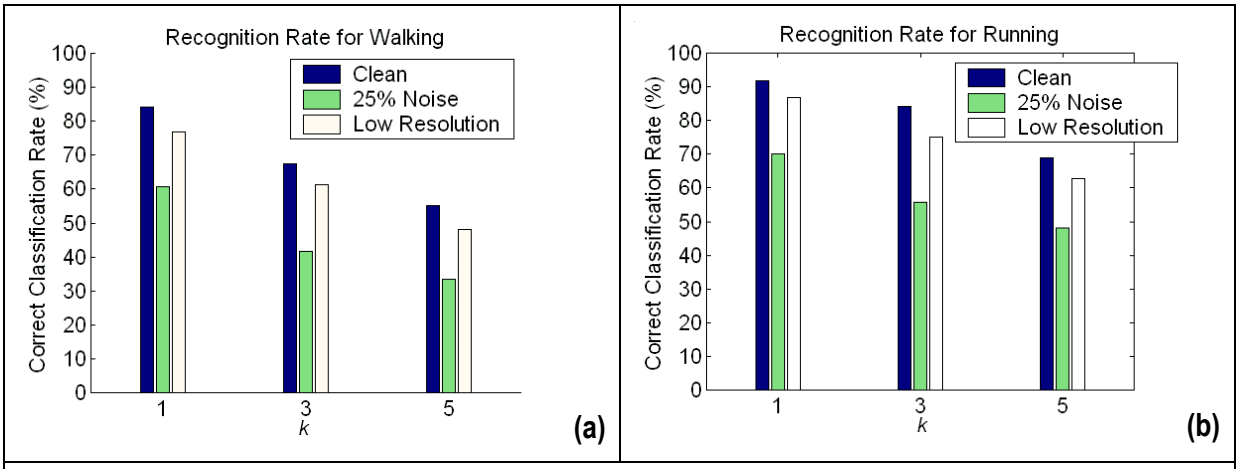

Figure 5.8: Performance analysis of walking and running

Performance analysis on 25% grey scale noise and low resolution (50% of the original resolution), has also been evaluated. The results by using the FCO model in **Figure 5.7** are included in **Figure 5.8** for comparison. As expected, the recognition rate decreased when images are contaminated with grey scale noise. The rate decreased

less when the technique was evaluated on images with lower resolution. That the rate does not decrease as much as when tested with noise could be due to measurement of the leg rotation angle being invariant to scaling.

5.4.2 Importance of Knee Rotation

Although both the magnitude spectrum of the thigh and the knee rotations are dominated by lower order components, this does not mean that both will offer similar potential in terms of discrimination. **Table 5.2** shows the values of $\bar{S}$ and σ^2 for the thigh and the knee rotations. Statistical measures show an increased value of $\bar{S}$ and σ^2 for the knee rotation for both the cases of walking and running. This suggests that the knee rotation may offer better discriminatory capability as it has more variation across the population. These measurements also suggest that the inclusion of knee rotation may greatly improve the discriminatory ability, especially for running as variance of the knee rotation increased by approximately 15 times when compared to that of the thigh rotation. A recent experiment also shows that in a statistical-based approach, not all parts of the silhouette are equally important for gait-based recognition, but only the lower 20% of the silhouette (approximately the portion from the knee downwards) is significantly accounted for recognition [Phillips'02]. **Figure 5.9** shows how this is reflected on the classification rate. Recognition rate based on the knee rotation alone outperforms the one when using the thigh rotation. Nevertheless, when combining the PWM of both the thigh and the lower leg, the correct classification rate is further increased. In the future, the discriminatory ability of the foot motion shall be investigated.

	Walking		Running	
	$\bar{S}$	σ^2	$\bar{S}$	σ^2
PWM for θ_T	0.0856	0.0061	0.0268	0.0009
PWM for θ_K	0.1601	0.0190	0.1272	0.0151

Table 5.2: Values of $\bar{S}$ and σ^2 show that the knee variation offers better discriminatory capability compared to that of the thigh rotation for both gaits.

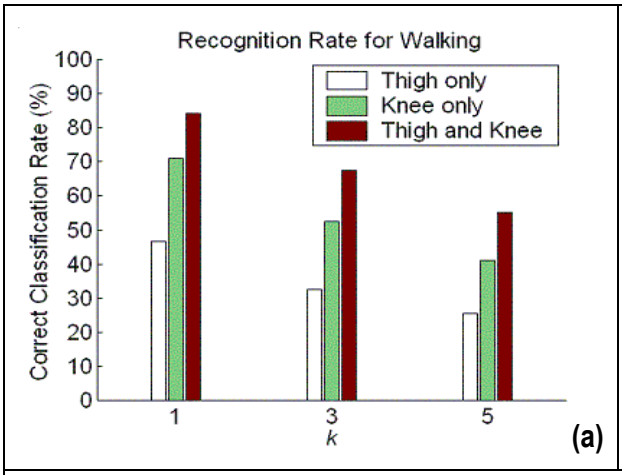

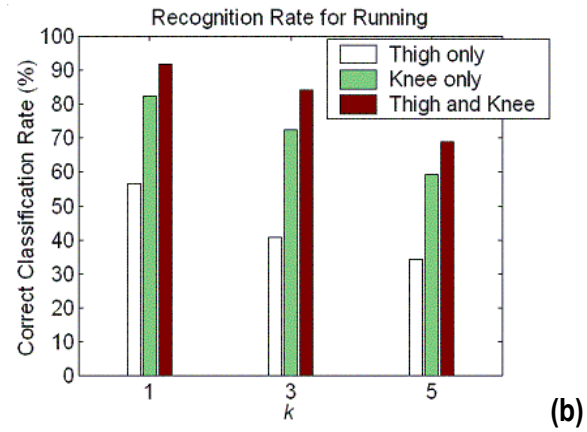

Figure 5.9: Comparing the performance of using only the thigh, the knee and both rotations in creating gait signatures.

5.4.2 Male and Female

As men have greater shoulder swing and women have greater hip swing [Mather'94], gender may have effects on the walking and running patterns. This is also reflected in our dataset as depicted by the classification rate for gender discrimination. Limited by the number of female subjects in this dataset, only 5 female and 5 male subjects are used for classification. **Figure 5.10** shows the result of gender discrimination of both gaits. High recognition rate suggest that locomotion patterns of male and female are indeed distinctive.

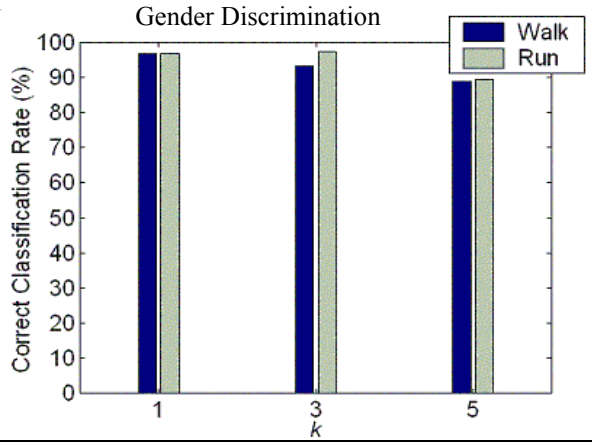

Figure 5.10: Gender discrimination for walking and running.

5.5 Conclusions

Frequency description is important in revealing the spatial-temporal characteristics of gaits. Statistical analysis describing class separation has been used to determine cluster separation. Measurements show that magnitude alone is not as promising as the phase-weighted magnitude in terms of discriminatory capability. However, phase and magnitude multiplication is not the only way of combining them. Also, higher order components may impede the discrimination potential. This may be due to the fact that higher order components are mainly dominated by noise. A simple classifier has been used to determine the genuine discrimination capability of the chosen features. Human locomotion patterns display unique characteristics for recognition purposes, with running being more potent. Performance analysis shows that the forced-coupled oscillator model outperforms the bilateral symmetric model. Also, this approach can tolerate noise and low resolution well. Besides being capable of distinguishing individuals, this technique can also discriminate the gender of a walker and runner. Interestingly, the knee rotation shows better discriminatory potential as compared with the thigh rotation. This may be because the knee rotation has more variations across the population. Also, the signature space depicts a unique mapping between walking and running signature of each subject, the next chapter will take a step further to investigate this relationship.

Chapter 6 : On the Relationship of Human Walking and Running

The intimacy of human walking and running gaits motivates the investigation in determining the existence of their relationship. This mapping, which is unique to each individual, can be expressed as a magnitude ratio and a phase difference in the frequency domain. It is useful in making the signature invariant to gait mode and also offers a convenient means of transforming from one gait made to another. These highly unique mappings can also be used alone as a condensed form of signature, or to buttress the original signatures. A neural network has been deployed in the search for a generic relationship between these two gait modes across a population.

6.1 Motivation

Human motion analysis has gained increasing attention from computer vision researchers. However, the relationship between human walking and running gaits (in computer vision) remains imperfectly understood. An understanding of the relationship between human walking and running is essential not only to further improve the existing automated person recognition approach using gaits, but also as a foundation for other studies e.g. biomechanics, robotics and computer graphics animation. Owing to the fact that these two gaits are derived from the same musculo-skeletal system, there must exist some correlation between them. Recall that, as stated in **Chapter 2.2**, Li suggests that the thigh and the leg co-ordination pattern for walking and running is similar under similar speed and stride frequency, although they are both functionally different [Li'99].

6.2 Unique Mapping

Examination of the signature space shows that there occur unique mappings between the walking and running signature for each subject, **Figure 5.6**. However, a generic mapping across the population cannot be determined (in this dataset) by visual inspection. Interestingly, the identical twins (in our dataset) who are "identical" by their visual appearance and physiological traits (**Figure 6.1**) appear unique in the way they walk and run. **Figure 6.2** shows the twins' gait signatures for walking and running where different symbols represent the two different subjects. Referring to **Figure 5.2(c-d)**, statistical analysis shows that these two classes, i.e. class 1 and class 11, are indeed very different, both in the walking and the running signature space. Perhaps what makes it seem unfeasible is that human gait is not only a physiological trait, but also a complex behavioural characteristic. That is, we *learn* how to walk and run when growing up and individuals with similar physiological traits may have their own particular way of walking and running.

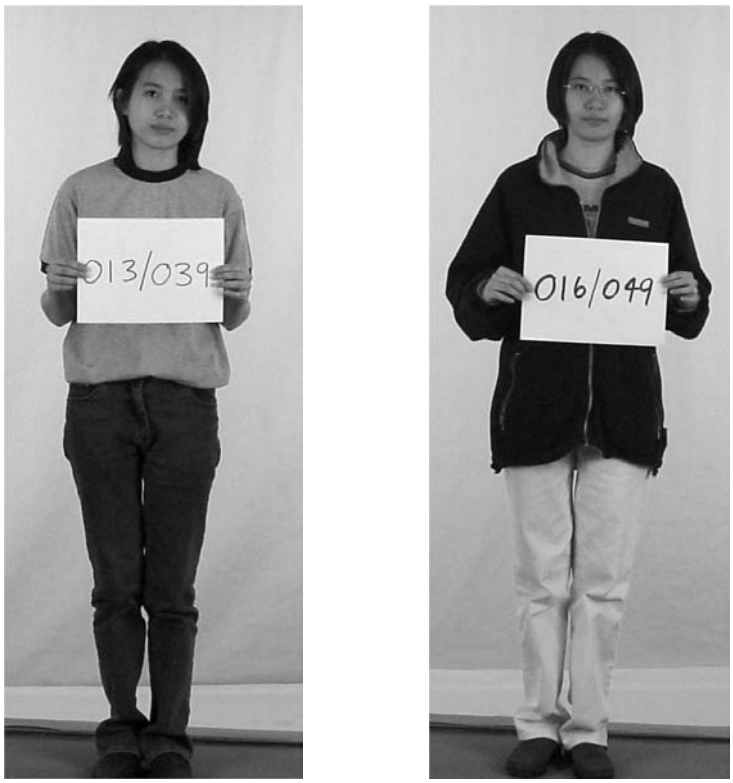

Figure 6.1: The identical twins with similar physical features. Images are the same scale.

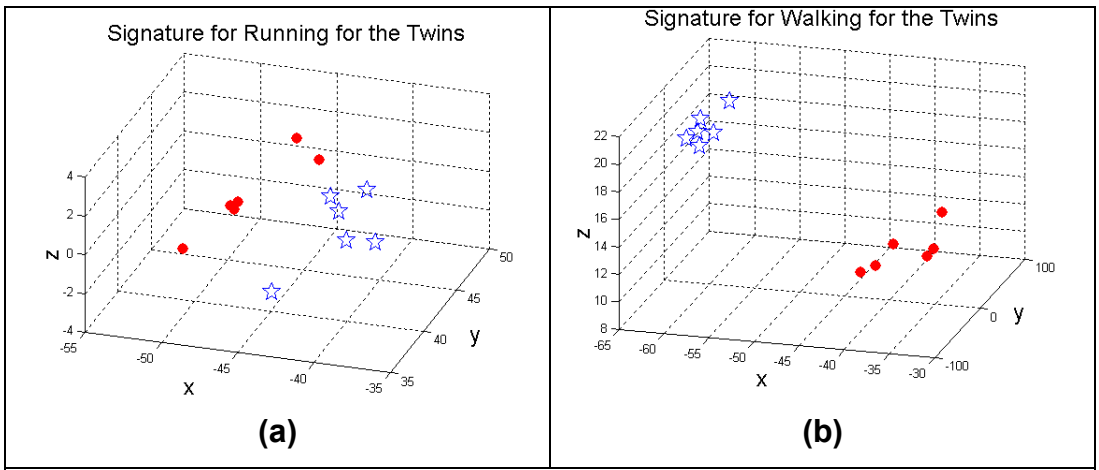

Figure 6.2: Signature for (a) running and (b) walking. x: 1st component of θ_T; y: 1st component of θ_K ; z: 2nd component of θ_K.

In the time domain, running can be regarded as a phase modulated version of walking (and vice versa), see **Figure 6.3**. Not only the range of movement made by the lower limbs and the manner in which the limbs swing when walking and running is different, the phase is also altered.

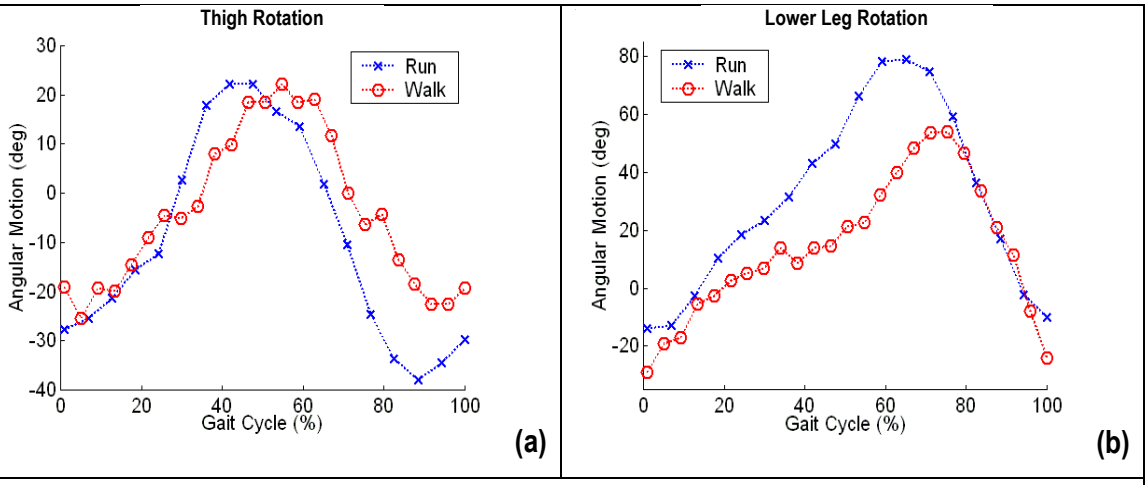

Figure 6.3: Angular motion of a particular subject when walking and running.

If $f(\omega t)$ is the signal for walking and the phase modulation signal is $Ke^{j\psi(t)}$, then the modulated signal (for running) is

$$g(\omega t) = Kf\left(\omega t + \psi(t)\right) \tag{6.1}$$

and likewise when transforming from running to walking. In the frequency domain, the spectra of the signals for walking and running can be easily related by the phase difference and magnitude ratio of each harmonic and these lead to a mapping, **T**, for N harmonics as

$$\mathbf{T} = \left[T_1, T_2, \ldots T_N\right] \tag{6.2}$$

Each element in **T** consists of the phase difference ϕ_{T_n} and the magnitude ratio M_{T_n} as

$$T_n = [\phi_{T_n}, M_{T_n}] \tag{6.3}$$

where ϕ_{T_n} is the phase difference between the spectral components for running, ϕ_{R_n}, and walking, ϕ_{W_n}

$$\phi_{T_n} = \phi_{R_n} - \phi_{W_n} \tag{6.4}$$

and M_{T_n} is the magnitude ratio of running, M_{R_n}, to walking, M_{W_n}

$$M_{T_n} = \frac{M_{R_n}}{M_{W_n}} \tag{6.5}$$

This mapping process shows how these two different gaits can be associated by the phase and the magnitude component in the frequency domain. **Figure 6.4** shows the phasor diagram of the mapping vector T_1 (the first harmonic) for θ_T and θ_K of 6 subjects. As shown, the components lie within a sector where the magnitude ratio and the phase difference show variability among different subjects as well as clustering for individual subjects, meaning that walking and running are closely related by their own unique mapping. That is, walking and running are not only distinguished by the range of movement made by the joints, but also by the forces that cause the movement. This also justifies the inclusion of the phase component in creating the gait signature and validates the assumption of phase modulation. Interestingly, the magnitude of the mapping for the thigh rotation of the first harmonic is not always bigger then unity. This suggests that this joint motion when running is not always larger then when walking. On the other hand, the magnitude of the mapping for the lower leg is generally bigger than unity indicating that the knee joint motion is usually more exaggerated during running. However, a note to make here is that the subjects in this experimental dataset are not professional (athletic) runners.

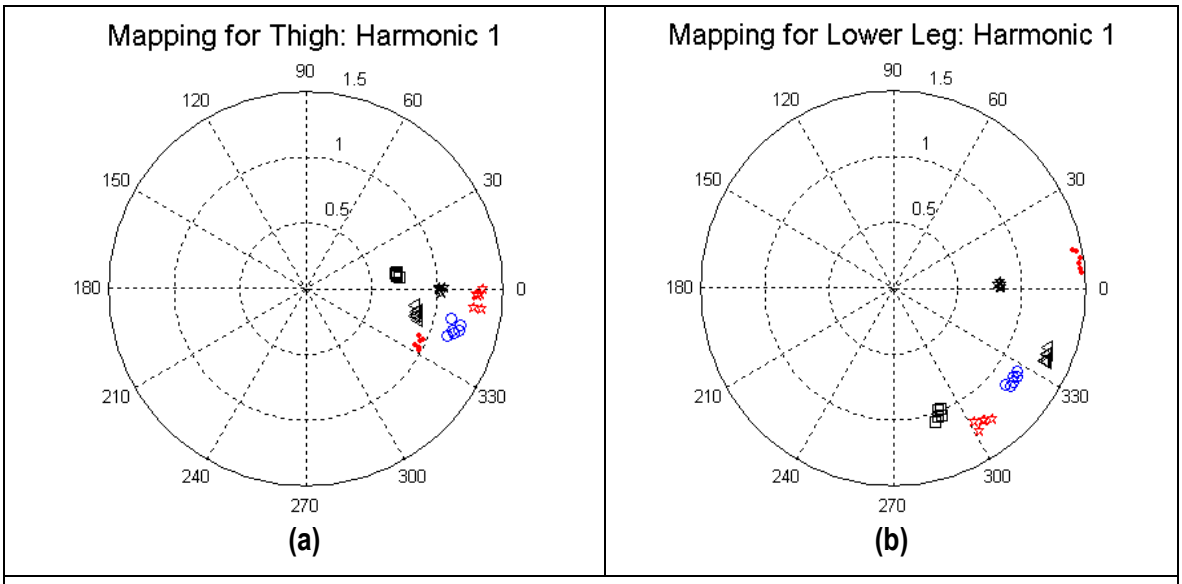

Figure 6.4: Phasor plot for the T_1 of the (a) thigh and the (b) lower leg; different symbols represent different subjects.

When evaluating the mappings, **T**, alone, the perfect classification rates (at least in this dataset) signify that the mapping is highly unique across the population and could be used as a compressed form of signature alone. The mapping is plotted in **Figure 6.5** for 13 subjects using spherical polar co-ordinates for 2 measures of phase and one of magnitude, superimposed on a unit sphere to aid visualisation, where different symbols represent different subjects. The dispersion of clusters confirms the high inter-class variability and low intra-class variability. This can be illustrated as the value of $\bar{S}$ in **Figure 6.6**. Almost all of the squares are bright, indicating high separation between classes. Also the value of $\bar{S}$ for **T** is 0.1803 and is larger than other values shown earlier in **Table 5.1**.

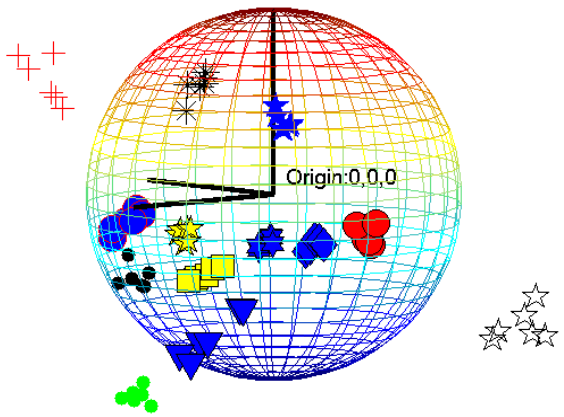

Figure 6.5: Part of the mapping in 3-D displays its uniqueness.

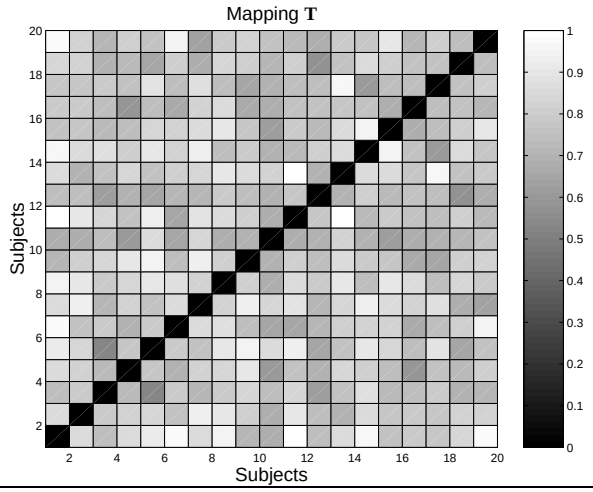

Figure 6.6: Pair-wise $\overline{S}$ -value for mapping T.

6.3 Gait Mode Invariant Signature

Recall that the gait signatures are created from the PWM. Having known the magnitude ratio and phase difference and hence the PWM for running, $\mathbf{PWM'}_R$, can be deduced from the phase and magnitude of walking signal (ϕ_W and M_W), as

$$\mathbf{PWM'}_R = (M_W \bullet M_T) \bullet (\phi_W + \phi_T) \qquad \textbf{(6.6)}$$

Similarly, the PWM for walking, $\mathbf{PWM'}_W$, can be deduced from the phase and magnitude of running (ϕ_R and M_R), as

$$\mathbf{PWM}'_W = \left(\frac{M_R}{M_T}\right) \bullet \left(\phi_R - \phi_T\right) \qquad \textbf{(6.7)}$$

The mapping, **T**, contains information directly related to both gaits, as such the features of the motion within both gaits are retained. One of the advantages is that it is reversible. The ability to describe the relationship in terms of phase and magnitude provides different information to enhance the signature. By means of the mapping, the gait signature can be made invariant and can be transformed from one form to another without losing discriminatory capability. Likewise, the mode of gait of a particular subject can be transformed easily by altering the phase and the magnitude of each harmonic according to its own mapping.

6.4 Evaluating the Unique Mapping

The unique mapping is evaluated over 20 subjects, with 6 samples of walking and running for each subject. The signatures for walking are derived using each individual's unique mapping, based on the signature of running obtained from the feature extraction process. The derived signatures for walking are then tested on the dataset of walking subjects and similarly for running. The results shown in **Figure 6.7** are promising and the process involved implies that the mapping offers invariance to signatures of different gait mode.

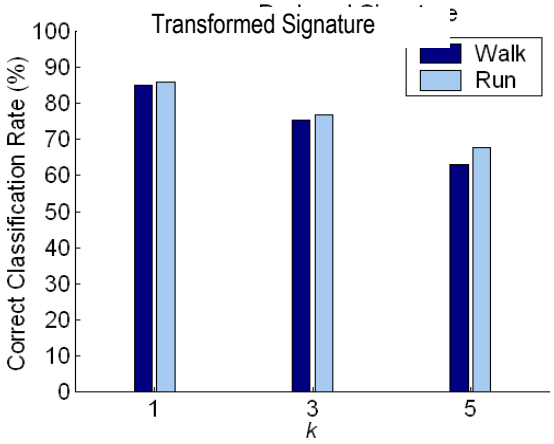

Figure 6.7: Performance of the transformed signature for walking and running.

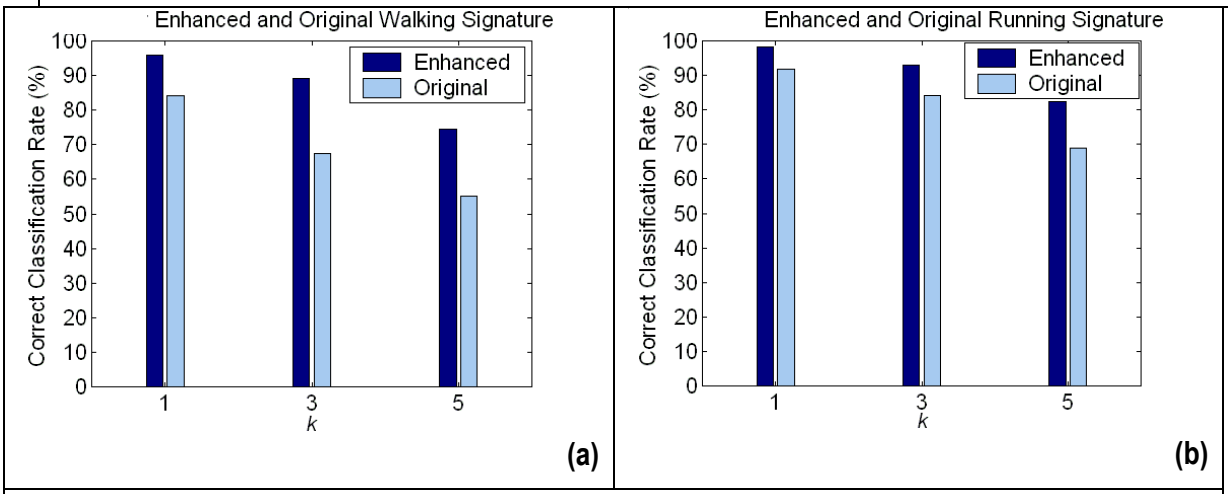

Figure 6.8: Performance of the enhanced and the original walking and running signature.

Finally, the idea of deploying **T** in enhancing the original gait signature again shows how the invariant mapping contains more descriptive information. Recall that the original signal comprises the lower PWMs and **T** is added to the signature vector to yield the enhanced signature. As depicted in **Figure 6.8**, the classification rate using the enhanced signature improves over the original signature for both walking and running. The clusters are more well defined in the enhanced signature space, as the rates do not fall as rapidly as when using the original gait signature whilst k increases. Hence, **T** can be used to enhance the original gait signatures.

6.5 Generic Mapping

As illustrated earlier, we have demonstrated how the signature of an individual's walking and running gait can be related. Nonetheless, due to the lack of understanding of the structure for the signature space, the earlier approach does not allow deduction of the signature of an unseen walker given his/her running gait signature, or vice versa. However, this may be possible if the structure for the generic relationship of these two signature spaces is determined. When classifying walking from running with similar approach (i.e. *k*-nn), it achieved over 90% correct classification rate, see F**igure 6.9**. This reflects the high separation between these two classes in the signature space. Now we shall aim to determine whether there is a generic transform between the signature of walking and running gaits. Here, we employed a neural network in investigating the existence of the generic relationship.

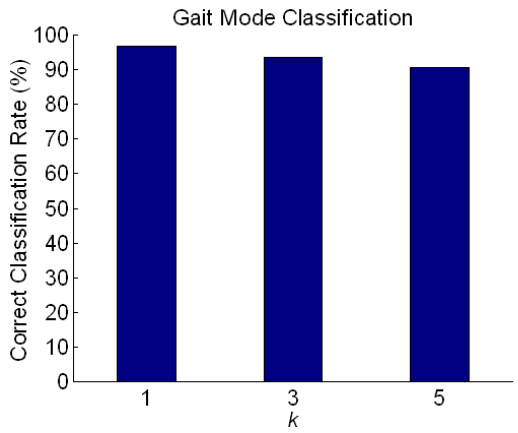

Figure 6.9: Classifying between walking and running gait signature by *k*-nn.

6.5.1 Implementing Neural Network

A neural network has common applications in *classification* and *regression* problems. In *classification*, the task is to assign new inputs to one of a number of discrete classes or categories, i.e. approximate the probabilities of membership of the different classes expressed as functions of the input variables; whereas in a *regression* problem, the outputs represent the values of continuous variables, i.e. regression function approximation. Here, we try to approximate a multi-dimensional regression

function via a neural network in the hope that this might give us some insight in finding the generic relationship and possibly the structure, if one exists. If there was a generic transform, we would expect the predicted signature to offer similar recognition performance as the original gait signature.

A multilayer feedforward network with the back propagation algorithm is the most commonly used architecture [Demuth'00]. Feedforward networks often have one or more hidden layers of sigmoid neurons followed by an output layer of linear neurons. Multiple layers of neurons with non-linear transfer functions allow the network to learn non-linear and linear relationships between input and output vectors. The network used here is illustrated in an abbreviated diagram in **Figure 6.10**, a comprehensive version can be found in **Appendix B**.

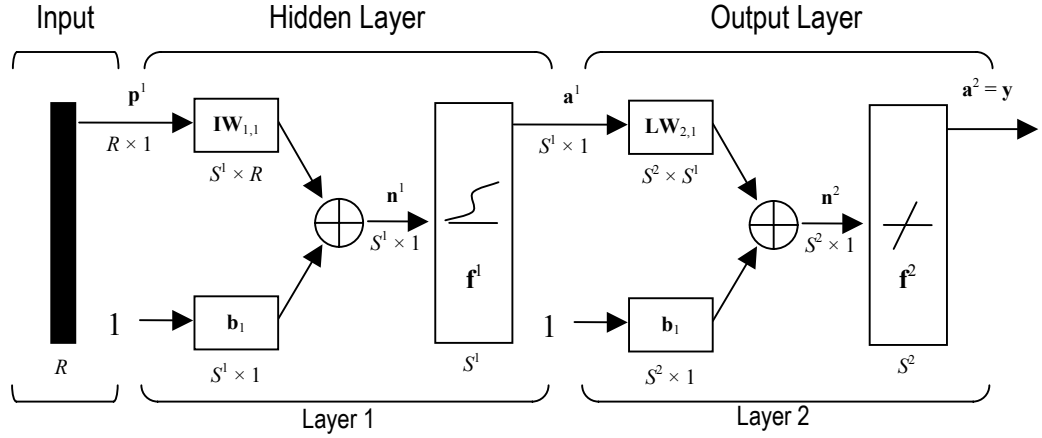

Figure 6.10: Feedforward network with 1 hidden layer and 1 output layer.

p is the input vector with *R* elements, **IW** is the input weight matrix, **LW** is the layer weight matrix, **n** is the transfer function input vector, **a** is the output vector, **b** is the bias vector, **y** is the output vector and *S* is the number of neurons in the layer. The transfer function in the hidden layer is log-sigmoid, and the output layer is a linear function. The network is trained using *resilient backpropagation*, a simple batch mode training algorithm with fast convergence and minimal storage requirements. This network is described by

$$\mathbf{a}^2 = \mathbf{f}^2\left(\mathbf{LW}_{2,1}\, \mathrm{f}^1\left(\mathbf{IW}_{1,1}\mathbf{p} + \mathbf{b}_1\right) + \mathbf{b}_2\right) = \mathbf{y} \qquad (6.8)$$

The task here is to approximate a regression function which describes the relationship between these two groups of signatures. The network is trained with walking signature vectors as the inputs and running signature vectors as the outputs to approximate their relationship. The network training is taken to have converged if the training error is below a threshold value of 10^{-3} for 50 subsequent epochs. Then the trained network is simulated with a seen walking signature vector to predict a running signature. Similarly in predicting a walking signature, another identical network is trained with running signature vectors as the inputs and walking signature as the outputs. And, this network is simulated by a seen running signature to predict a signature for walking. Then classification is carried out between walking and running, by comparing these simulated walking and running signature obtained from the neural network against the original signature space. Again, classification is done via *k*-nn and cross-validated by the leave-one-out rule. **Figure 6.11(a)** shows the result of using the first five harmonics of PWMs in approximating the regression function whereas **Figure 6.11(b)** is the result of using the first ten harmonics. As depicted, the correct classification rate is similar. This could be due to the fact that the dominating component may be from the lower order. Although the rate does not exceed 90%, this preliminary research does suggest the possible existence of a generic mapping between these two biomechanically distinct gaits.

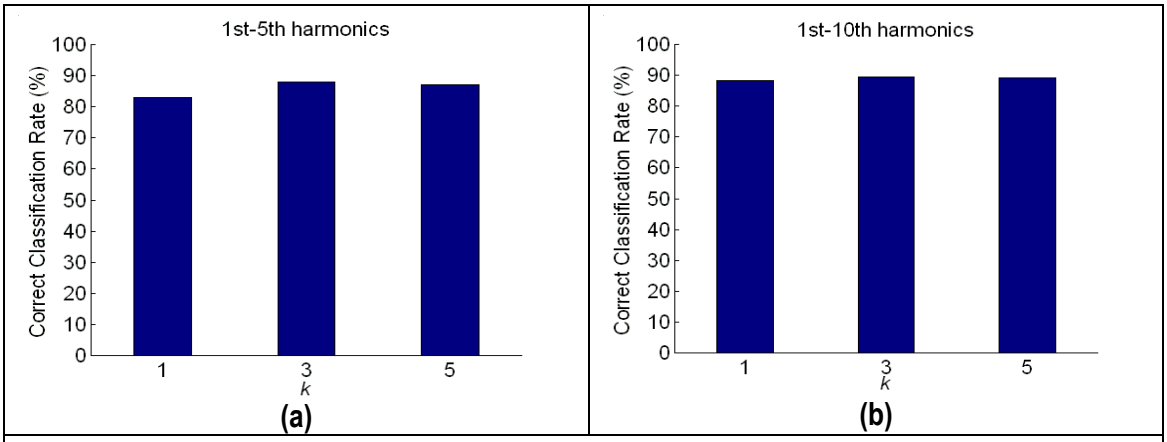

Figure 6.11: Performance of signature predicted via neural network for walking and running.

6.6 Discussion and Conclusions

Frequency representation of the motion not only provides useful features for recognition, but also serves as the basis for the analysis of the relationship between walking and running gaits. The new and interesting findings are: *(i)* a relationship between walking and running gait of a particular subject can be regarded as a phase modulation of each other. This mapping can be described by its unique magnitude ratio and phase difference, capturing the motion features of both gaits; *(ii)* the mappings are highly unique: not only can they be used for recognition alone and to enhance the original gait signature, but also to make signatures invariant to gait mode and to provide a means to transform from one gait mode to another; and *(iii)* the neural network experiment shows that the generic mapping may exist.

Naturally, we shall in the future aim to determine more precisely the nature of the mapping between running and walking, and whether it can be modelled. The understanding of the relationship between walking and running gait not only strengthens the automated person identification approach by gait (biometrics), but also may play an important role in other areas such as biomechanics, robotics and computer graphics animation. This novel idea particularly favours the computer animation of human locomotion as it offers a convenient morph from one gait mode to another. Furthermore, similar ideas could be deployed in motion analysis when walking on a treadmill and on the floor, or across different terrains and etc.

Although this work confirms the existence of the individual mapping, nevertheless, due to the inadequate richness of this dataset the structure of the generic mapping (or the parametric formula to explicitly describe the structure) could not be drawn at this initial stage. However, observations do suggest that this relationship does exist. The next phase of work that could possibly be followed is to find the structure of these relationships. Last but not least, the next challenge would be: does there exist an individual mapping within the generic mapping?

Chapter 7 : Trajectory Invariance

Most of the laboratory-based studies constrain the subjects to walk or run in a plane normal to the camera's sagittal view and have ignored the effects of different view angles. Unfortunately, the effect of trajectory of a moving person on their gait signature is one of the major application issues in a gait-based biometric. Hence, view angle invariant gait signature is essential in terms of practicality. Till now, we have only considered the fronto-parallel view of a moving person for the convenience of evaluating various techniques and algorithms. Preliminary research shows how the camera sagittal view will affect the gait signature, which is effectively the frequency representation of gait patterns. Moreover, experiments show that this automated feature extraction technique can extract the angular motion of both the thigh and the lower leg precisely for the range of -50^{o} to 50^{o} without any adjustment.

7.1 Looking from Different Camera Sagittal Views

To start, let us understand the setup of the camera and various planes. **Figure 7.1** illustrates the camera setup and various planes, and defines the camera sagittal view. For example, when a subject is walking towards and away from the camera, then the trajectory angle/camera sagittal view is said to be normal to (90^o and -90^o, respectively) the camera. So far, we have only considered subjects walking at an trajectory angle of 0^o where the trajectory plane is parallel to the principal plane.

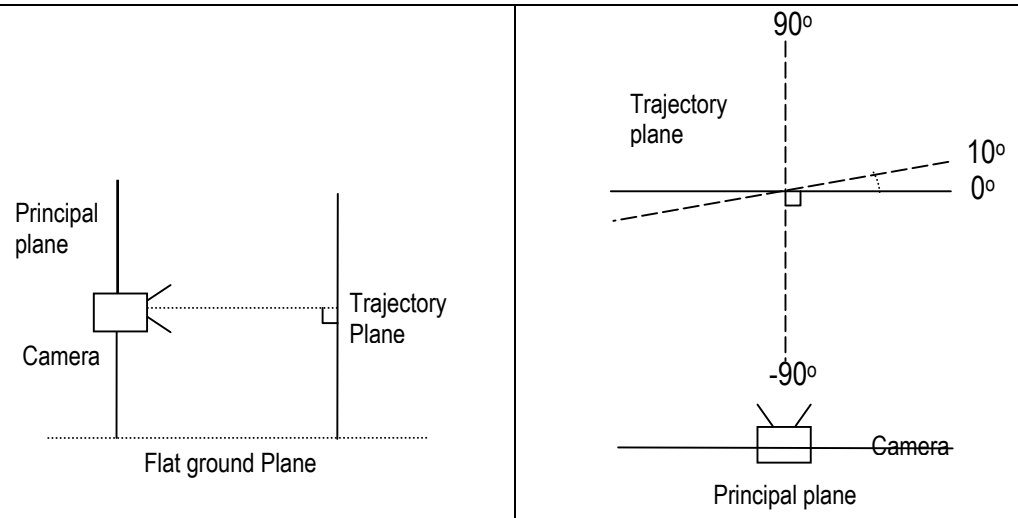

Figure 7.1: Setup for the camera and various planes.

A moving thin rod resembling a pendulum swinging on a plane with simple harmonic motion was created and projected at different camera sagittal view ranging from -90^o to 90^o at increments of 10^o. Then, the rotation angles of the pendulum projected on the camera's principal plane (depicted in **Figure 7.2**) are extracted and Fourier analysis is performed.

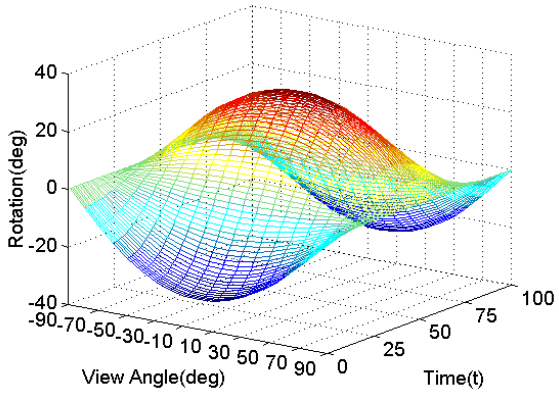

Figure 7.2: Angles of rotation at various camera sagittal views.

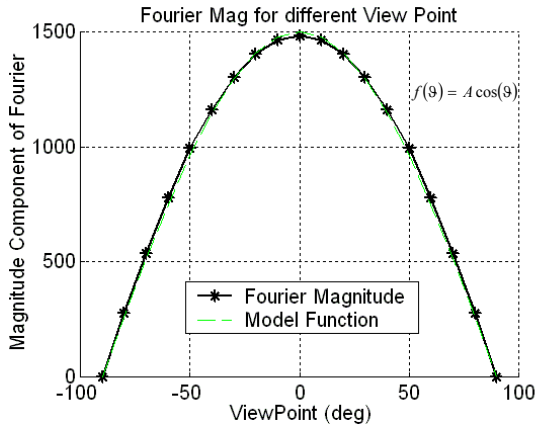

(a)

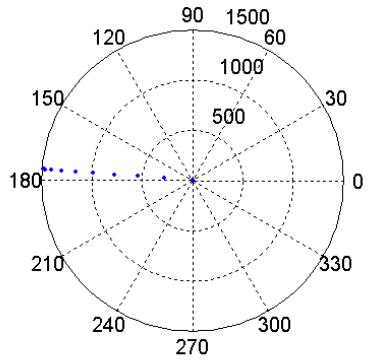

(b)

Figure 7.3: Fourier description of the angular motions perceived from different view angles.

As expected, changes in camera view angle only affect the magnitude spectrum in the frequency domain (**Figure 7.3(a)**), but not the dynamics of the motion as the phase spectrum remains unaltered. The phasor plot in **Figure 7.3(b)** shows the consistency of the phase. Therefore, the angles of motion can be conveniently mapped with a linear relation to the true motion angles (those when viewed from 0^o) by a scaling factor that reads

$$\theta(t, \vartheta) = \theta(t) f(\vartheta) \qquad \textbf{(7.1)}$$

where

$$f(\vartheta) = A\cos(\vartheta) \quad , -\frac{\pi}{2} \le \vartheta \le \frac{\pi}{2} \tag{7.2}$$

and ϑ is the camera sagittal view angle or effectively the trajectory angle. Carter [Carter'99] showed that a model-based approach can be used to extract a gait signature from a sequence of motion that is invariant to pose. It is assumed that the camera is placed at the subject's height, parallel to the ground plane and the subjects walk with various trajectory angles, and the leg is swinging in a plane. Also, it is found that the true thigh rotation angle can be expressed as a linear function of the trajectory and the perceived thigh inclination angle. However, Spencer found that if the trajectory of a walker and elevation angles of the camera are to be considered, the geometric correction for the thigh motion is no longer of a linear relationship [Spencer'02].

7.2 Synthesised Human

The effects of the camera sagittal view angle on the magnitude and phase spectrum when considering a very thin rod has been introduced. Now we shall see if this relationship holds when a synthesized walking human is to be considered. This dataset consists of a gait cycle of a synthesised human with 3-D motion obtained from a real subject. Sequences of various trajectory angles are generated using *Pinocchio*, an in-house software package. This software package allows a user to synthesise a walking human with user-defined camera viewing positions. **Figure 7.4** shows examples of a synthesised human viewed at -90^o to 90^o at increments of 10^o. It is assumed that subjects walk on flat ground. Angular motion of the thigh and lower leg is extracted using the evidence gathering technique illustrated in **Chapter 3**. Results show that this technique is able to extract the motion well when the legs occlude each other at various camera views. **Figure 7.5** shows example results of extraction at ϑ = 20^o and 0^o and they are accurately extracted. Also this technique is capable of extracting the leg motion within the range of -50^o $\le \vartheta \le$ 50^o without any parameter adjustment, but starts to show errors when ϑ approaches -60^o or 60^o. **Figure 7.6** shows the example results of this feature extraction technique. As depicted, leg motion is accurately extracted even at $\vartheta = \pm$ 50^o but did not match the image data well at $\vartheta = \pm$

80°. As the trajectory angle gets larger, the motion dynamics perceived by the machine vision is no longer the same.

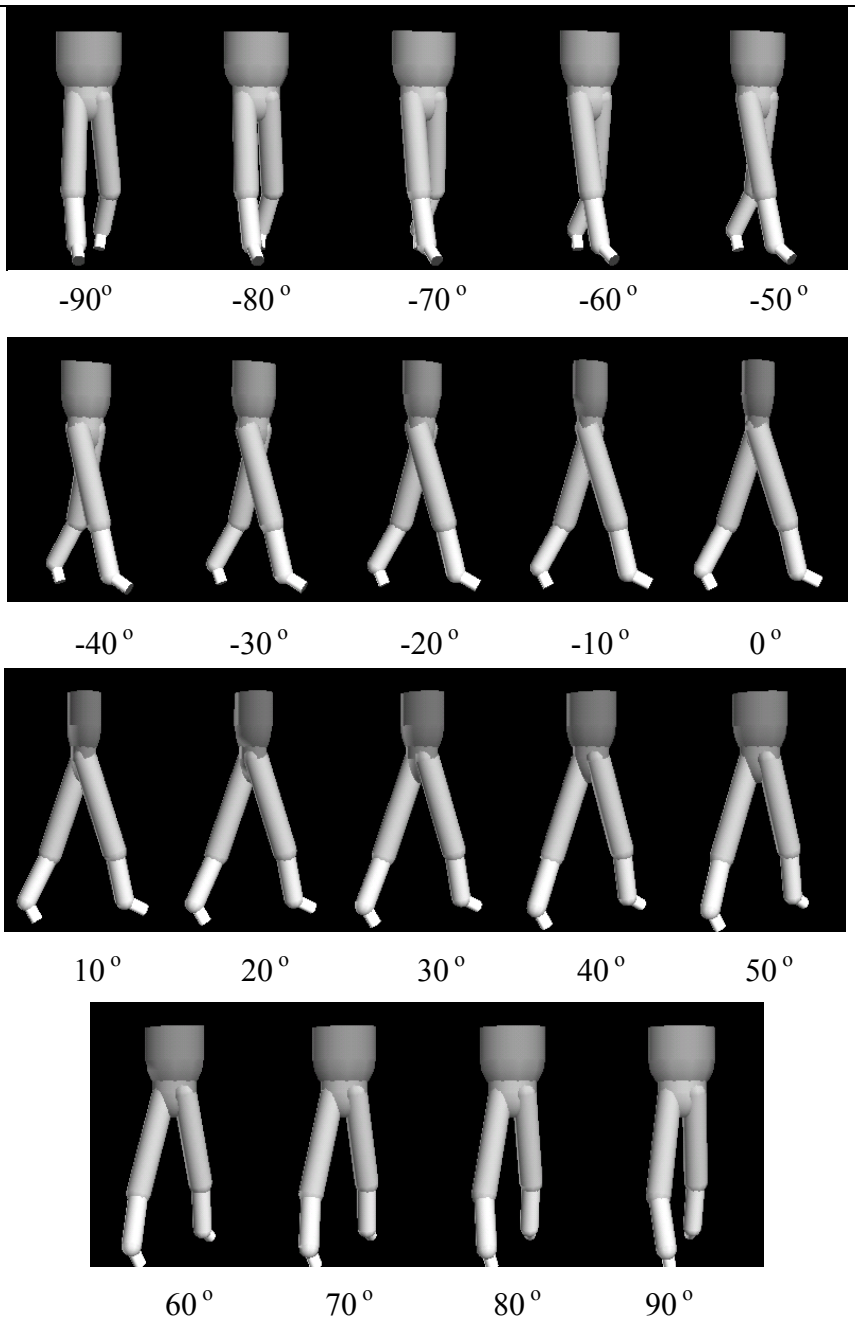

Figure 7.4: Viewing from different sagittal angles.

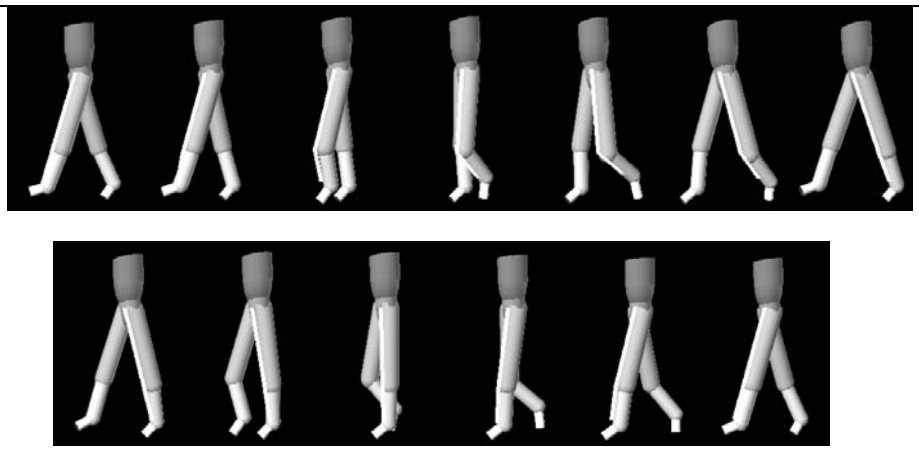

(a) 20°

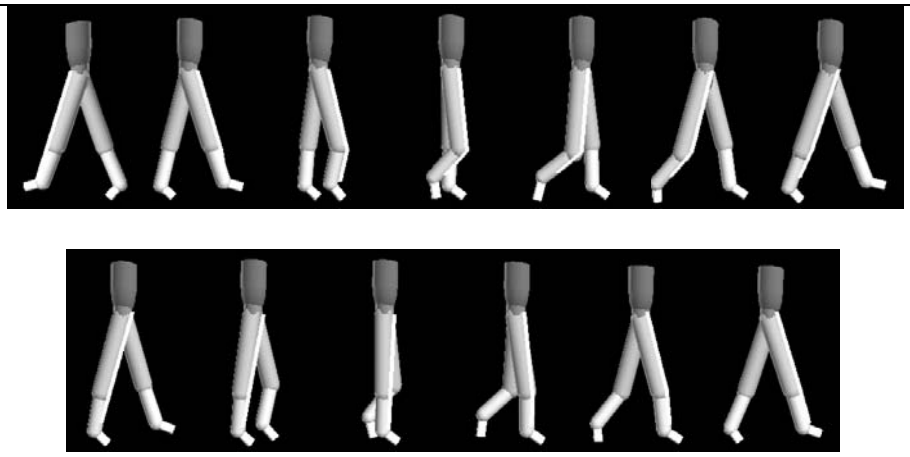

(b) 0°

Figure 7.5: Feature extraction results for sagittal view angle at 20° and 0°.

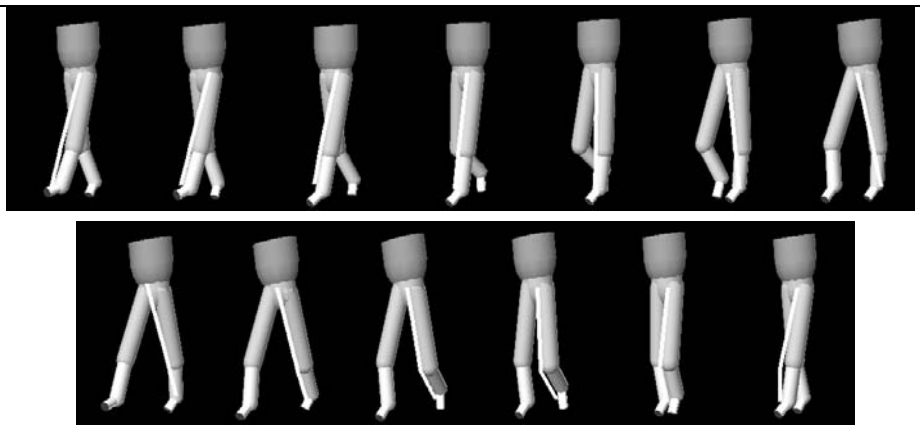

(a) 50°

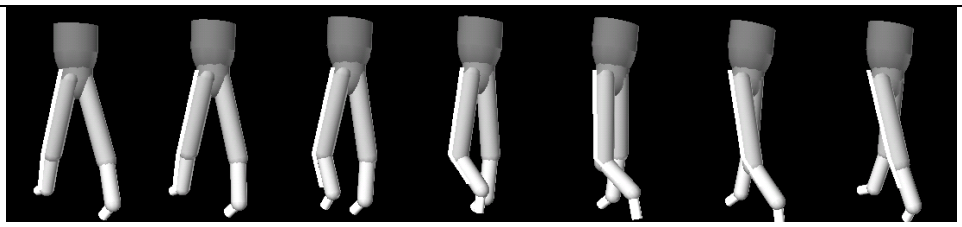

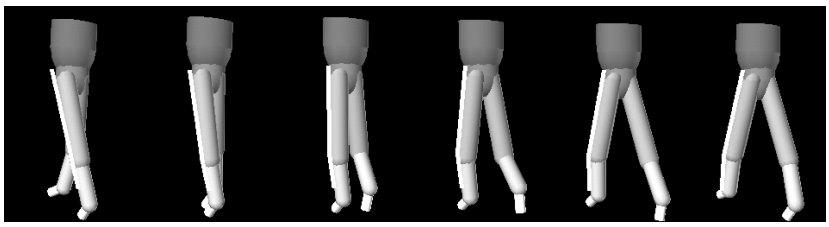

(b) - 50^{o}

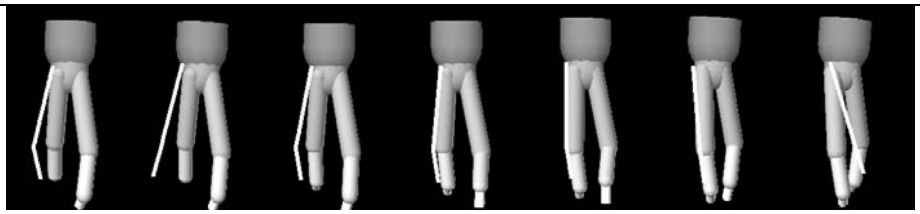

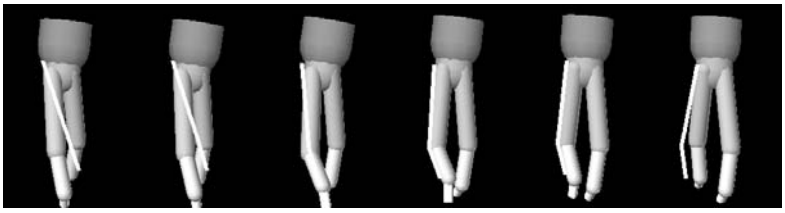

(c) 80^{o}

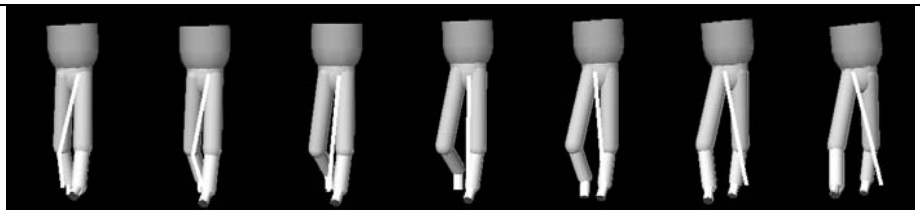

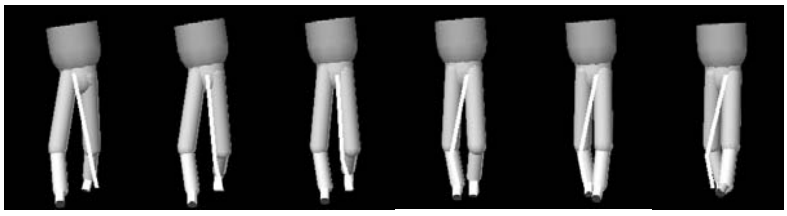

(d) - 80^{o}

Figure 7.6: Samplar results for the feature extraction technique at various camera sagittal view angles.

7.3 Trajectory Angle and Signature Vector

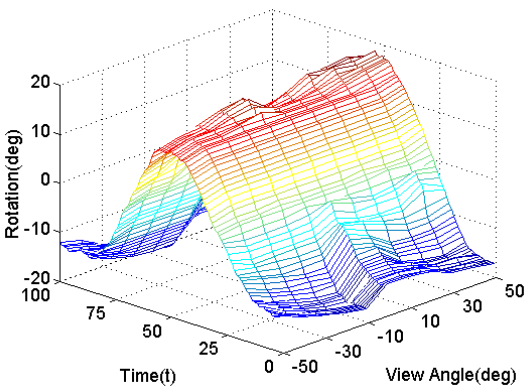

(a) Thigh rotation

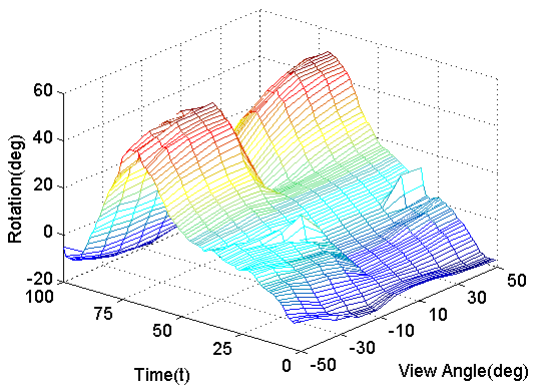

(b) Lower leg rotation

Figure 7.7: Angular motion projected on the principal plane with trajectory angles ranging from -50° to 50° extracted by the evidence gathering technique.

Figure 7.7 illustrates the rotation angles of **(a)** thigh and **(b)** lower leg projected on the camera's principal plane when viewed from -50° to 50°. These angles are extracted automatically by the evidence gathering. Motion angles are changing smoothly with the viewing angle.

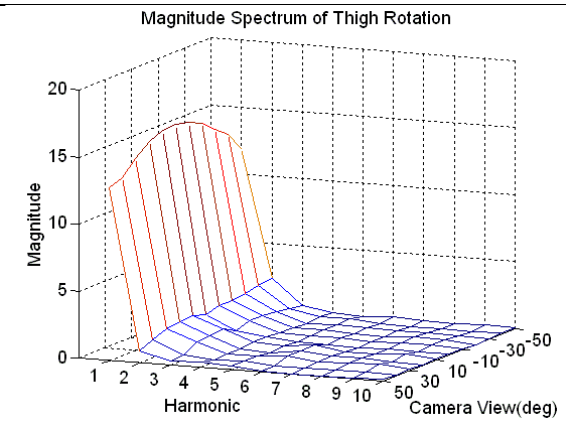

(a)

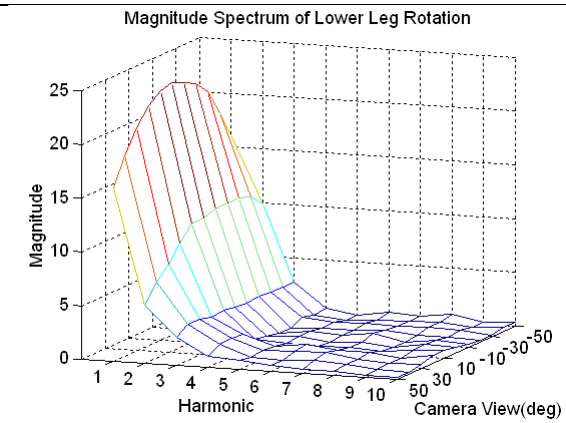

(b)

Figure 7.8: Changes of magnitude spectrum with camera view angles from -50 ° to 50°.

Fourier description of the automatically extracted angles show the effects of different trajectory angles on the magnitude. In **Figure 7.8**, the magnitude spectrum of the thigh and lower leg motion changes smoothly with the camera sagittal view angles and is symmetric at $\vartheta = 0^o$, similar to that of the thin rod depicted in **Figure 7.3**. When the magnitude decreases with the higher harmonics, the changing pattern no longer similar to that of the lower harmonics. This is mainly due to the fact that the higher harmonics are likely to be dominated by noise. Unlike the case of a thin rod shown**,** when a cylinder (which represents the limbs of a subject in this case) is considered, the phase changes with the camera sagittal view angle. Interestingly, the changes are also symmetric at $\vartheta = 0^o$, as shown in **Figure 7.9**, the phasor diagram of the magnitude and phase spectrum. The phases of thigh and lower leg rotation change accordingly with similar symmetry. The arrow indicates the change from -50^o to 50^o at a step of 10^o and changes direction at $\vartheta = 0^o$ for the first harmonic of both the thigh and the lower leg rotations. Therefore, these linear relationships can be potentially exploited to make a gait signature (made up of magnitude and phase) invariant to trajectory angle.

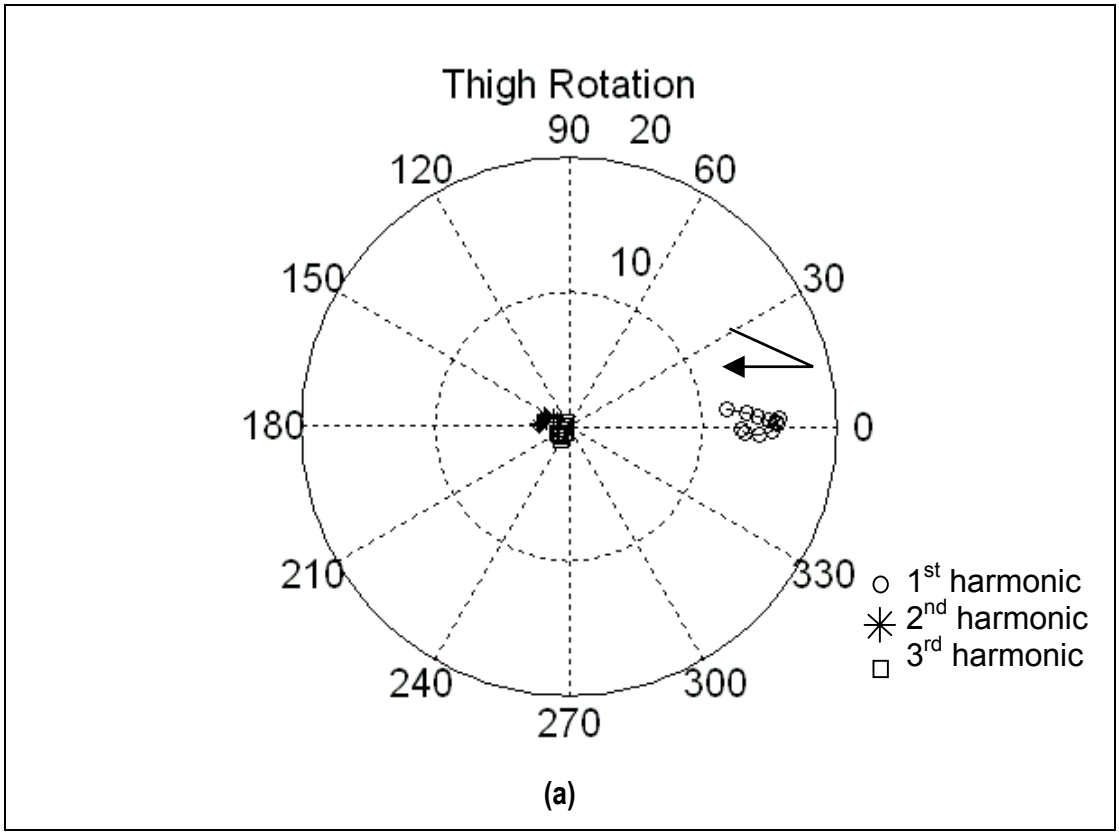

(a)

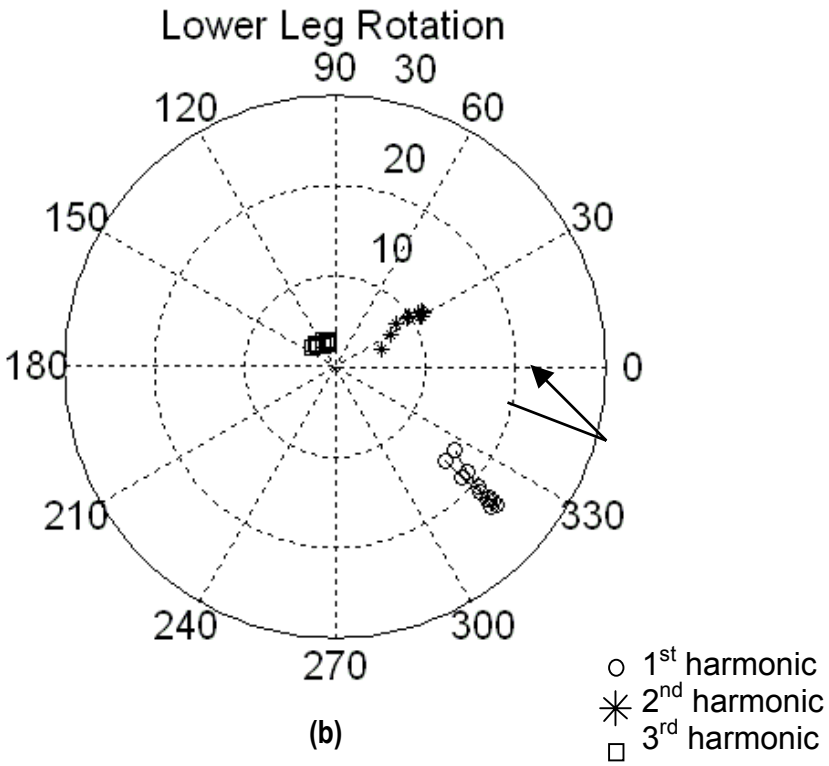

Figure 7.9: Phasor plot showing the changes of phase spectrum with camera view angle from -50 o to 50o.

The variation in phase may be due to both the volumetric and dynamic factor. Instead of a thin line, we are now considering a volume of cylinder (in real life it is a tapered cylinder) which will cast an effect when viewed from a different angle. Also, the hip's transversal rotation may be a dynamic factor that contributes to the alteration in phase. As the real life data is limited, a more precise model for the relationship of the phase change and the trajectory angle is difficult to draw, and this shall be further investigated in the future.

7.4 Conclusions

Experiments show that this automated feature extraction technique can well tolerate various camera sagittal views ranging from -50^o to 50^o without any human intervention or adjustment. This may benefit many applications not only in biometrics, but also clinical-based applications. Results show that the phase and the magnitude

change in a linear fashion with the camera sagittal view. Interestingly, both show a symmetric pattern. Time domain gait patterns can be conveniently mapped to that of $\vartheta = 0^{o}$ (true angle) by exploiting this linearity for the convenience of analysis. More importantly, a gait signature can be made invariant to camera sagittal view under certain constraints. As this is only a preliminary research on the effect of trajectory on the gait signature, further work should investigate generalisation issues on camera various positions, such as elevation and rotation to develop a more realistic model to handle the real world scenario.

Chapter 8 : Finale

We shall now recapitulate the essence of this work by drawing again the motivation, and summing up the conclusions and contributions. Last but not least, to discuss other possible areas for deployment of this novel biometric technique and to suggest possible future work.

8.1 Motivation Revisited

Humans have the natural ability to recognise people by various biological traits, be they physical or behavioural. This actuates the idea of teaching machines about this natural ability of humans, to recognise an individual by their biological traits – **biometrics**. Although there are a number of commercially available biometric systems such as iris pattern and fingerprint recognition system, many others are still in their experimental stage. Gait is one of the emerging biometrics and only attracted attention a decade ago. Much research has been focused on investigating the potential of human walking gait, however, the potential of running gait is yet to be unleashed. Although there has been little quantitative study on the uniqueness of gait, many studies, including those of psychology and biomechanics, do suggest that gait is indeed unique. Furthermore, gait has the potential to overcome some of the limitations that restrict other biometrics. Among the advantages, the most important are, gait *i)* can be perceived from a distance making acquisition non-invasive and convenient, *ii)* does not require high resolution images, *iii)* is difficult to disguise without impeding one's natural gait, and *iv)* has the least impact on privacy issues. This form of biometric is ideal for a scenario where other biometrics such as face and fingerprints are not available. An example will be in a crime scene where the only footage captured by CCTVs is the way the criminal walks in and runs away to escape. Not only do these advantages seem attractive, above all, they provide an alternative biometric approach aiming to achieve a more secure environment.

8.2 Conclusions and Contributions

We have introduced a new biometric approach and outlined the potential of both walking and running gaits as a biometric. There are two major methods in approaching the problem of using gait as a biometric, the most popular being statistical-based methods. However, important characteristics are described by the inter-relationship of the structural description. Therefore, a model-based approach may be of advantage here. Our main objective is to develop a new approach for an automated non-invasive model-based human recognition system by walking and

running via computer vision and pattern recognition techniques. Now we shall recapitulate the conclusions and more importantly, the contributions of this work to the world of biometrics.

1. Human walking and running are two different gaits distinguished mainly by the existence of *double support* or *double float* in respective gait patterns. Despite the functional differences of these two gaits, there occur topological similarities under similar speed and stride frequency. Thus, two **gait-mode invariant motion models** have been developed upon these phenomena and evaluated, and the (untested) third model being potentially as capable.

2. The two motion models are: i) a **bilateral symmetric** model which is developed following the observation on gait patterns. Although the upper pendulum representing the thigh is swinging with a simple harmonic motion, however, the motion model of the lower leg is rather empirical; and ii) a **forced coupled oscillator** model which is developed following the hypothesis of human locomotion being considered as an imperfect pendulum, with substantial energy loss. This new model solves the differential equations obtained from the dynamic motions of the two pendula representing the thigh and the lower leg. The upper pendulum swings with a simple harmonic motion, whilst the lower pendulum is affected by the force introduced by the upper pendulum. The potentially **third** (untested) motion model describes the lower leg as a damped pendulum driven by a periodic force introduced by its suspension point. It shows adherence to the knee rotation when it reaches a steady state.

3. These two models each have their unique strengths and limitations. The **bilateral symmetric** model enjoys its simplicity requiring fewer parameters to describe both the thigh and the knee rotation, as compared with the earlier model. This model, when used as the underlying temporal template for the evidence gathering technique, can extract the thigh and the lower leg motion reasonably well. Though, this model requires selection of a parameter for different gait mode. On the other hand, the **forced coupled oscillator** model requires no parameter selection.

Moreover, when used within the feature extractor, it achieves remarkable results by promising higher accuracy and higher correct classification rate compared to that of the bilateral symmetric model. Owing to the fact that human gaits (walking and running) are bilaterally symmetric and locked by a half a period phase-lock, this enables the models to be extended to describe both legs simultaneously. Nevertheless, a more precise model could be achieved by Fourier series, but at the expense of complexity. However, performance analyses show that this may be unnecessary for our purpose here.

4. This is the first experimental **dataset** to contain the fonto-parallel images of 20 subjects walking and running on a motorised treadmill at their preferred speeds, with 6 samples or sequences of complete gait cycle for each subject. Various conditions such as 25% random greyscale noise and low resolution (65×95) are incorporated in the dataset. Some may argue that treadmill may incur changes to the normal gait, though this remains a constant debate among biomechanics and psychology communities. Although features may change, with respect to one another, the change is assumed to be insignificant. Moreover, treadmill offers many advantages for laboratory-based experiment including controlling environmental factors, space requirement, selectability of locomotion speeds, and repeatability.

5. Gait is naturally rhythmic and periodic. It is no surprise that the patterns of walking and running satisfy **spatial** and **temporal symmetry**. Therefore, dynamic characteristics which are the angular motions of the thigh and the lower leg, are exploited for recognition purposes.

6. **Feature extraction** by temporal and local evidence gathering has successfully captured the motion dynamics of the thigh and the lower leg within a gait cycle. Furthermore, this automated angular motion extraction technique proved to be possible even within the range of -50^{o} to 50^{o} of camera sagittal view angle without any human intervention or parameter adjustment.

7. The **gait signature** is created from the Fourier description by multiplying the magnitude and the phase spectrum to yield phase-weighted magnitude (PWM).

This gives encouraging correct recognition rates. Statistical analysis demonstrated that the inter-class distance measure is higher when the PWM is used, compared with the magnitude component only. Also, only lower order PWM is necessary for creating a reasonably unique signature as higher orders are mainly dominated by noise. This conforms to biomechanics studies which show that the frequency content of the human body when walking is 5 Hz [Angeloni'94]. Furthermore, it is demonstrated that the knee rotation significantly accounted for discrimination. Nonetheless, discrimination capability increases when it is combined with the thigh rotation.

8. **Performance analyses** have been performed on clean images, images contaminated with 25% random greyscale noise and low resolution images (half of the original) by using the two motion models within this novel biometric approach. Results show that when the forced coupled oscillator model is used as the underlying temporal template for the evidence gathering process, it promises an increase of an average of 15.2% and 10.6% recognition rates for the cases of running and walking, respectively, compared to that of the bilateral symmetry model. Also, this technique can tolerate noise reasonably well and is less sensitive to resolution. This may be due to the fact that angles are invariant to scaling. More importantly, analyses demonstrate the potential of walking and running gait as biometrics, with running gait being more potent. This may be due to the many variations of running styles. Moreover, not only this technique can be used to identify individuals, it can also distinguish different gaits and genders.

9. There exists a highly unique **individual mapping** between one's walking and running pattern. In the time domain, a walking signal may be considered as a phase modulated version of a running signal, and vice versa. This relationship can be expressed as the phase difference and magnitude ratio of each other. A gait signature can therefore made invariant to gait mode by exploiting this linear relationship besides offering means for transforming from one gait mode to another. Furthermore, this highly unique (achieving 100% correct classification rate in this dataset) mapping capturing the dynamics of both gaits can be used as a

condensed form of gait signature or to buttress the original signature. A neural network has been employed in search for the **generic mapping** between walking and running across a population. Observations suggest its possible existence, however, the structure of this generic mapping could not be drawn at this early stage.

10. To cope with one of the many application issues, the effects of different **camera sagittal view angles** have been studied. When a subject is walking at different angles from the camera, this casts an effect on the gait pattern perceived by the machine vision. The frequency domain representation changes as both of the magnitude and phase components are affected, though in a linear fashion. Interestingly, both changes are symmetrical at $\vartheta = 0^{o}$, i.e. the fonto-parallel view. The phase change may possibly be due to the hip's transversal rotation, an important dynamic factor for 3-D motion capture. However, the effect is undetermined due to insufficient data and required further investigation. The linear relationship between the camera view angle and the frequency descriptions offers several advantages. The most important in our case here is that the gait signature can be made invariant to camera sagittal view by exploiting this linearity. Furthermore, this may provide a way to map the angular motion obtained from various camera views to that of fonto-parallel view for convenience of gait analysis, be it biometrics or biomechanics.

The above are the main conclusions and contributions drawn from this work. Now, we shall see how this technique may benefit other areas of research.

8.2 Possible Deployment in Other Areas

Interesting and new findings from this research will not only benefit the biometrics arena, they may be helpful in other areas of research such as avatar and medical domain. The following are some suggestions.

Avatar

The two new human locomotion models may offer an alternative method for animating human locomotion based on some biomechanics properties. The beauty of these two models is the invariance to gait mode and requirement of relatively few parameters. Above all, the unique mapping (which can capture the characteristics of both gaits) is expressed by a simple function which particularly favours character animation. This novel idea offers a convenient way for morphing from one gait mode to another with individual characteristics.

Medical

This automated marker-less and non-invasive manner of extracting human leg motion offers a new means for clinical application e.g. biomechanical studies, rehabilitation and psychological studies to study human locomotion in a natural way. This may have an positive impact on clinical gait analysis as many of the current approaches are either not extensively automated, or employ invasive methodologies.

8.3 Future Work

As illustrated, this work offers many contributions to several research domains, particularly biometrics. Nonetheless, research may be brought further either to further enhance the existing technique or approach, or may trigger other interesting areas of research.

First of all the human locomotion model can be improvised by including the highly fluctuating angular motion of the ankle. Besides, a more flexible forcing function may be developed to further improve the precision of the motion model. This modelling method can be extended to include the 3-D motion of human locomotion. Motions from all the three planes, namely, transverse, sagittal and frontal plane can be modelled at the expense of complexity. The major advantage of having a 3-D model is that it may offer more features for discrimination, as with incorporating the ankle

rotation into the motion models. A 3-D model will also have a positive impact on camera view invariance issue. Recall that one of the important factors that may affect the gait patterns viewed at different angles is the hip's transversal rotation. Further research shall be focused on the development of a more precise transfer function to provide camera view invariance.

Last but not least, this work has confirmed the unique mapping for individuals' walking and running pattern. Observations do suggest the possible existence of a generic mapping across a population, nonetheless, the structure of this generic relationship is undetermined, at least not by this approach. The next phase of work that could possibly be followed up is to find the structure of this relationship. If the structure of this generic relationship is found, perhaps there is an individual mapping within the generic mapping?

Appendix A: Comparison of Manual Labelling and Vision Extraction

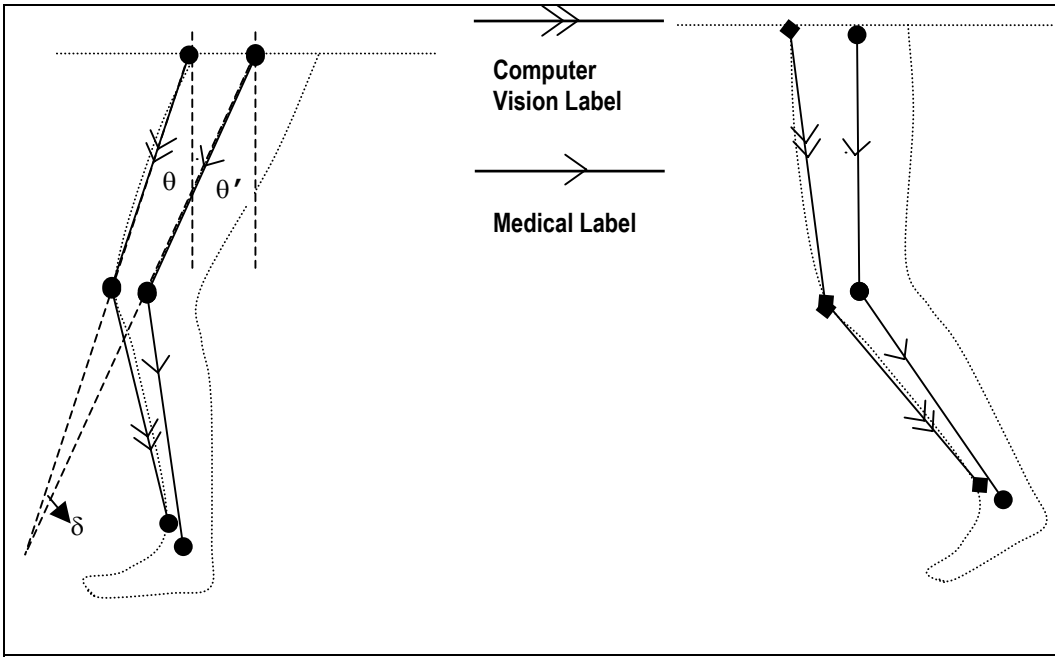

Figure A.1: Medical labelling and computer vision labelling.

The front part of the leg is chosen because clothing adheres most to the front of a moving leg. Unfortunately the location of the bone is unknown by this computer vision approach (and it is not the medial position). Although it is impossible to label the bone (by manual labelling) for analysis, we can assume that the front line and the bone form a rigid body. The relative position of these two lines is always fixed (**Fig. A.1**), therefore the perceived dynamics of the motion are not affected. Assuming that the two lines representing the bone and the front part of the leg form a rigid body, i.e. the relative position is fixed , then they can be related by a linear function (**Eq. A.1**). Such an offset hardly affects the recognition process.

$$\theta' = \theta + \delta \qquad \textbf{(A.1)}$$

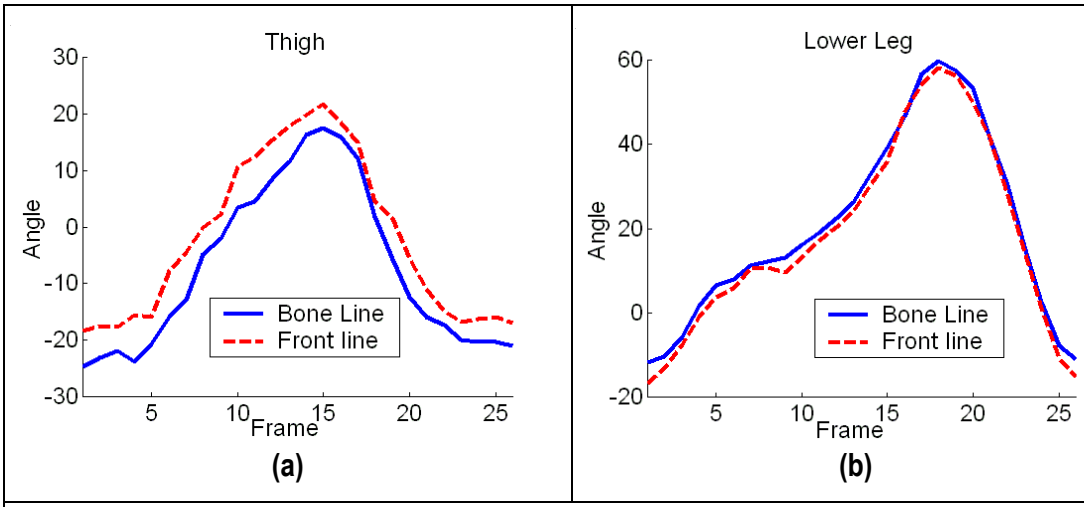

Figure A.2: Difference of medical and computer vision labelling on the thigh and the lower leg rotation

Here, markers are fixed to a subject's leg and measurement is taken from the markers and also the front part of the leg for comparison, see **Figure. A.2**. Having found the offset δ, the angle of rotation extracted by computer vision can be related or corrected to one that match clinical observations if necessary. This will provide an alternative approach to extract leg motion automatically without human intervention. Note that the offset for the thigh rotation is larger then that of the lower leg rotation as this is because less muscle tissue is located at the front of the tibia.

Appendix B: Comprehensive Version of Neural Network

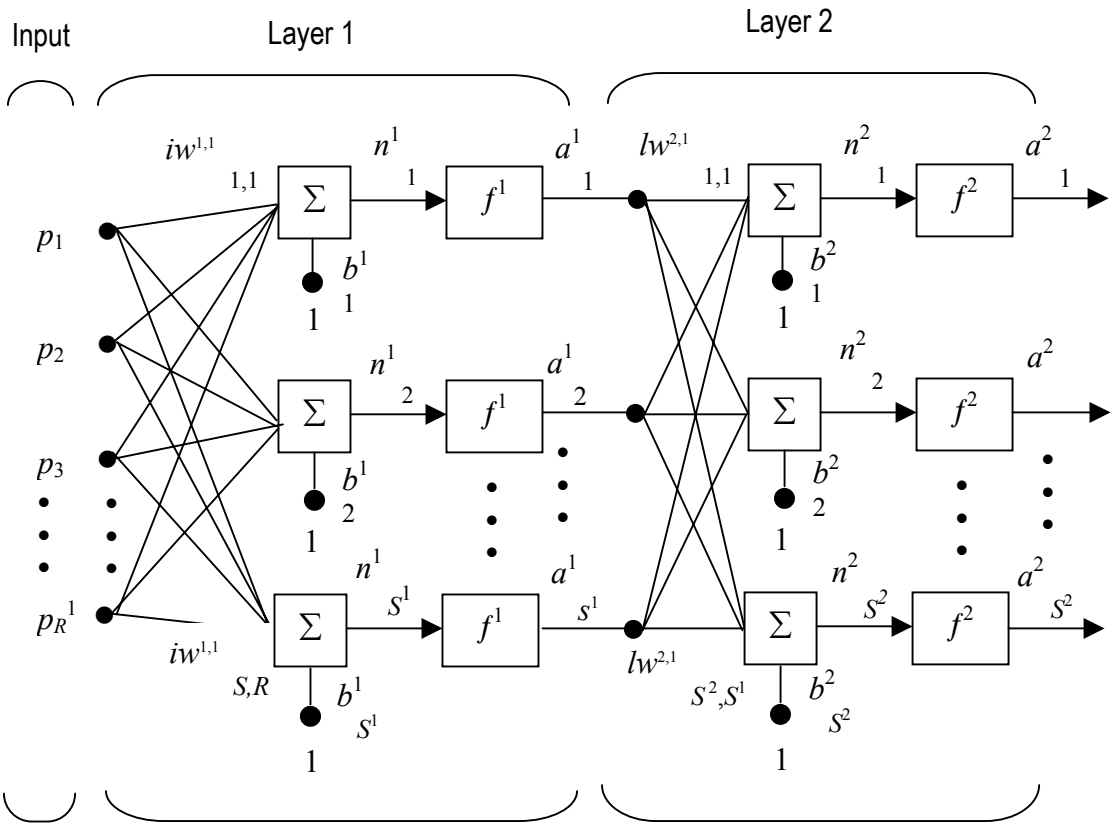

Figure B.1: Neural network with two layers of neurons.

The symbols are:

p = input to the neural network

n = input to the transfer function

a = output

b = bias

S = number of neurons in a layer

R = number of elements in an input vector

lw = layer weight

iw = input weight

References

[Abdelkader'01] C. B. Abdelkader, R. Cutler, H. Nanda and L. Davis, EigenGait: Motion-Based Recognition Using Image Self-Similarity, *Proc. 3rd Audio- and Video-Based Biometric Person Authentication*, pp 289-294, 2001.

[Abdelkader'02] C. B. Abdelkader, R. Cutler and L. Davis, Stride and Cadence as a Biometric in Automatic Person Identification and Verification, *Proc. 5th International Conference on Automatic Face and Gesture Recognition*, pp 372-377, 2002.

[Akita'84] K. Akita, Sequence Analysis of Real World Human Motion, *Pattern Recognition*, **17**(1), pp 73-83, 1984.

[Angeloni'94] C. Angeloni, Riley, P.O. and Krebs, E.D., Frequency Content of Whole Body Gait Kinematic Data, *IEEE Trans. on Rehabilitation Engineering*, **2**(1), pp 40-46, 1994.

[Bader'99] J. P. Bader, J. Buhler, J. Endrass, A. Klipstein and D. Hell, Muscle Power and Gait Patterns of Depressed Persons, *Nervenarzt*, **70**(7), pp 613-619, 1999.

[Bernstein'35] N. A. Bernstein, *Studies in Biomechanics of Locomotion*, Moscow: Ull-Union Institute of Experimental Medicine, 1935.

[Bianchi'98] L. Bianchi, D. Angelini and F. Lacquaniti, Individual Characteristics of Human Walking Mechanics, *Pflugers Archiv - European Journal of Physiology*, **436**, pp 343-356, 1998.

[Boyd'97] J. E. Boyd and J. J. Little, Global versus Structured Interpretation of Motion: Moving Light Display, *IEEE Proc. Computer Society Workshop on Motion of Non-Rigid and Articulated Objects*, pp 18-25, 1997.

[Boyd'01] J. E. Boyd, Video Phase-Locked Loops in Gait Recognition, *IEEE Proc. 8th International Conference on Computer Vision*, pp 696-703, 2001.

[Braune'87] W. Braune and O. Fisher, *The Human Gait*, New York: Springer Verlag, 1987.

[Cai'96] Q. Cai and J. K. Aggarwal, Tracking Human Motion Using Multiple Cameras, *IEEE Proc. International Conference on Pattern Recognition*, pp 68-72, 1996.

[Campbell'95] L. W. Campbell and A. F. Bobick, Recognition of Human Body Motion using Phase Space Constraints, *IEEE Proc. 5th International Conference on Computer Vision*, pp 624-630, 1995.

[Carter'99] J. Carter and M. Nixon, On measuring Gait Signatures which are Invariant to their Trajectory, *Measurement and Control*, **32**, pp 265-269, 1999.

[Cavanagh'90] P. R. Cavanagh, *Biomechanics of Distance Running*, Human Kinematics Books, 1990.

[Chen'92] Z. Chen and H. J. Lee, Knowledge-guided Visual Perception of 3-D Human Gait from a Single Image Sequence, *IEEE Trans. Systems, Man and Cybernetics*, **22**(2), pp 336-342, 1992.

[Cunado'99a] D. Cunado, M. S. Nixon and J. N. Carter, Automatic Gait Recognition via Model-Based Evidence Gathering, *Proc. AutoID99: IEEE Workshop on Automated ID Technologies Summit*, pp 27-30, 1999.

[Cunado'99b] D. Cunado, J. M. Nash, M. S. Nixon and J. N. Carter, Gait Extraction and Description by Evidence-Gathering, *Proc. Audio- and Video-based Biometric Person Authentication*, pp 43-48, 1999.

[Cutting'77] J. E. Cutting and L. T. Kozlowski, Recognizing Friends by their Walk: Gait Perception without Familiarity Cues, *Bulletin of the Psychonomic Society*, **9**(5), pp 353-356, 1977.

[Davis'01] J. W. Davis, Visual Categorization of Children and Adult Walking Styles, *Proc. 3rd Audio- and Video-Based Biometric Person Authentication*, pp 295-300, 2001.

[Davis'02] J. W. Davis and S. R. Taylor, Analysis and Recognition of Walking Movements, *IEEE Proc. 16th International Conference on Pattern Recognition*, 2002.

[Demuth'00] H. Demuth and M. Beale, *Neural Network Toolbox User's Guide, Version 4*, The MathWorks, Inc., 2000.

[Fairhurst'94] M. C. Fairhurst and P. Brittan, An Evaluation of Parallel Stratergies for Feature Vector Construction in Automatic Signature Verification Systems, *International Journal of Pattern Recognition and Artificial Intelligence*, **8**(3), pp 661-678, 1994.

[Foster'01] J. Foster, M. Nixon and A. Prugel-Bennett, New Area Based Metrics for Automatic Gait Recognition, *Proc. British Machine Vision Conference*, pp 233-242, 2001.

[Foti'00] T. Foti, J. R. Davids and A. Bagley, A Biomechanical Analysis of Gait during Pregnancy, *Journal of Bone and Joint Surgery - American Volume*, **82A**(5), pp 625-632, 2000.

[Grant'02] M. G. Grant, M. S. Nixon and P. H. Lewis, Extracting Moving Shapes by Evidence Gathering, *Pattern Recognition*, **35**, pp 1099-1114, 2002.

[Hayfron-Acquah'01] J. Hayfron-Acquah, M. Nixon and J. Carter, Recognising Human and Animal Movement by Symmetry, *IEEE Proc. International Conference on Image Processing*, pp 290-293, 2001.

[Holt'90] K. G. Holt, The Force-Driven Harmonic Oscillator as a Model for Human Locomotion, *Human Movement Science*, **9**, pp 55-68, 1990.

[Hreljac'95] A. Hreljac, Determinant of the Gait Transition Speed During Human Locomotion: Kinematic Factors, *Journal of Biomechanics*, **28**, pp 669-677, 1995.

[Huang'99] P. S. Huang, C. J. Harris and M. S. Nixon, Human Gait Recognition in Canonical Space using Temporal Template, *IEE Proc. Vision, Image and Signal Processing*, **146**(2), pp 93-100, 1999.

[Jain'99] A. K. Jain, *Biometrics - Personal Identification in Networked Society*, Kluwer Academic Publishers, 1999.

[Johnson'01] A. Y. Johnson and A. F. Bobick, A Multi-View Method for Gait Recognition Using Static Body Parameters, *Proc. 3rd Audio- and Video-Based Biometric Person Authentication*, pp 301-311, 2001.

[Kale'02] A. Kale, A. N. Rajagopalan, N. Cuntoor and V. Kruger, Gait-based Recognition of Humans Using Continuous HMMs, *Proc. 5th International Conference on Automatic Face and Gesture Recognition*, pp 336-341, 2002.

[Kozlowski'77] L. T. Kozlowski and J. E. Cutting, Recognizing the Sex of a Walker from a dynamic Point-Light Display, *Perception and Psychophysics*, **21**(6), pp 575-580, 1977.

[Kreyszig'93] E. Kreyszig, *Advanced Engineering Mathematics*, John Wiley & Sons, Inc., 1993.

[Li'99] L. Li, E. C. H. v. d. Bogert, G. E. Caldwell, R. E. A. v. Emmerik and J. Hamill, Coordination Patterns of Walking and Running at Similar Speed and Stride Frequency, *Human Movement Science*, **18**, pp 67-85, 1999.

[Little'98] J. Little and J. Boyd, Recognising People by Their Gait: the Shape of Motion, *Videre, International Journal of Computer Vision*, **14**(6), pp 83-105, 1998.

[Mather'94] G. Mather and L. Murdoch, Gender Discrimination in Biological Motion Displays based on Dynamic Cues, *Proc. Royal Society*, (258), pp 273-279, 1994.

[McGeer'90a] T. McGeer, Passive Dynamic Walking, *The International Journal of Robotics Research*, **9**(2), pp 62-82, 1990.

[McGeer'90b] T. McGeer, Passive Walking with Knees, *IEEE Proc. Robotics & Automation Conference*, pp 1640-1645, 1990.

[Moenssens'71] A. Moenssens, *Fingerprint Techniques*, Chilton Book Company, London, 1971.

[Murase'96] H. Murase and R. Sakai, Moving Object Recognition in Eigenspace Representation: Gait Analysis and Lip Reading, *Pattern Recognition Letters*, **17**, pp 155-162, 1996.

[Murray'64] M. Murray, A. Drought and R. Kory, Walking Patterns of Normal Men, *Journal of Bone Joint Surgery*, **46-A**(2), pp 335-360, 1964.

[Murray'67] M. P. Murray, Gait as a Total Pattern of Movement, *American Journal of Physical Medicine*, **46**(1), pp 290-332, 1967.

[Murray'70] M. P. Murray, R. C. Kory and S. B. Sepic, Walking Patterns of Normal Women, *Archives of Physical Medicine and Rehabilitation*, 1970.

[Murray'85] M. P. Murray, G. B. Spurr, S. B. Sepic and G. M. Gardner, Treadmill vs. Floor Walking: Kinematics, Electromyogram, and Heart Rate, *Journal of Applied Physiology*, **59**, pp 87-91, 1985.

[Nash'97] J. M. Nash, J. N. Carter and M. S. Nixon, Dynamic Feature Extraction via the Velocity Hough Transform, *Pattern Recognition Letters*, **18**, pp 1035-1047, 1997.

[Nixon'02] M. S. Nixon and A. Aguado, *Feature Extraction and Image Processing*, Butterworth Heinmann, 2002.

[Niyogi'94] S. A. Niyogi and E. H. Adelson, Analyzing and Recognizing Walking Figures in XYT, *Proc. Conference of Computer Vision and Pattern Recognition*, pp 469-474, 1994.

[Ounpuu'94] S. Ounpuu, The Biomechanics of Walking and Running, *Clinics in Sports Medicine*, **13**(4), pp 843-863, 1994.

[Penycate'01] J. Penycate, *Identify Theft: Stealing Your Name*, Business, BBC News, 18 June 2001.

[Phillips'02] P. J. Phillips, S. Sarkar, I. Robledo, P. Grother and K. Bowyer, The Gait Identification Challenge Problem: Data Sets and Baseline Algorithm, *Proc. 16th International Conference on Pattern Recognition*, 2002.

[Polana'94] P. Polana and R. Nelson, Low Level Recognition of Human Motion (or how to get your man without finding his body parts), *IEEE Proc. Computer Society Workshop on Motion of Non-Rigid and Articulated Objects*, pp 77-82, 1994.

[Sabatini'98] A. M. Sabatini and V. Colla, A Method for Sonar-based Recognition of Walking People, *Robotics and Autonomous Systems*, **25**, pp 117-126, 1998.

[Sadeghi'00] H. Sadeghi, P. Allard, F. Prince and H. Labelle, Symmetry and Limb Dominance in Able Bodied Gait: A Review, *Gait and Posture*, **12**, pp 34-45, 2000.

[Samson'01] M. M. Samson, A. Crow, P. L. de Vreede, J. A. G. Dessens, S. A. Duursma and H. J. Verhaar, Differences in Gait Parameters at a Preferred Walking Speed in Healthy Subjects due to Age, Height and Body Weight, *Aging-Clinical and Experimental Research*, **13**(1), pp 16-21, 2001.

[Schenau'80] G. J. V. I. Schenau, Some Fundamental Aspects of the Biomechanics of Over Ground versus Treadmill Locomotion, *Medicine & Science in Sports & Exercise*, **12**, pp 257-261, 1980.

[Shakhnarovich'01] G. Shakhnarovich, L. Lee and T. Daarrell, Integrated Face and Gait Recognition from Multiple Views, *Proc. Conference on Computer Vision and Pattern Recognition*, pp 439-446, 2001.

[Shutler'01] J. D. Shutler and M. S. Nixon, Zernike Velocity Moments for Description and Recognition of Moving Shapes, *Proc. British Machine Vision Conference*, pp 705-714, 2001.

[Spencer'02] N. M. Spencer and J. N. Carter, Viewpoint Invariance in Automatic Gait Recognition, *IEEE Proc. 3rd Workshop on Automatic Identification Advanced Technologies*, pp 1-6, 2002.

[Stevenage'99] S. V. Stevenage, M. S. Nixon and K. Vince, Visual Analysis of Gait as a Cue to Identity, *Applied Cognitive Psychology*, **13**, pp 513-526, 1999.

[Stewart'99] I. Stewart, Symmetry-breaking Cascades and the Dynamics of Morphogenesis and Behaviour, *Science Progress*, **82**(1), pp 9-48, 1999.

[Thordarson'97] D. B. Thordarson, Running Biomechanics, *Clinics in Sports Medicine*, **16**(2), pp 239-247, 1997.

[Wall'80] J. C. Wall and J. Charteris, The Process of Habituation to Treadmill Walking at a Different Velocities, *Ergonomics*, **23**, pp 425-435, 1980.

[Weber'36] E. Weber and W. Weber, *Mechanik der Mensclichen Gehwerkzeuge. Eine Anatomisch Physiologische Untersuchung*, Gottingen, 1836.

[Wolfram] Wolfram, Eric Weisstein's World of Mathematics: A Wolfram Web Resource, *http://mathworld.wolfram.com/*

[Yam'01] C.-Y. Yam, M. S. Nixon and J. N. Carter, Extended Model-based Automatic Gait Recognition of Walking and Running, *Proc. 3rd Audio- and Video-Based Biometric Person Authentication*, pp 284-294, 2001.

[Yam'02a] C.-Y. Yam, M. S. Nixon and J. N. Carter, Gait Recognition by Walking and Running: A Model-based Approach, *Proc. 5th Asian Conference on Computer Vision*, pp 1-6, 2002.

[Yam'02b] C.-Y. Yam, M. S. Nixon and J. N. Carter, Performance Analysis on New Biometric Gait Motion Model, *IEEE Proc. 5th Southwest Symposium on Image Analysis and Interpretation*, pp 31-34, 2002.

[Yam'02c] C.-Y. Yam, M. S. Nixon and J. N. Carter, On the Relationship of Human Walking and Running: Automatic Person Identification by Gait, *IEEE Proc. 16th International Conference on Pattern Recognition*, 2002.

[Yam'02d] C.-Y. Yam, M. S. Nixon and J. N. Carter, Automated Markerless Analysis of Human Walking and Running by Computer Vision, *Proc. 4th World Congress Biomechanics*, 2002.

[Zatsiorky'94] V. M. Zatsiorky, S. L. Werner and M. A. Kaimin, Basic Kinematics of Walking: Step Length and Step Frequency. A Review, *The Journal of Sports Medicine and Physical Fitness*, **34**(2), pp 109-134, 1994.

[Zwick'98] D. Zwick, R. Czajkowski, A. Dhage, L. Larina, K. Montgomery and A. J. Nelson, The Effects of Asymmetric Load Carrying on Selected Parameters of Gait, *Journal of Back and Musculoskeletal Rehabilitation*, **10**(2), pp 61-68, 1998.

Publications Associated with this Thesis

1. C.-Y. Yam, M. S. Nixon and J. N. Carter, Extended Model-based Automatic Gait Recognition of Walking and Running, *Proc. 3rd Audio- and Video-Based Biometric Person Authentication*, pp 284-294, 2001.
2. C.-Y. Yam, M. S. Nixon and J. N. Carter, Gait Recognition by Walking and Running: A Model-based Approach, *Proc.5th Asian Conference on Computer Vision*, pp 1-6, 2002.
3. C.-Y. Yam, M. S. Nixon and J. N. Carter, Performance Analysis on New Biometric Gait Motion Model, *Proc. 5th IEEE Southwest Symposium on Image Analysis and Interpretation*, pp 31-34, 2002.
4. C.-Y. Yam, M. S. Nixon and J. N. Carter, On the Relationship of Human Walking and Running: Automatic Person Identification by Gait, *Proc. 16th International Conference on Pattern Recognition*, 2002.
5. C.-Y. Yam, M. S. Nixon and J. N. Carter, Automated Markerless Analysis of Human Walking and Running by Computer Vision, *Proc. 4th World Congress Biomechanics*, 2002.
6. C.-Y. Yam and M. S. Nixon, Automated Non-Invasive Human Locomotion Extraction Invariant to Camera Sagittal View, *Proc. International Congress on Biological and Medical Engineering*, 2002.
7. C.-Y. Yam, M. S. Nixon and J. N. Carter, Automated Person Recognition by Walking and Running via Model-based Approach, *Pattern Recognitio*n, under review.